Dissertations, Master's Theses and Master's Reports

2019

AN EXPERIMENTAL STUDY OF A PASSIVE NOx ADSORBER (PNA) FOR THE REDUCTION OF COLD START DIESEL EMISSIONS

Conor Berndt
Michigan Technological University, ctberndt@mtu.edu

www.manaraa.com

AN EXPERIMENTAL STUDY OF A PASSIVE NOx ADSORBER (PNA) FOR THE
REDUCTION OF COLD START DIESEL EMISSIONS

By

Conor T. Berndt

A THESIS

Submitted in partial fulfillment of the requirements for the degree of

MASTER OF SCIENCE

In Mechanical Engineering

MICHIGAN TECHNOLOGICAL UNIVERSITY

2019

© 2019 Conor T. Berndt

This thesis has been approved in partial fulfillment of the requirements for the Degree of MASTER OF SCIENCE in Mechanical Engineering.

Department of Mechanical Engineering – Engineering Mechanics

Thesis Co-Advisor: *Dr. Jeffrey D. Naber*

Thesis Co-Advisor: *Dr. John H. Johnson*

Committee Member: *Dr. Boopathi S. Mahadevan*

Department Chair: *Dr. William Predebon*

Table of Contents

iv

List of Figures

List of Tables

Acknowledgements

Many organizations and individuals made it possible for me to pursue this higher education and supported me throughout. I would like to thank those past and present who are responsible for this accomplishment.

I would like to thank my advisors Dr. Jeffrey Naber and Dr. John Johnson for their continued support and expertise throughout my research. Also, for providing me with the opportunity to continue my education and gain such a valuable experience. I would like to thank Dr. Boopathi S. Mahadevan for being on the committee for my defense. Dr. Scott Miers for his invaluable teaching influence on my undergraduate studies. Dr. Darrel Robinette, for being an excellent professor during my undergraduate degree and influencing me to pursue my master's degree. Zachary Stanchina, William Hansley, and Tyler Miller for assisting with the experimental testing. Henry Schmidt and Bill Atkinson for hiring me at the Michigan Tech AERB and helping me obtain a graduate research assistantship. Andreas from AVL for his support with the Pierburg 5-gas bench. Xiaobo Song from Cummins for supplying software licensure and replacement engine instrumentation. Paul Dice, for his support with the engine test cell, and many others.

I would also like to thank Tucker Alsup for working with me to design and construct the experimental test setup and to conduct experimental testing. Without his help I can honestly say I would not be here and for that I am grateful.

I would also like to thank my friends and family for their unconditional support and encouragement throughout these past two years.

List of Abbreviations

dCSC™ – Johnson Matthey Diesel Cold Start Concept

DOC – Diesel Oxidation Catalyst

PNA – Passive NOx Adsorber

CARB – California Air Resources Board

EPA – Environmental Protection Agency

NAAQS – National Ambient Air Quality Standards

HC – Total Hydrocarbons

NO – Nitric Oxide

NO_2 – Nitrogen Dioxide

NOx – NO + NO_2

N_2O – Nitrous Oxide

CO – Carbon Monoxide

CO_2 – Carbon Dioxide

ATS – Aftertreatment System

ULN – Ultra-Low NOx

H_2O – Water

O_2 – Oxygen

JM – Johnson Matthey

SCR – Selective Catalytic Reduction

SCR-F – Selective Catalytic Reduction Catalyst on a Diesel Particulate Filter

EGR – Exhaust Gas Recirculation

DPF – Diesel Particulate Filter

CPF – Catalyzed Particulate Filter

PM – Particulate Matter

CDA – Cylinder Deactivation

SwRI – Southwest Research Institute

LLC – Low Load Cycle

REAL – Real Emissions Assessment Logging

NI – National Instruments™

DAQ – Data Acquisition

VGT – Variable Geometry Turbo

AFR – Air-to-Fuel Ratio

GHG – Greenhouse Gas

PGM – Platinum Group Metals

Ar – Argon

Pd – Palladium

Pt - Platinum

Abstract

Medium and heavy-duty diesel engines contribute nearly a third of all NOx emissions nationwide. Further reduction of NOx emissions from medium and heavy-duty diesel engines is needed in order to meet National Ambient Air Quality Standards (NAAQS) for ambient particulate matter and ozone. Current diesel engine aftertreatment systems are very efficient at reducing NOx emissions at exhaust temperatures above 200 °C, however at exhaust temperatures below 200 °C there are significant NOx emissions at the tailpipe. Therefore, a reduction of diesel engine cold start and low speed/load operation emissions, where exhaust temperatures are below 200 °C, is needed. Utilizing a passive NOx adsorber (PNA) to adsorb NOx emissions at temperatures below 200 °C and reduce tailpipe NOx emissions is part of the solution. In this research, over 200 hours of experimental testing was carried out on a Johnson Matthey Diesel Cold Start Concept Catalyst (dCSC™), a passive NOx adsorber with hydrocarbon trapping ability on an oxidation catalyst.

Storing NOx emissions while the aftertreatment system downstream of the PNA is at temperatures below 200 °C needs to be supplemented by externally heating the aftertreatment system downstream of the PNA. This would reduce the time the aftertreatment system is at temperatures below 200 °C. The faster the aftertreatment system reaches operating temperature the less risk of substantial NOx emissions at the tailpipe, because the storage capacity of the dCSC™ is finite. Methods such as electric heaters, fuel burners, engine calibration, engine hardware changes, and others to quickly reach desired aftertreatment temperatures are being researched. The EPA and CARB are preparing to monitor the emissions regulation compliance of medium and heavy-duty diesel engines by using on-board diagnostics, throughout the useful life of the engine. They are also investigating thermal and chemical catalyst poisoning in order to accurately age and predict the life of the aftertreatment system. Improving processes and reducing contaminants in fuels can reduce the risk of chemical catalyst poisoning.

A 2013 6.7L Cummins ISB (280 hp) diesel engine was used for a series of experiments to quantify the NO, NO_2, and NOx storage and release performance of the dCSC™. NOx storage experiments were performed at a range of temperatures from 80 to 250 °C and NOx release experiments were performed at temperatures from 200 to 450 °C. The portion of NO, NO_2, and NOx that is converted and the portion that remains stored on the dCSC™ and the oxidation characteristics of the dCSC™ at these temperatures were also quantified.

Peak NOx storage capacity of the dCSC™ was found to be at temperatures from 125 to 150 °C. Throughout the testing, a decrease in the total NOx storage capacity was observed. However, the 200-second dCSC™ NOx storage capacity remained constant throughout testing. The percentage of stored NOx released was observed to be over 70% if the dCSC™ temperature ramped through 200 to 265 °C and/or reached 350 °C. These temperatures coincide with the desired operating temperatures of current aftertreatment systems. The dCSC™ also shows over 50% NO to NO_2 oxidation at temperatures from 200 to 400 °C and a peak oxidation performance of 90% at 300 °C. At temperatures of 150 °C and above, the dCSC™ oxides 90 to 100% of CO to CO_2. At 80 to 125 °C, the dCSC™ oxidizes 50 to 70% of the CO entering the substrate to CO_2.

1 Introduction

The purpose of this chapter is to give background information and the goals and objectives of the research conducted. Specifically, why the research is being conducted and what need does it fill. For decades, diesel engine aftertreatment system research has been continuously driven by increasingly stringent emissions standards. The Environmental Protection Agency (EPA) and California Air Resources Board (CARB) have worked in conjunction for years to develop new emissions standards, test cycles, compliance monitoring, useful life determinations, and advanced protocols to simulate real world deterioration of the components in the diesel engine aftertreatment system.

1.1 Background

The current heavy-duty diesel engine aftertreatment systems can reduce tailpipe emissions with very high efficiencies once they reach their operating temperature [1]. One such system from Cummins Emissions Solutions consists of (from upstream to downstream) a DOC, DPF, DEF injector, decomposition reactor, and SCR [2]. The DOC, or Diesel Oxidation Catalyst, oxidizes CO to CO_2, HC to CO_2 and H_2O, and NO to NO_2. The DPF, or Diesel Particulate Filter, filters the particulate matter (PM). The DEF, or Diesel Exhaust Fluid injector injects atomized DEF into the decomposition tube. The decomposition tube decomposes the atomized DEF into ammonia (NH_3) and water (H_2O), and mixes the NH_3 uniformly with the exhaust gas. The SCR, or Selective Catalytic Reduction, receives the NH_3-exhaust gas mixture and reduces the NOx in the exhaust gas to nitrogen (N_2) and water (H_2O). There is a need to periodically actively regenerate the DPF due to excess PM by performing a late diesel injection [2]. The efficiency of the SCR catalyst has been increased to 90% at temperatures as low as 200°C [3]. However, when these systems are below 200 °C, during startup or low speed/load operation, their NOx conversion efficiency is low. One of the goals of the EPA and CARB partnership is to reduce or even eliminate these NOx emissions [3, 4, 5].

Currently, heavy-duty trucks contribute a third of the NOx emissions produced in California and are projected to contribute a third nationwide by 2025 [3]. Further NOx emissions regulations are required in order for the South Coast Air Basin to achieve the National Ambient Air Quality Standards (NAAQS) requirement for ambient PM and Ozone [3]. NOx emissions are a precursor to PM, this makes them especially important to meeting the NAAQS PM requirement. The current NOx reduction goal is an Ultra-Low NOx (ULN) standard of 0.02 gNOx/bhp-hr on the FTP and RMC-SET cycles [3]. The Federal Test Procedure (FTP) and Supplemental Emission Test Ramped Modal Cycle (RMC-SET) are the drive cycles currently used to certify medium and heavy-duty diesel engines [3]. The drive cycles command sequences of vehicle speed (chassis dynamometer) or engine load (engine dynamometer) and tailpipe emissions are measured. The tailpipe emissions measurements determine whether or not the specific drive cycle emissions regulations are met. Southwest Research Institute (SwRI) is working closely with CARB and the EPA to determine realistically achievable emissions levels for the drive cycles and the methods for doing so. "Per reference [3], SwRI has achieved 0.034 gNOx/bhp-hr NOx level over the FTP and a 0.038 g/bhp-hr NOx level over the RMC-SET [3]". The latest feasibility assessment from the CARB staff is that MY 2024 through 2026 heavy and medium-duty engines could be required to meet 0.05 to 0.08 gNOx/bhp-hr on the FTP and RMC cycles [3, 6]. PM emissions standards will also see a reduction to 0.005 g/bhp-hr by MY 2024. MY 2027 will see an even further reduction in NOx emissions levels [3, 6]. CARB and the EPA have reduction targets for greenhouse gas (GHG) and petroleum use as well. CARB Phase 2 GHG emissions standards will be implemented alongside the NOx and PM regulations in 2021, 2024, and 2027. These Phase 2 GHG emissions standards require a 5.1% fuel efficiency improvement from the 2017 fuel efficiency levels, by model year 2027 [3].

A new "Low Load Cycle" (LLC) has been developed by SwRI to simulate the low speed and load of "urban tractor and vocational vehicle operations" [3, 7]. The current FTP and RMC-SET cycles fail to capture the low load and speed operation of medium and heavy-duty diesel engines. It is important to capture the low speed/load operation because

2

exhaust temperatures are low at these conditions: causing the current ATS to be ineffective [3, 7]. The LLC emissions requirements for NOx will be between 1 to 3 times the FTP and RMC-SET requirements (0.05 to 0.24 gNOx/bhp-hr) [3, 6].

During low speed/load operation, the ATS temperatures fall well below 200°C. Increasing exhaust temperatures can be done via engine calibration, hardware, or external heat sources, and can ensure that the ATS temperature is above 200°C during startup and normal operation. In addition, improving ATS efficiencies at temperatures below 200°C can help reduce low speed/load emissions. This could involve improving the efficiency of current SCR systems at low temperatures; or employing a passive NOx adsorber (PNA) to store NOx emissions at low temperatures. Current ULN ATS solutions employ both the increase in exhaust temperatures and improving catalyst efficiencies at lower temperatures [1, 4, 5, 8].

The main goal of the ULN ATS is to reduce NOx and HC emissions during low load/speed operation and cold start. Storing NOx and HC emissions until the ATS is at operating temperature is a promising strategy. This can be achieved through the use of a PNA catalyst with zeolites to trap HC [1, 5, 8]. Figure 1.1 shows a schematic of proposed ULN ATS configurations compared to today's ATS systems [9]. The schematic was put together by Daimler Trucks to reflect the proposals from references [3, 5].

3
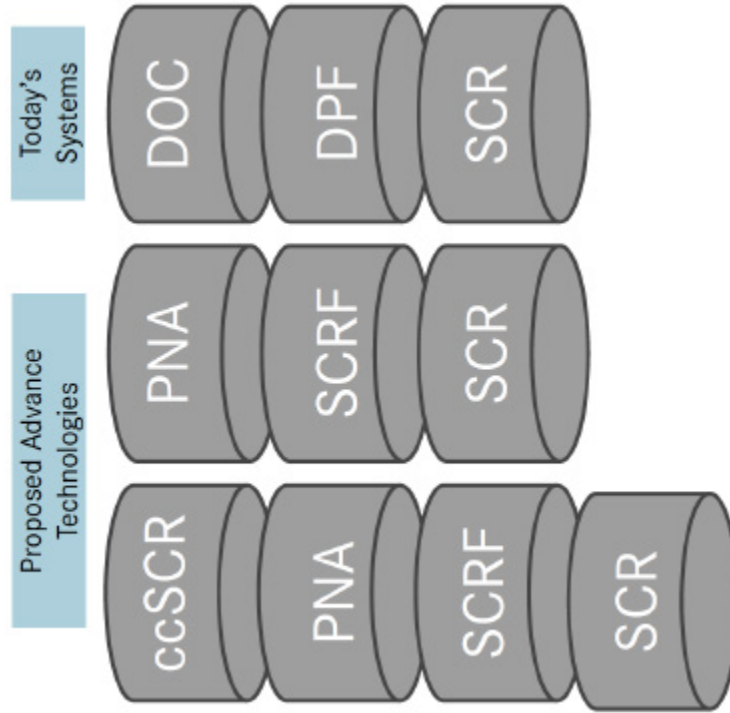
Figure 1.1 Possible ULN ATS Compared to Current ATS [9]

Both "Proposed Advance Technology" systems in Figure 1.1 include the utilization of a PNA to store NOx emissions at temperatures below 200 °C [3, 5, 9]. PNA technology developed by Johnson Matthey to store HC, CO, and NOx emissions at low temperatures and release them at high temperatures has been developed. The device consists of a PNA with HC trapping ability on an oxidation catalyst i.e. the Diesel Cold Start Concept (dCSC™) [1, 8]. The goal of this catalyst is to store emissions while the downstream ATS heats up. Externally heating the downstream ATS will reduce the time the PNA has to adsorb NOx, HC, and CO emissions and improve ATS efficiency [4, 5, 9]. Once the downstream ATS is at its operating temperature, the dCSC™ will release these emissions to the downstream ATS to be reduced and oxidized [5, 8]. The ATS will have a complex control system that will require accurate thermal management in order to achieve desired tailpipe emissions [10].

The dCSC™ has a limited NOx and HC storage capacity. Therefore, increasing exhaust temperatures quickly and keeping them above 200°C is still a primary goal of the ULN

4

ATS. As stated before, exhaust temperatures can be increased through engine calibration, hardware, or external heat sources like electric heaters. Late fuel injections are currently a common tool used to manage the ATS temperature; research is also being done to develop external heat sources such as electric heaters and fuel burners [3, 4, 5, 10, 11]. Figure 1.2 shows that a reduction in engine AFR increases exhaust gas temperatures [12]. Reducing AFR can be achieved by throttling, reducing boost, valve timing, EGR, and cylinder deactivation [4, 12]. Some of these are engine hardware changes while some of them are calibration changes will likely be needed. In Figure 1.2 the AFR was decreased through cylinder deactivation and late intake valve closing. A mixture of engine hardware and calibration changes. In this case the figure is reporting turbine outlet temperature which is at the inlet to the ATS. Cases where the turbine outlet temperature falls well below the curve are cases with high EGR rates [12].
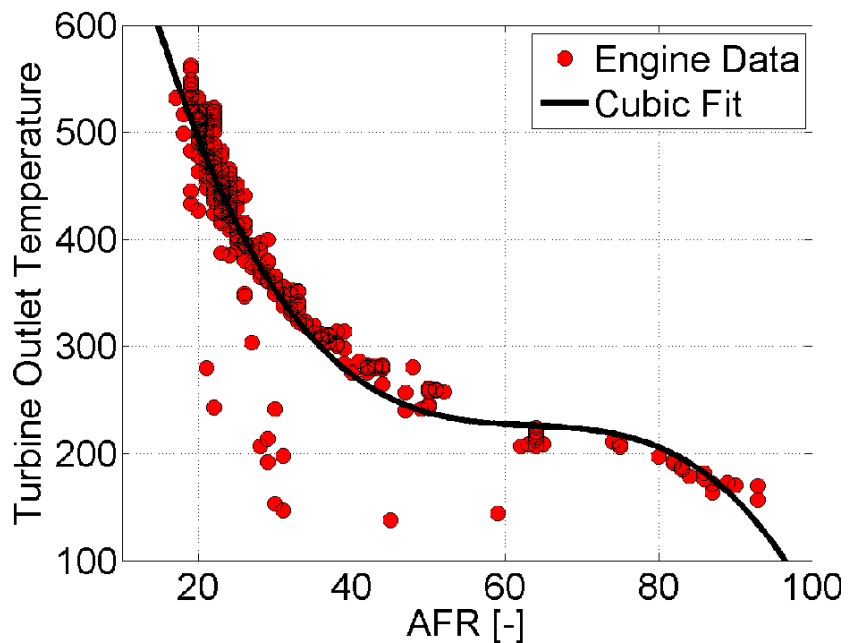
Figure 1.2 Engine Turbo Outlet Temperature vs. AFR [11].

Another objective of the EPAs Cleaner Trucks Initiative and CARB is to "ensure in-use emissions reductions [4, 12]." One of the ways to do this is to properly determine the useful life of ATS components. This will ensure the compliance with regulations once the ATS is exposed to real world conditions. Current ATS aging procedures for certification

5

are not reflective of actual real-life deterioration factors [3]. Aging methods are extremely important to developing ATS components that will be required to perform throughout the useful life of the product. Properly aging the ATS with the correct deterioration factors will allow for more accurate ATS useful life estimates and service dates. Chemical poisoning is the primary cause for catalyst malfunction. This is usually caused by fuel contaminants that could be avoided through improved fuels and processes. Understanding all of the aging effects on the ATS is vital to achieving the goal of technology with a useful life of up to 1 million miles [3, 4].

CARB has proposed a program called Real Emissions Assessment Logging or REAL. REAL aims to utilize onboard data loggers to monitor compliance and enforce emissions regulations. They are investigating the feasibility of using NOx sensors to monitor and determine emissions compliance. NOx sensor data could be logged for future inspection or monitored in "real" time to detect emissions compliance issues [3].

The reduction of NOx and PM emissions, ensuring the reduction of emissions through real-time monitoring, and advanced testing capabilities that are reflective of actual "real-world" situations are the overall goals of the EPA and CARB [3, 4].

1.2 Goals and Objectives

The goal of this research is to acquire experimental data on the dCSC™ device, characterize the device's performance, and calibrate a high-fidelity 2D flow through model. This model would aid in the development of the ULN ATS and the overall goals the EPA and CARB. To achieve these goals, an engine test cell and test procedure had to be developed as well as a statistical test matrix. Determining the correct test cell instrumentation to acquire the data for the model was also needed. The specific objectives developed to achieve the research goals are as follows:

1. Perform a literature study on the dCSC™, and other PNAs, related to experimental studies, in order to develop a set of objectives to achieve from the dCSC™ experimental data.
2. Determine the experimental data needed in order to calibrate the high-fidelity 2D flow through model to simulate the Johnson Matthey Cold Start Concept (dCSC™).
3. Develop the engine test cell setup to perform experimental research on the dCSC™.
4. Develop experimental testing procedures and a statistical test matrix.
5. Quantify the NO, NO_2, and NOx storage performance of the dCSC™ at temperatures from 80°C to 250°C during the cold start period and NOx release performance at temperatures from 200°C to 450°C.
6. Quantify the portion of the stored NO, NO_2, and NOx that is converted and the portion that remains stored during the warm-up period.
7. Quantify the oxidation characteristics of the dCSC™ during the experimental testing.

1.3 Thesis Outline

This chapter gives background on the motivation for the research herein. The National Ambient Air Quality Standards (NAAQS) drive the CARB/EPA vehicle and engine emission standards for medium and heavy-duty diesel emissions. These standards drive research to be conducted and options to be explored. This research was to better understand the dCSC™ performance during storage and release experiments.

Chapter 2 is a literature review on the dCSC™, related experimental studies, and similar technologies. These technologies are all directed towards meeting future Ultra-Low NOx standards.

Chapter 3 is an overview of the test cell setup: engine, dynamometer, instrumentation, emissions analyzers, and the methodology used to process the data. Also described is the

experimental test procedure developed to achieve the research goals, as well as the experimental test matrix. A test procedure was developed for varying engine conditions, steady-state dCSC™ temperatures, and temperature ramp rates.

Chapter 4 covers the results and the Summary/Conclusions from the experimental data. A more extensive description of the instrumentation and the data analysis calculations, time plots, control plots, and other data acquired can be found in Appendices A-H.

2 Literature Review

2.1 Ultra-Low NOx Aftertreatment Systems

EPA and CARB are planning to reduce NOx from medium and heavy-duty diesel engines in model years 2024 and 2027 [3, 4]. The ULN standard for 2027 has not been set, but could potentially be a 90% reduction from the current 0.2 to 0.02 gNOx/bhp-hr on the FTP cycle. A study performed by SwRI achieved 0.034 gNOx/bhp-hr over the FTP cycle on a 2014 MY 13.0L Volvo diesel engine [3]. Engine hardware changes to aide ATS thermal management and strategic control of ATS thermal management would improve the results of the reference [5]. Figure 2.1 shows the ULN ATS used on the engine at SwRI to achieve the 0.034 gNOx/bhp-hr on the FTP cycle. The system features a PNA at the outlet of the engine exhaust.
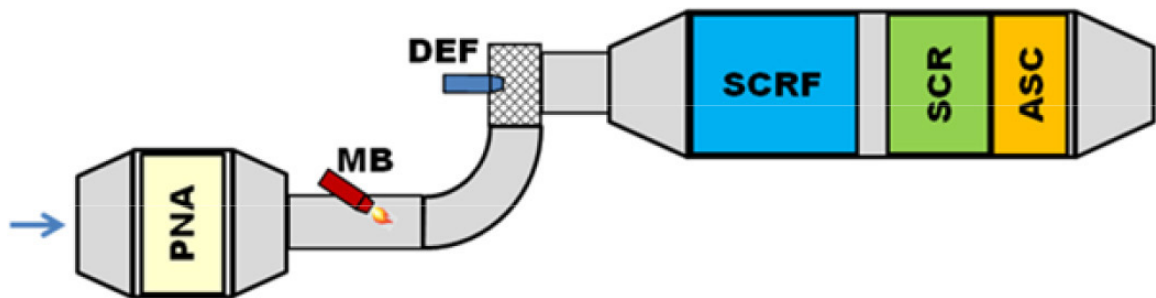
Figure 2.1 ULN ATS used on a Volvo MY 13.0L Diesel Engine at SwRI [5]

The PNA in Figure 2.1 is followed by a diesel fueled mini-burner, DEF injector, SCR-F, SCR, and an ammonia slip catalyst (ASC). The diesel-fueled mini-burner was used as supplemental heat to achieve an SCR-F inlet temperature of 250-350°C [13]. The ASC compensates for slip of NH_3 from the SCR, leading to NH_3 emissions at the tailpipe. The ASC oxidizes NH_3 slip from the SCR into N_2 [14]. The PNA adsorbs NOx, CO, and HC at low temperatures while the diesel-fueled mini-burner heats the rest of the ATS to its operating temperature (250-350 °C) [13]. Once the SCR is at its operating temperature, it can reduce the NOx in the exhaust gas [15]. The ability of the PNA to store emissions is finite. Therefore, the mini-burner must heat the SCR to its operating temperature (250-

9

350 °C) before the PNA reaches its storage capacity. Instead of needing a separate DOC, the PNA serves as the DOC for the system as well. The PNA replaces the DOC with no added thermal mass to the ATS. This is the general architecture of the ULN ATS used at SwRI to conduct the ULN feasibility study on behalf of CARB and the EPA [5].

Another ULN ATS architecture being evaluated, shown in Figure 1.1, is to have a close-coupled SCR (ccSCR) or a LO-SCR in front of the PNA in Figure 2.1. Positioning this SCR in front of all of the other ATS components and as close to the engine as possible will allow it to heat up quickly. It would not reduce NOx at its highest efficiency, but the amount of NOx it does reduce would reduce the workload of the PNA to store NOx during cold start. The LO-SCR would also supplement the ATS during hard acceleration events where a spike in tailpipe NOx emissions is possible [16]. Multiple SCR's within the system would require complex dosing system with the ability to dose at low temperatures. Therefore, the dosing system must be externally heated so that it can effectively deliver DEF to the ATS [16].

Cold start is not the only operation in which NOx emissions must be reduced. The development of the Low Load Cycle (LLC) will test the ULN ATS systems efficiency during low speed and load medium and heavy-duty diesel engine operation. Therefore, it is important that the ATS reaches operating temperature quickly, but also stays at operating temperature (above 200 °C). This will be achieved through properly packaging, positioning, and insulating the ATS to reduce thermal losses [16].

2.2   PNA Fundamentals

NOx storage or adsorption is a viable strategy for controlling cold start NOx emissions by using PNA technology that can adsorb NOx emissions at temperatures below 200 °C. Common PNA formulations include ceria/alumina-supported Pd/Pt and zeolite supported Pd. Ceria/alumina-supported and zeolite supported Pd allows the PNA to store NOx at temperatures below 200 °C as opposed to the alkaline earth oxide that is used on Lean NOx Trap's. Zeolite supported Pd formulations have superior resistance to sulfur and HC

10

poisoning over the ceria/alumina and alkaline earth oxide Pd/Pt [17]. In addition to adsorption of NOx the Pd zeolite's serve as an HC trap as well. The combination of an HC trap and NOx adsorber, and good resistance to Sulphur and HC poisoning, makes the zeolite Pd PNA catalyst the best current option for cold start emissions control [1, 8, 17, 18].

Figure 2.2 illustrates NO adsorption on a PNA catalyst, from a flow reactor study at the University of Houston [19]. The gas mixture to the reactor was 80 °C and contained 400 ppm NO, 2% O_2, balance Ar. The gas mixture was comprised of all NO and no NO_2 because diesel engine outlet NOx is 90-95% NO. The catalyst was fed with the gas for 5 minutes and the downstream NO, NO_2, and NOx concentrations were measured. There is 400 ppm NO at the catalyst inlet, therefore a measurement less than 400 ppm of total NOx at the catalyst outlet indicates NO storage or adsorption. The x-axis shows test time in seconds and the y-axis shows downstream PNA NO, NO_2, and NOx concentrations in ppm. The downstream PNA NOx concentrations are much lower than 400 ppm during the first 100 seconds. Indicating during the first 100 seconds, a large amount of NO is being adsorbed. During the 100 to 300 second time, the downstream PNA NO and NOx concentrations are over 350 ppm which is less than 50 ppm lower than the 400 ppm at the PNA inlet. During these 200 seconds the PNA reaches its NOx adsorption/storage capacity. There is a constant 0 ppm NO_2 concentration at the PNA outlet for the duration of the adsorption process that is occurring. The inlet gas temperature, 80 °C, is too low for the PNA to oxidize NO to NO_2. Therefore, 0% of the upstream NO is oxidized to NO_2 [19].
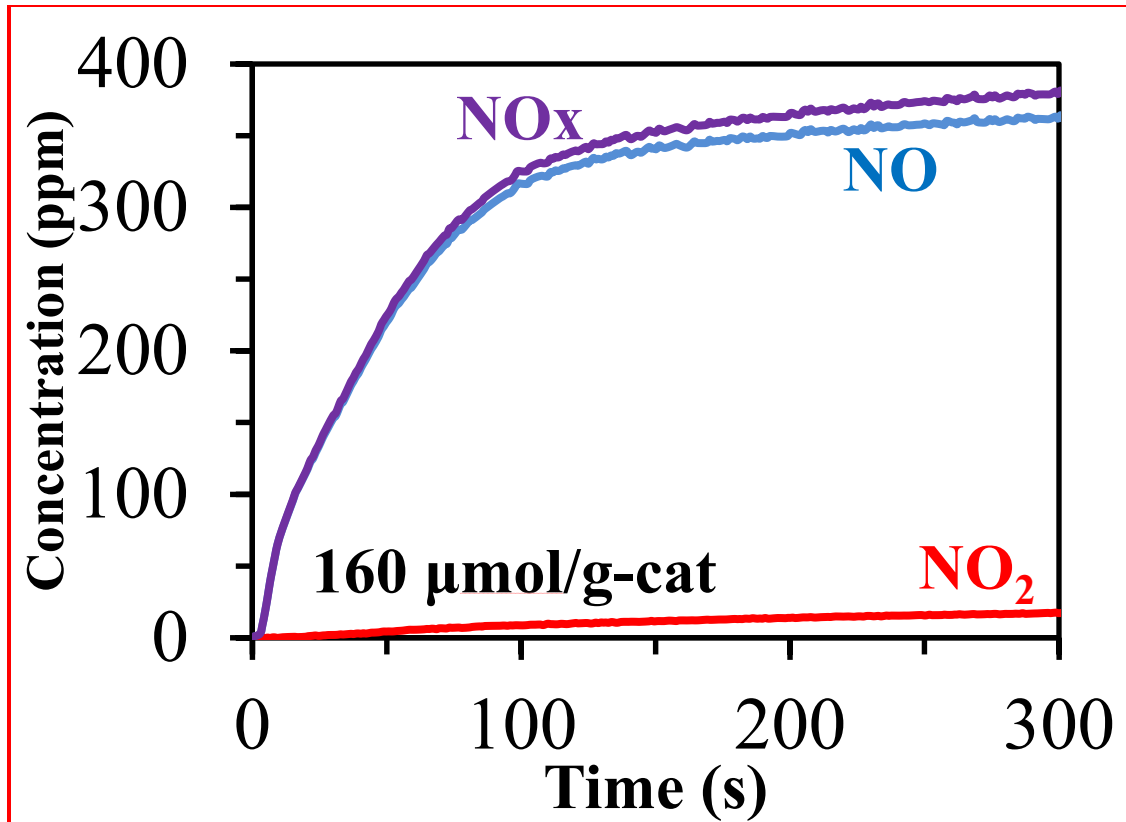
Figure 2.2 NO Adsorption Profile [19]

A NOx desorption profile from the same study, is shown in Figure 2.3. The x-axis shows feed gas temperature in °C and the y-axis shows downstream PNA NO, NO_2, and NOx concentrations in ppm. The y-axis starts at 0 ppm, to properly compare the NO, NO_2, and NOx desorption profiles. In Figure 2.3 the PNA is being fed with the same feed gas as Figure 2.2 except for the 400 ppm NO. In this figure, the PNA has reached its NOx peak storage capacity at 80 °C from the adsorption event in Figure 2.2. The temperature of the feed gas is increasing at a rate of 20 °C per minute from 80 to 500 °C. As the feed gas temperature increases, the downstream PNA NO, NO_2, and NOx concentrations increase. The PNA inlet NO concentration is not increasing and the outlet concentration is increasing indicating NOx is being desorbed from the PNA. The downstream PNA NOx concentration reaches a peak as the feed gas temperature reaches 150 °C. The PNA continues to release NOx until the feed gas temperature reaches 250°C. The presence of NO_2 downstream of the PNA indicates the PNA is oxidizing NO to NO_2. The d_{200} = 52%

12

in the top right corner of Figure 2.3 indicates that by the time the feed gas temperature reached 200 °C, 52% of the adsorbed NOx had been desorbed.
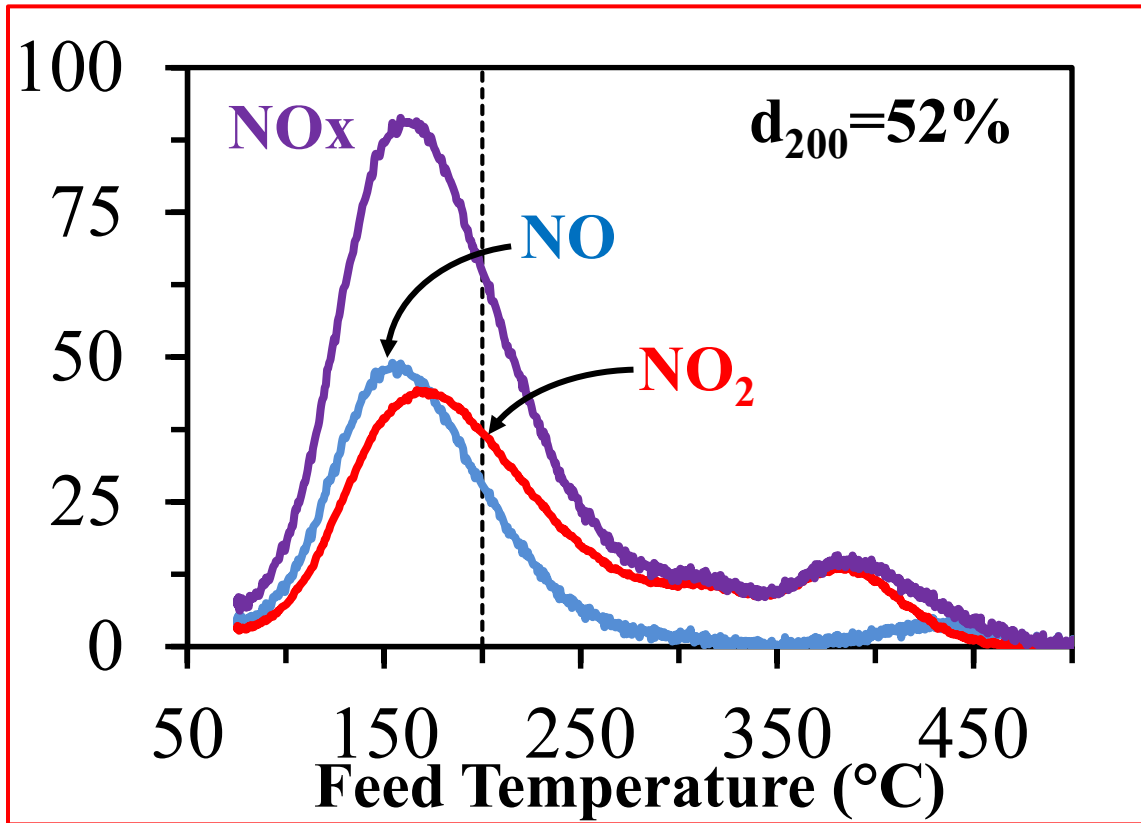
Figure 2.3 NOx Desorption Profile [19]

Similar profiles are observed for the storage and release of other exhaust gas constituents: such as CO and HC. The presence of H_2O in the exhaust gas can inhibit the ability of the PNA to adsorb HC and NOx. The presence of CO in exhaust gas can mitigate this inhibition [20].

The same experiment as Figure 2.2 was conducted three times in Figure 2.4. Of those three experiments, two were conducted with the addition of 5% H_2O in the feed gas and one was conducted with no H_2O in the feed gas. Of those two experiments containing 5% H_2O in the feed gas, one was "oxytreated" beforehand. The "oxytreatment" consists of a 10% O_2 balance Ar feed gas to the reactor at 750°C for two hours. The data in Figure 2.4

illustrates the inhibition of water on NOx adsorption by comparing the PNA NOx adsorption profiles from the three experiments [19].
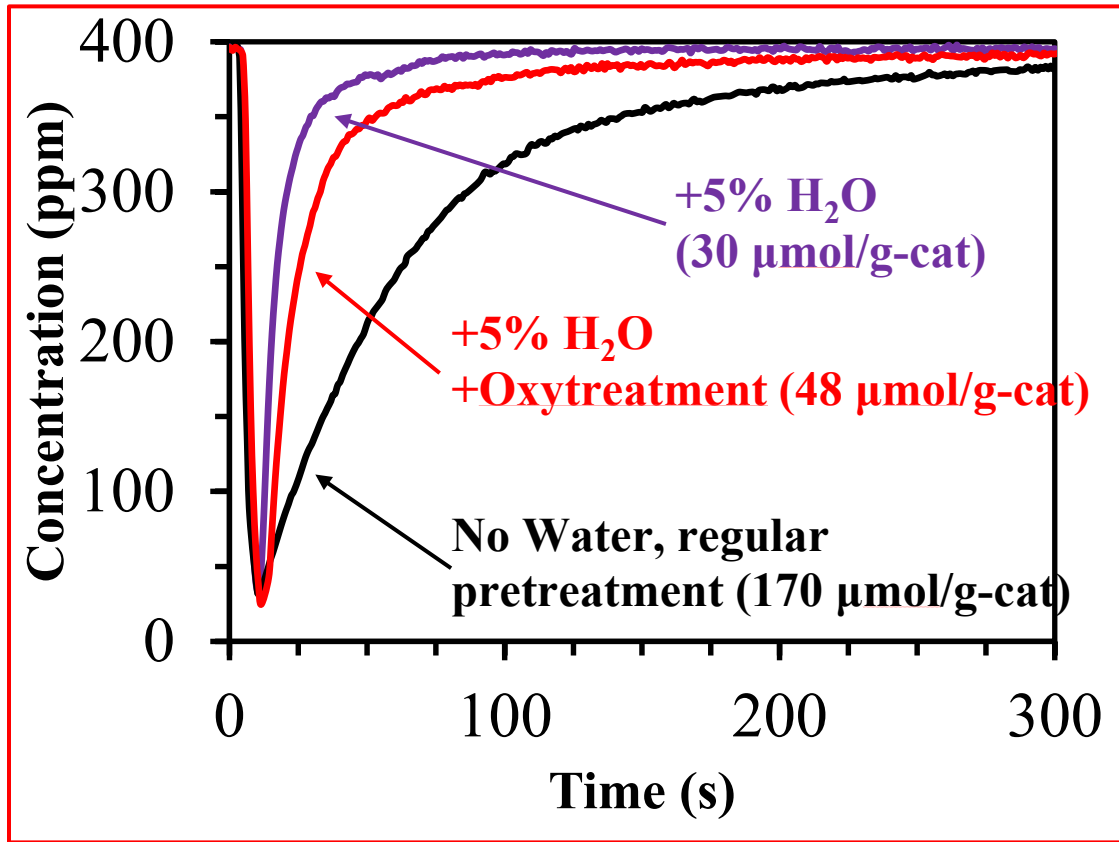
Figure 2.4 H$_2$O Effects on NOx Storage Capacity [19]

The y-axis shows NOx concentration in ppm and the x-axis shows time, in seconds. The addition of water in the exhaust will inhibit the PNA's ability to store NOx. Therefore, higher NOx concentrations will be observed sooner at the PNA outlet with increasing H$_2$O concentrations. The oxytreatment attempts to reduce this water inhibition. At the 50 second time, the NO concentration downstream of the PNA with no H$_2$O in the feed gas and no oxytreatment was 200 ppm. The NO concentration downstream of the PNA that was fed with feed gas containing 5% H$_2$O and no oxytreatment was 375 ppm at the 50 second time. The NO concentration downstream of the PNA that was oxytreated and fed with feed gas containing H$_2$O was 345 ppm. Therefore, the "oxytreated" experiment, containing 5% H$_2$O in the feed gas, experienced less NOx storage inhibition than the

14

experiment containing the 5% H_2O without oxytreatment. Therefore, it can be deduced that the oxytreatment reduced the inhibition effect of H_2O in the feed gas. In both the oxytreated and non oxytreated case, the 5% H_2O present in the feed gas caused the downstream PNA NO concentration to increase more rapidly than the experiment with no H_2O.

2.3 PNA, DOC, and Cold Start Concept Catalyst Performance

The Johnson Matthey Diesel Cold Start Concept (dCSC™), is a PNA with HC trapping ability on an oxidation catalyst [1, 8]. In reference [1], the dCSC™ was compared to a separate DOC and PNA to show the advantages of the dCSC™ which has coupling of DOC and PNA technologies [1].

The dCSC™, DOC, and PNA were exposed to 5% H_2O, balance air, at 750 °C, for 16 hours. The substrates were then fed gas containing 10% O_2, 5% CO_2, 5% H_2O, balance N_2 at 650 °C to clean the substrates of any stored emissions. All three substrates were then cooled to a temperature of 80 °C with the same feed gas composition. Once the substrates reached a steady state temperature of 80 °C, 200 ppm NO, 200 ppm CO, and 500 ppm decane (on a C_1 basis) was added to the feed gas for 100 seconds. At the conclusion of the 100 seconds, the temperature of the feed gas was increased from 80 to 650 °C at a rate of 100 °C per minute [1].

During this experiment, CO concentrations were measured downstream of the dCSC™, PNA, and DOC. Figure 2.5 shows the CO oxidation comparison between the dCSC™, DOC, and PNA. The dCSC™ is referred to in the plot legend as the CSC. At the 50 second point in the experiment, the downstream dCSC™ and PNA CO concentrations are around 50 ppm and the downstream DOC CO concentration is around 175 ppm. The amount of PGM on each substrate effects the CO oxidation capabilities of each substrate [1]. The PNA and dCSC™ contain a significantly higher amount of PGM than the DOC substrate. This is why the CO oxidation of the PNA and dCSC™ is greater than the DOC.

100 seconds into the experiment, the feed gas starts its temperature ramp from 80 to 650 °C. As soon as the feed gas temperature starts increasing, the downstream PNA and dCSC™ CO concentrations start decreasing. Both downstream PNA and dCSC™ CO concentrations reach 0 ppm before the feed gas temperature reaches 140 °C. The downstream DOC CO concentration does not start decreasing until the feed gas temperature reaches 140 °C and reaches 0 ppm once the feed gas temperature reaches 200 °C [1].
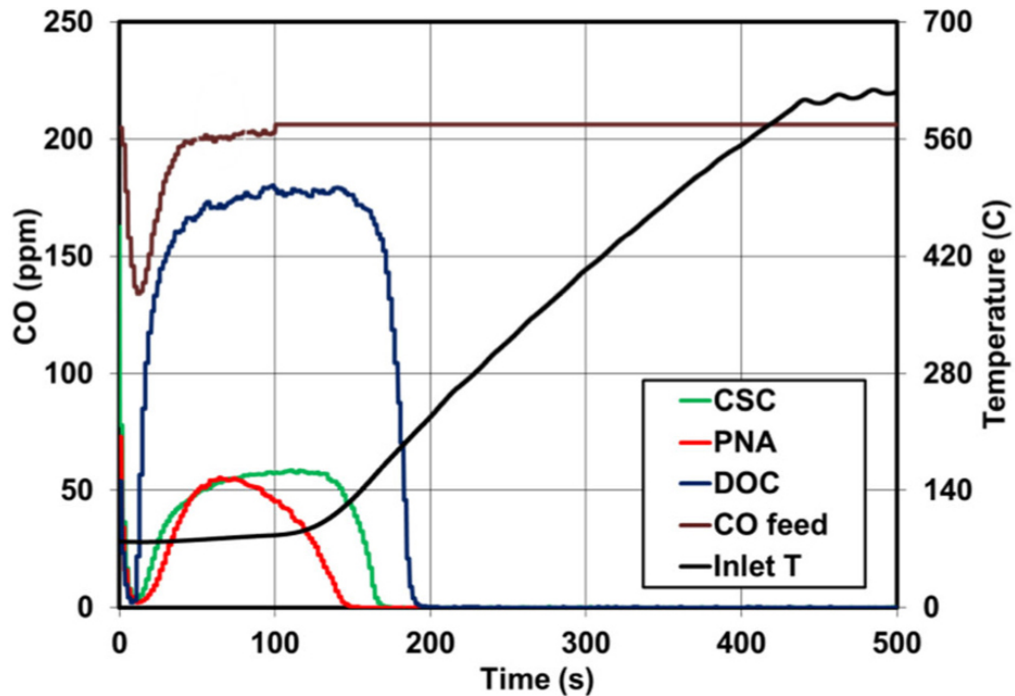
Figure 2.5 Downstream DOC, PNA, and dCSC™ CO Concentrations vs. Time and Temperature [1]

The dCSC™ and PNA show significantly higher CO oxidation than the DOC [1]. During the same experiment as Figure 2.5, downstream dCSC™, DOC, and PNA HC concentrations were measured. Figure 2.6 shows the HC concentrations downstream of the substrates. From time 0 to 100 seconds, the downstream HC concentrations of all three substrates are less than 50 ppmC (on C_1 basis), while the upstream HC concentration is 500 ppmC. Therefore, all three substrates show significant HC adsorption per reference [1].

16

At the 100 second point, the inlet gas temperature starts increasing from 80 to 650 °C. When the inlet gas temperature reaches 150 °C, the downstream DOC and PNA HC concentrations begin to increase indicating desorption of HC. The downstream dCSC™ HC concentration does not start increasing until the inlet gas temperature reaches 200 °C. At 220 °C inlet gas temperature of all three downstream substrate temperatures peak. The downstream PNA concentration peaks highest at 120 ppmC, the downstream DOC HC concentration peaks at 100 ppmC, and the downstream dCSC™ HC concentration peaks at slightly over 50 ppmC. The peak downstream dCSC™ HC concentration is less than half of the peak downstream DOC and PNA HC concentrations. This shows that the dCSC™ more effectively converts the stored HC than the DOC and PNA substrates. Once the inlet gas temperature reaches above 250 °C, all three substrates show 100% HC oxidation efficiency [1].
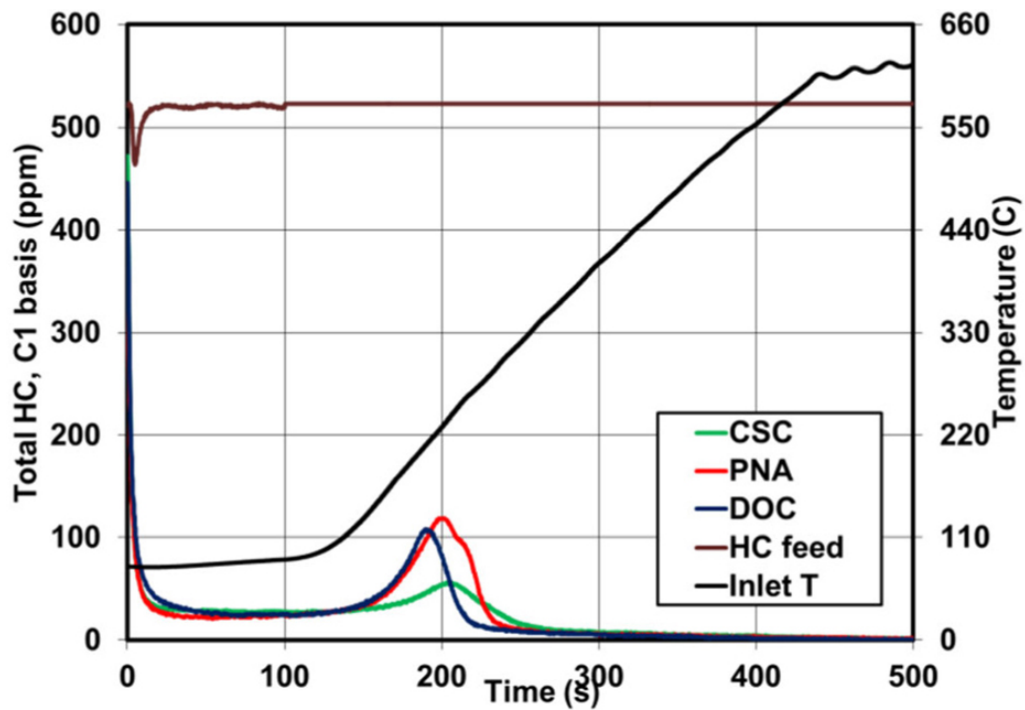
Figure 2.6 Downstream DOC, PNA, and dCSC™ HC Concentrations vs. Time and Temperature [1]

It was determined during further testing in reference [8] that during the temperature ramp in Figures 2.5 and 2.6 that N_2O is produced due to the HC lean NOx reductions

17

occurring. Peak downstream substrate N_2O concentrations observed were 126, 74, and 30 ppm for the DOC, PNA, and dCSC™ substrates, respectively [8].

An additional experiment was run in reference [1] to characterize steady state NO to NO_2 oxidation activity of the DOC and dCSC™. Figure 2.7 shows the steady state NO_2/NOx ratio downstream of the DOC and dCSC™ substrates vs. temperature. The same feed gas containing 200 ppm NO, 200 ppm CO, 500 ppmC decane (C_1 basis), 10% O_2, 5% CO_2, 5% H_2O, balance N_2 was fed to the DOC and dCSC™ at temperatures from 200 to 550 °C, in 50 °C intervals. The gases were fed to the DOC and dCSC™ substrates for 30 minutes to ensure steady state NO to NO_2 oxidation was occurring [1].

The dCSC™ substrate shows slightly less NO to NO_2 oxidation than the DOC. Both the dCSC™ and DOC have peak NO_2/NOx oxidation performance at a substrate temperature of 300°C. At 300 °C the dCSC™ converts 45% of the upstream NO to NO_2 and the DOC converts 55%. The NO oxidation of both is substantial from 250°C to 350°C. At substrate temperatures lower than 250 °C and higher than 350°C the NO oxidation decreases significantly [1].
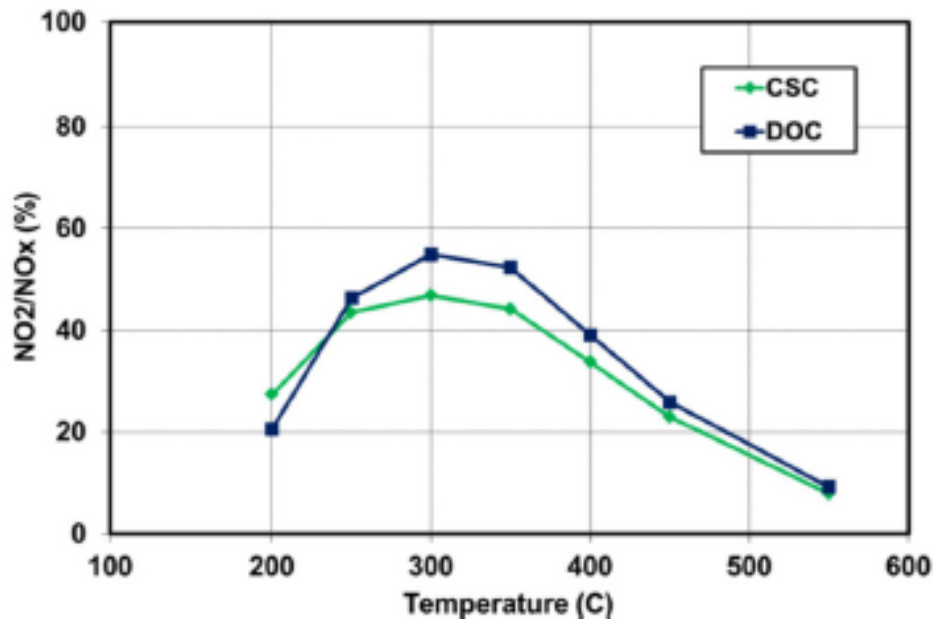
Figure 2.7 Downstream dCSC™ and DOC NO_2/NOx Ratio vs. Temperature [1].

18

Figure 2.8 shows the 200-second NOx storage capacity of the Johnson Matthey Diesel Cold Start Concept (dCSC™) [8]. In addition to the experiments above, experiments were performed in reference [8] to quantify the NOx storage capability of the dCSC™. In reference [8], multiple cold start concept substrates containing PNA catalyst with HC trapping ability and an oxidation catalyst were prepared. All of the experiments took place in a laboratory reactor. First, the substrates were hydrothermally aged at 650 °C for 2 hours with various feed gas compositions to reflect different air-to-fuel ratios.

NOx adsorption experiments were performed with feed gas mixtures comprised to emulate exhaust gas from a diesel engine during cold start. The substrates were preheated to 500 °C in feed gas of 10% O_2, 5% CO_2, 5% H_2O, and a balance of N_2. The substrates were held at 500 °C to ensure desorption of any emissions from all of the active NO storage sites on the catalysts. The substrates were then cooled to low temperatures ranging from 80 to 250°C with the same feed gas composition. Once the substrates reached the temperature setpoint for the certain test, 200 ppm NO, 200 ppm CO, and 500 ppmC decane (on a C_1 basis) was added to the feed gas. The substrates were fed with this gas from 10 minutes to ensure complete saturation of all of the available NOx storage sites [8].

The NOx storage capacity of the substrates at temperatures of 80 to 250°C is characterized in Figure 2.8. The optimal temperature of the substrates to store NOx emissions is observed from 125 to 175°C where the NOx storage capacity peaks [8]. The storage capacity falls off from 125 to 80 °C. As feed gas temperature decreases from 125 to 80 °C, H_2O presence in the feed gas increases, this presence of water inhibits the NO storage sites from storing the NO in the feed gas. Storage capacity also decreases as temperature increases from 200 to 250°C. This is due to the NO storage sites becoming unstable above 200 °C [8].

19
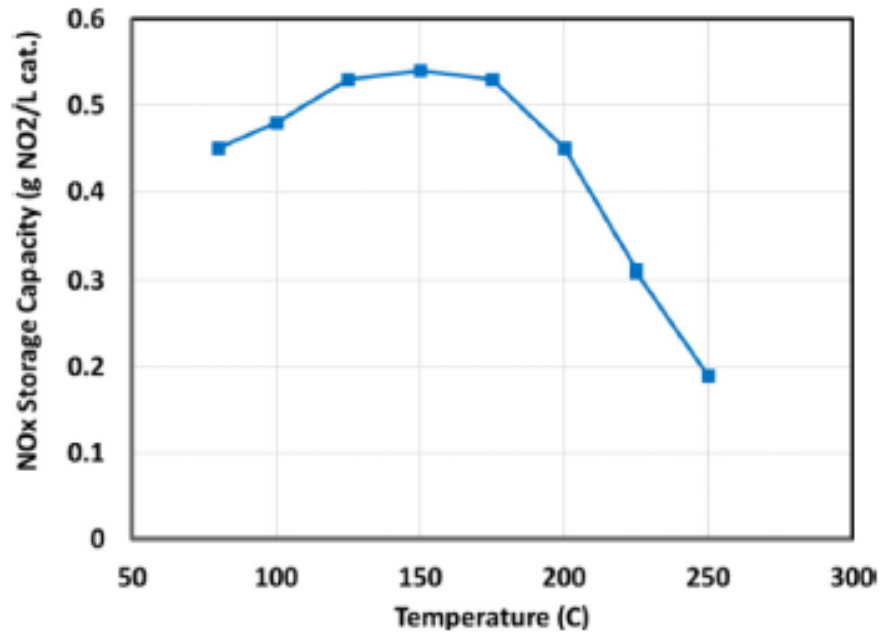
Figure 2.8 200-Second dCSC™ NOx Storage Capacity vs. Temperature [8]

2.4 Summary

The dCSC™ device would integrate into the ULN ATS in Figure 2.1 as the PNA. Followed by an external heat source of some sort, to reduce the time the SCR and the rest of the ATS needs to reach operating temperature [11, 16]. The goal of the system is to meet ULN regulations for medium and heavy-duty diesel engines for 2024, 2026, and subsequent MY's. The EPA and CARB also plan for regulations over time to include emissions compliance for all use-cases, extended warranty requirements, accurate useful life determinations, and real time emissions logging capabilities [3].

Research has consisted of laboratory reactor studies on various substrates [1, 8, 19, 16], engine dynamometer studies on ULN ATS architectures [5, 13], engine hardware and calibration changes, [5, 16, 12], the development of new test cycles [7], and additional research studies to evaluate the feasibility and methods for achieving regulations laid out in reference [3].

20

The goal of this research is to acquire experimental data on the dCSC™ device, characterize the device's performance, and use the data to calibrate a high-fidelity 2D flow through model of the dCSC™. The model will be able to accurately predict outlet dCSC™ species concentrations, 2D temperature distributions, delta pressure, etc. This may be the first model of the dCSC™ and it will be very useful for the development of the ULN ATS, aiding the efforts being made by the EPA, CARB, and companies that need to meet future regulations.

3 Experimental Setup and Procedures

The experimental set-up was developed in order to carry out the experiments to gather the data needed to meet the objectives outlined in the Introduction. The test procedures and the experiments were then designed to get the data needed for the dCSC™ model and to determine the effect of the various variables on the storage, release, and oxidation of NO, NO_2, CO, and N_2O. The calculation procedures and equations used for analyzing the experimental data are also explained.

3.1 Experimental Setup

This section covers the general test cell layout, engine and dynamometer, fuel properties, exhaust heater, and ATS. The purpose of this section is to give background information on the experimental setup, engine, fuel properties, electric heater capability, and the aftertreatment system components.

3.1.1 Test Cell Layout

Figure 3.1 shows the layout of the Michigan Tech diesel engine aftertreatment test cell which was specifically modified to perform the dCSC™ research. Additions to the test cell included the Thermo Fisher 46i N_2O analyzer, a Cambustion fNOx400 NOx analyzer, and a Cambustion HFR 400 Fast FID total hydrocarbon analyzer. The ambient air inlet and valve B were also added.
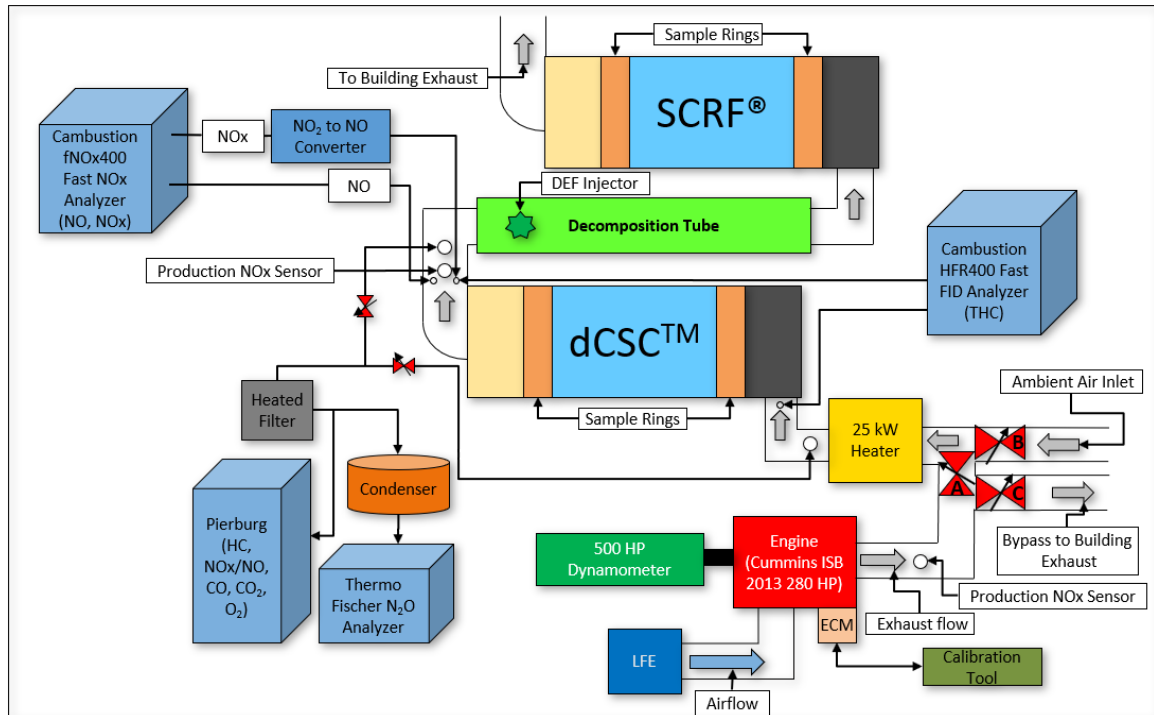
Figure 3.1 Test Cell Layout

The 2013 6.7L 6-cylinder Cummins ISB engine is coupled to a 500 HP dynamometer. The engine is controlled by the Calterm calibration tool provided by Cummins. A laminar flow element accurately measures the mass flow rate of air into the engine. A 25-kW heater from Watlow is in-line to control exhaust temperature to desired setpoints. See Appendix A for additional information on the exhaust heater. There are two NOx sensors in the ATS. One sensor measures the engine outlet NOx concentrations and the other measures downstream dCSC™ NOx concentrations. See Appendix B for additional information on the NOx sensors. The Pierburg 5-gas analyzer and N_2O analyzer can measure emissions upstream or downstream of the dCSC™. Appendices B.1 and B.4 have additional information on the Pierburg 5-gas bench and Thermo Fisher N_2O analyzer, respectively. Two fast response analyzers from Cambustion are part of the instrumentation. One of the analyzers measures NO and NOx and the other measures HC. For more information on the Cambustion analyzers see Appendices B.2 and B.3. Each Cambustion analyzer has two channels, one upstream and one downstream of the dCSC™. There is a DEF injector downstream of the dCSC™ and upstream of the

23

SCRF®. The SCRF® is a Selective Catalytic Reduction catalyst on a Diesel Particulate Filter (DPF).

3.1.2 Engine and Dynamometer

As stated earlier, a 2013 6.7L inline 6-cylinder Cummins ISB engine, rated for 280 HP at 2400 rpm, was used to conduct the experimental testing. A list of engine specifications is shown in Table 3.1. The engine is coupled to a Dynamatic water-cooled eddy current dynamometer rated for 500 HP from 1700-7000 rpm. The dyno controls engine speed through a Digalog dynamometer controller.

Table 3.1 Engine Specifications

Model	Cummins ISB
MY	2013
Displacement	6.7 L, 408 in^3
Cylinders	6
Aspiration	Holset Variable Geometry Turbocharger
Bore & Stroke	107 x 124 mm
EGR System	Electronically controlled and cooled
CR	17.3 : 1
Firing Order	1-5-3-6-2-4
Fuel System	High pressure common rail, Bosch DI
Rated power and speed	280 HP at 2400 rpm
Rated torque and speed	660 lb-ft at 1600 rpm

3.1.3 Fuel Properties

A batch of summer blend #2 ultra-low sulfur diesel (ULSD #2) was purchased and stored at Krans Oil in Lake Linden for the dCSC™ testing. A fuel sample was sent to Paragon Laboratories in Livonia, Michigan for analysis and the results are shown in Table 3.2. For the complete analysis results from Paragon see Appendix C.

24

Table 3.2 ULSD #2 Fuel Properties used in Engine

Fuel Type	ULSD #2
Carbon (Wt%)	86.55%
Hydrogen (Wt%)	13.45%
API Gravity at 15.56 °C	34.5 °API
Density at 15.56 °C	0.8516 g/mL
Specific Gravity at 15.56 °C	0.8524
LHV	19669 BTU/lb 45.749
NLHV	18442 BTU/lb 42.895
Cetane	51.7
Air to Fuel Ratio (CH-based)	14.58
Hydrogen to Carbon Atomic Ratio	1.852

3.1.4 Exhaust Heater

A 25-kW heater was used to control exhaust gas temperatures to the desired setpoints for the dCSC™ testing. The heater and the heater controller were manufactured by Watlow. Controller PID's were tuned to eliminate temperature oscillations and they ensure temperature setpoint accuracy. Additional details on the exhaust heater and heater PID tuning are in Appendix A.

3.1.5 Aftertreatment System

The ATS consists of a Johnson Matthey dCSC™ upstream of an SCRF® previously used to conduct research at MTU [21, 22]. The dCSC™ was degreened before the experimental testing began. The dCSC™ was degreened by running the engine at 1660 rpm, 550 N-m, and with 32 mg/stroke of late fuel injection. The 25-kW heater was set to 700°C and the dCSC™ was held at temperatures between 650 and 700°C for 2 hours. This was done to emulate the hydrothermal aging done on the cold start concept technology testing in [1, 8]. The dCSC™ substrate specifications are shown in Table 3.3.

Table 3.3 dCSC™ Substrate Specifications

Material	Cordierite
Diameter (inch)	10.5
Length (inch)	6
Cell Geometry	Square
Total Volume (L)	8.51
Open Volume (L)*	7.72
Cell Density /in^2	400
Cell Width (in)	0.046
Open Frontal Area (in^2)	78.5
Channel Wall Thickness (in)	0.004
Wall Density (g/cm^3)	1.2
Porosity (%)	35
Number of Inlet Cells	31,415

*Total Volume minus No Flow Zone

3.2 Instrumentation

This section introduces the instrumentation used to record the data needed to meet the research objectives. Numerous thermocouples, pressure transducers, emission analyzers, and DAQ systems were utilized to gather the data needed.

3.2.1 Temperature Measurement

The dCSC™ substrate is instrumented with 32 thermocouples. These thermocouples are 16-inch Omega K-type MQSS series thermocouples with a 304 stainless steel sheath. The temperature data are used to monitor the 2D temperature distribution during testing. Figure 3.2 shows the location of each thermocouple in the dCSC™.

26
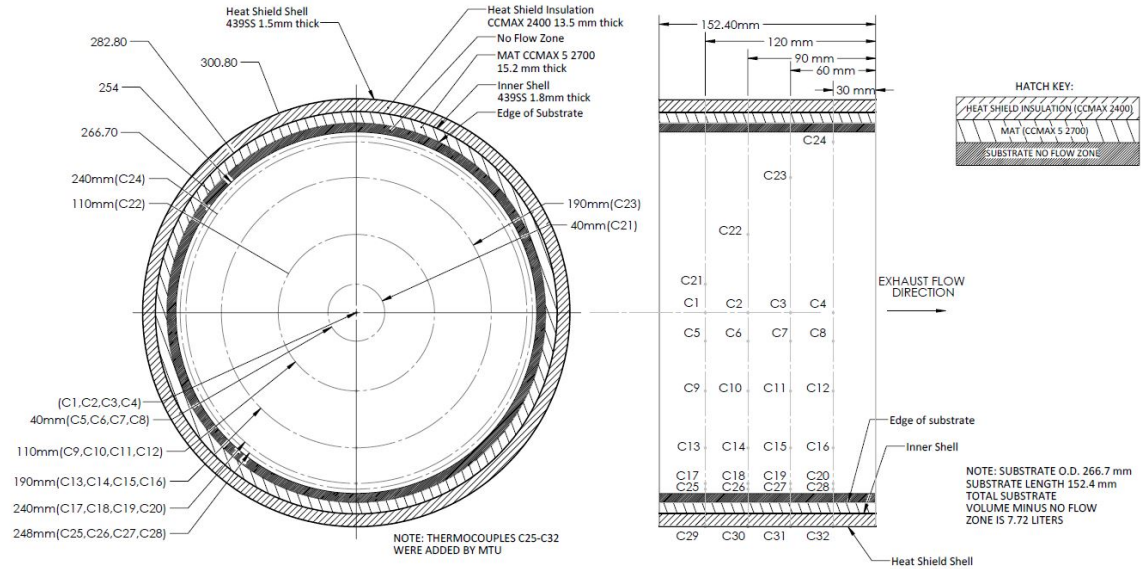
Figure 3.2 dCSC™ Thermocouple Layout

3.2.2 Pressure Measurement

Intake air flow is monitored by an engine intake manifold pressure sensor and a laminar flow device upstream of the intake manifold. The laminar flow device's delta pressure is monitored with an Omega high accuracy oil-filled pressure transducer. The dCSC™ delta pressure is monitored with a similar transducer.

3.2.3 Emission Analyzers

Exhaust gas constituents are measured by a number of analyzers. A 5-gas analyzer from Pierburg measures O_2, CO_2, CO, NOx, and total hydrocarbons. However, the sampling system is not conducive to measuring hydrocarbons; the sample lines are too long and the hydrocarbons get adsorbed on the sample lines. N_2O concentrations in the exhaust gas are measured by a Thermo Fisher 46i N_2O analyzer. Both the Pierburg 5-gas bench and Thermo Fisher N_2O analyzer are setup to measure either upstream or downstream dCSC™ NOx concentrations. This is done by opening a pneumatic valve to either the upstream or downstream sample site and closing the other. There are two production NOx sensors in the system to measure engine out and downstream dCSC™ NOx

27

concentrations. A Cambustion fNOx400 CLD is used to measure downstream dCSC™ NOx and NO concentrations. One of the fNOx400 channels was converted from NO measurement to NOx measurement. See Appendix B for additional details on all of the emission analyzers.

3.2.4   Data Acquisition Modules

National instruments NICDAQ modules are used to log temperatures, pressures, flow rates, Cambustion fNOx400 NOx concentrations, and numerous other signals. NI LabVIEW is used to monitor and log these signals as well as control the sampling system for the Pierburg 5-gas bench and the Thermo Fisher 46i N_2O analyzer. Electronic solenoids, controlled in LabVIEW, allow compressed air to open one-way valves to either an upstream or downstream dCSC™ sampling system, for these two analyzers.

3.3   Test Procedures and Experimental Conditions

This section lays out specific test procedures that were developed to conduct the experiments and the test conditions for those experiments. The procedures were developed by running test experiments before starting the research testing. During the test experiments, heater PID controls were tuned, engine controls were calibrated, and the overall setup was refined.

3.3.1   Test Procedure

Figure 3.3 shows engine load, engine speed, turbine outlet temperature, and the temperature of the thermocouple at the front and middle of the dCSC™ substrate (C1 Thermocouple), during a test. The Phases of every test are illustrated in Figure 3.3 as well.
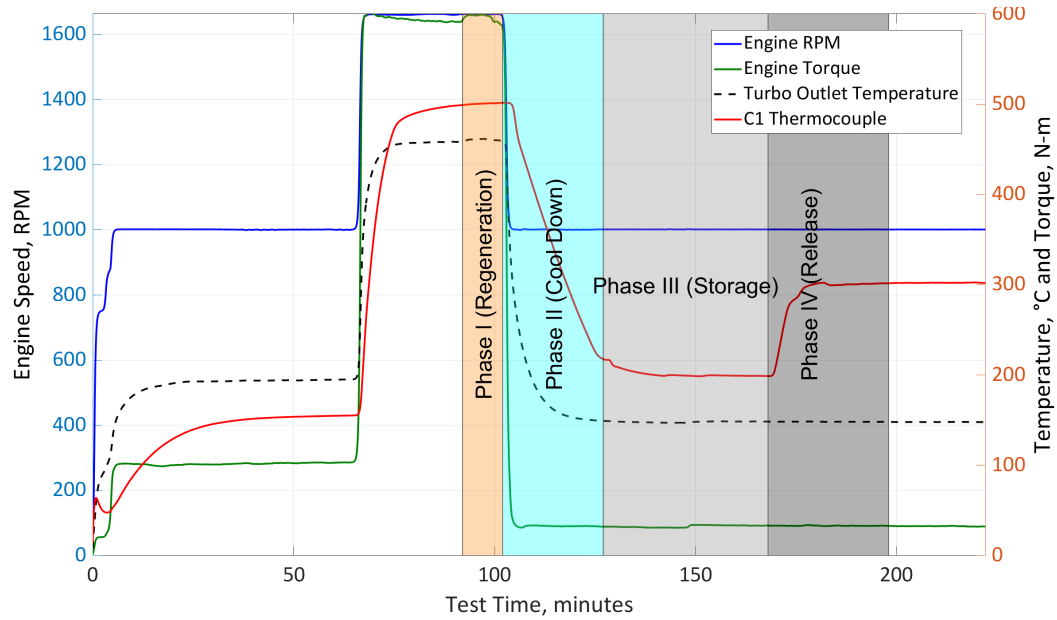
Figure 3.3 dCSC™ Control Test

Prior to Phase I of the test, the engine is warmed up to a steady state coolant temperature. This ensures the engine-out emissions will be constant during Phases III and IV.

Phase I of the test, is called regeneration. During this Phase, the engine is set to 1660 rpm and 600 N-m and exhaust is routed to the aftertreatment system. With the aid of the heater, the dCSC™ will reach 500 °C and will be kept at that temperature for 10 minutes to clean the surface of the substrate and ensure the release of all emissions from the substrate [1, 8, 19]. When the 10 minutes is over, the exhaust is routed directly to the building exhaust and Phase II begins.

During Phase II (Cool Down) the building exhaust is allowed to pull ambient air through the heater to the aftertreatment system. This allows the temperature of the aftertreatment system to be controlled by the heater to the desired temperature for Phase III. During Phase II the engine is also set to the desired condition for the test. The engine will remain at this condition for the remainder of the test. Once the dCSC™ is controlled to the desired temperature for Phase III (Storage), the ambient air inlet to the aftertreatment

29

system is sealed off. Once the ambient air inlet is sealed off, the exhaust flow is routed to the aftertreatment system. At this time, Phase III (Storage) begins.

Phase III (Storage) is the portion of the test where dCSC™ emissions storage capacity is calculated. The dCSC™ is controlled to a desired constant temperature for Phase III by the 25-kW heater heating exhaust gas upstream of the dCSC™. The Pierburg 5-gas bench and the Thermo Fischer 46i N_2O analyzer are both measuring downstream emissions for the entirety of Phases III & IV. Phase III is 40 minutes long to ensure that the dCSC™ emissions storage sites are saturated and steady state emissions can be measured. At the conclusion of Phase III, the 25-kW heater is set to heat the exhaust gas upstream of the dCSC™ so that the dCSC™ temperature will ramp up to a desired constant temperature for Phase IV. As soon as the temperature ramp begins, so does Phase IV.

Phase IV (Release) is the portion of the test where dCSC™ emissions' release performance is calculated. Once the dCSC™ temperature reaches the desired constant temperature, it is held there for 20 minutes in order to ensure the dCSC™ is finished releasing emissions and steady state emissions can be measured.

At the conclusion of Phase IV, the Pierburg 5-gas bench and the Thermo Fischer 46i N2O analyzer are used to measure upstream dCSC™ emissions concentrations.

3.3.2 Engine Test Conditions

In order to re-create cold start conditions, the three low-load engine conditions shown in Table 3.4 were determined. These are the engine conditions used in Phases III and IV of each experiment, shown in Figure 3.3. The conditions allowed for low dCSC™ temperatures to be achieved during Phase III (storage phase) of tests. The use of condition 2 was vital to achieving a high dCSC™ temperature during Phase IV (release phase) of tests. Condition 2 was also used to achieve a higher temperature ramp rate of 40 °C/min from Phase III to Phase IV. The ramp rate was achieved by changing from engine condition 1 to 2 at the beginning of Phase IV. Engine condition 3 was needed in order to achieve dCSC™ temperature of 80 °C during Phase III of a test. Engine condition is set

30

before Phase III begins and remains at that condition for the entirety of Phases III and IV. The only exception to the previous statement is the test where a 40 °C/min temperature ramp rate was desired. During this test engine condition changes from 1 to 2 at the start of Phase IV, to achieve the temperature ramp rate of 40°C/min in the dCSC™. Table 3.4 also shows engine out or upstream dCSC™ emissions concentrations at each engine condition, measured by the Pierburg 5-gas bench. The air-to-fuel ratio at each engine condition was calculated from the measured fuel flow and air flow into the engine. They were measured with a Coriolis fuel mass flow rate meter and a laminar flow element instrumented to measure air mass flow rate. The H_2O concentration out of the engine was calculated using the AFR and the fuel properties from Table 3.2.

Table 3.4 Engine Test Conditions

Engine Parameter	Condition 1	Condition 2	Condition 3
Speed (rpm)	1000	1290	750
Load (N-m)	35	46	22
Exhaust Flow Rate (kg/min)	3.5	4.9	2.6
Turbine Outlet Temperature (°C)	140	180	110
Air-to-Fuel Ratio (AFR)	100	83	130
EGR (%)	0	0	0
O_2 (%)	17.5	17.1	18.0
CO_2 (%)	2.5	2.9	1.8
H_2O (%)	1.9	2.3	1.5
CO (ppm)	86	95	75
NO (ppm)	175	209	211
NO_2 (ppm)	10	7	18
NOx (ppm)	185	216	229

3.3.3 Experimental Test Conditions

Table 3.5 shows a list of desired dCSC™ temperatures for Phase III. These temperatures were decided upon based on findings from other dCSC™, PNA, and DOC research publications [1, 8, 17, 18, 24]. Refer to Chapter 2 Figure 2.8 for temperatures tested on the dCSC™ in reference [8]. These tests were all conducted with a dCSC™ temperature of 300 °C during Phase IV of the test.

Table 3.5 Emissions Storage Test Plan

Engine Test Condition	Phase III (Storage) Emissions Temperature, °C
1	100, 125*, 150, 200, 225, 250
2	115, 150, 200, 250
3	80

The use of "*" next to a number in Tables 3.5-3.7 indicates that the test is a repeat of a test in one of the other two tables.

Based on downstream dCSC™ ATS operating temperatures, a list of desired dCSC™ temperatures was determined for Phase IV of the dCSC™ testing. This list of temperatures is referred to as the emissions release/conversion test plan in Table 3.6. The dCSC™ temperature during Phase III and engine condition for Phases III and IV is in Table 3.6 as well. Engine condition 1 and 150°C Phase III (storage) dCSC™ temperature was tested at 200-450°C Phase IV (release) dCSC™ temperatures. This was done in order to characterize the temperature of the dCSC™ vs. its ability to regain its NOx storage capacity.

Table 3.6 Emissions Release/Conversion Test Plan

Engine Test Condition & Phase III (Storage) Temperature, °C	Phase IV (Release) Emissions Temperature, °C
Condition 1 & 150	200, 250, 300*, 350*, 400, 450
Condition 2 & 150	300*, 350
Condition 1 & 125	300*
Condition 1 & 200	300*, 400

The use of "*" next to a number in Tables 3.5-3.7 indicates that the test is a repeat of a test in one of the other two tables.

Testing was completed to compare the release/conversion performance to temperature ramp rate. Two tests were run with the same Phase III and Phase IV temperature setpoints, but with different temperature ramp rates between the two. Details of these two tests are in Table 3.7. The first test was completed with a ramp rate of 20 °C/min and the second with a rate of 40 °C/min. In order to achieve the 40 °C/min ramp rate, the engine condition changes from condition 1 to 2 at the conclusion of Phase III and the start of Phase IV.

Table 3.7 Emissions Release/Conversion vs. Temperature Ramp Test Plan

Engine Test Condition & Phase III (Storage) Temperature, °C	Ramp Rate, °C/minute	Engine Test Condition & Phase IV (Release) Temperature, °C	Ramp Time, minutes
Condition 1 & 150*	20	Condition 1 & 350	10
Condition 1 & 150	40	Condition 2 & 350	5

A complete list of tests that were run can be found in Appendix D. A MATLAB vector containing the numbers 1 through 25 was randomized using the command 'randperm' to generate the test run order. In between each test in the run order, test 4, the control test, was run. The control test is performed at engine condition 1, 200 °C Phase III dCSC™ temperature, and a 300 °C Phase IV dCSC™ temperature.

3.3.4   ATS Thermal Management

Characterizing the dCSC™ performance at different temperatures is presented in Chapter 4. The data will be used to calibrate a model of the dCSC™ characteristics at different temperatures. Therefore, controlling the ATS temperature during the experiments is vital. Figure 3.4 shows the system (also shown in Figure 3.1) for controlling the temperature in the ATS.
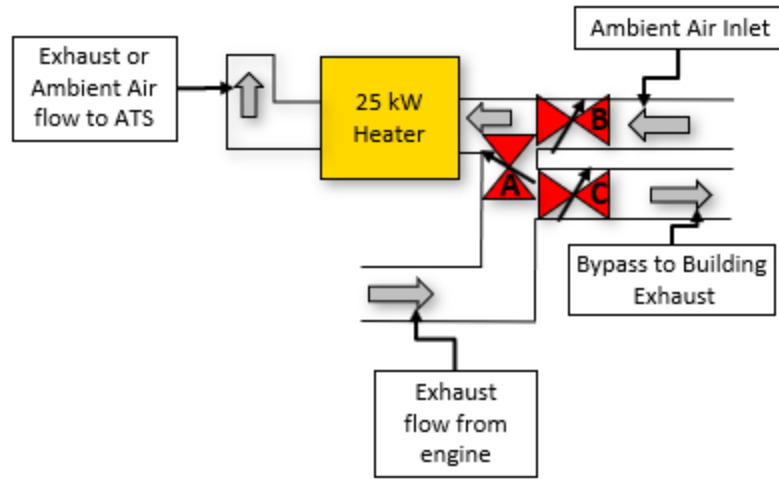
33

Figure 3.4 ATS Thermal Management

The exhaust flow from the 2013 Cummins ISB engine can be routed to the ATS by closing valves C and B and opening valve A. The exhaust can also be routed directly to the building's exhaust by closing valve A and opening valve C. While valve A is closed, valve B can be opened to allow ambient air to be pulled through the ATS. This strategy is utilized to cool the ATS while also controlling the ATS temperature with the 25-kW heater. This allows the dCSC™ temperature to be controlled and stabilized at the desired temperature for Phase III of the test. This strategy also minimizes the possibility of the building exhaust vacuum pulling engine exhaust past valve A when it is closed. This is because the building exhaust will be able to pull ambient air through an open valve B rather than deadheading on valve A.

Figure 3.5 shows the dCSC™ temperatures and a calculated dCSC™ volume weighted temperature. Equation 3.7 and Appendix E describe how the volume weighted temperature is calculated. In Figure 3.5 the dCSC™ temperatures are measured by thermocouples C1, C2, and C18. The location of these thermocouples is shown in Figure 3.2. C1 and C4 are located on the centerline of the dCSC™ substrate. C1 is 32.4 mm from the upstream face and C4 is 30 mm from the downstream face of the substrate. C18 is 120 mm radially from the center of the dCSC™ and 30 mm downstream of C1, axially.

34

The thermocouple data in Figure 3.5 shows how the dCSC™ temperature is accurately and actively controlled during the experiment.
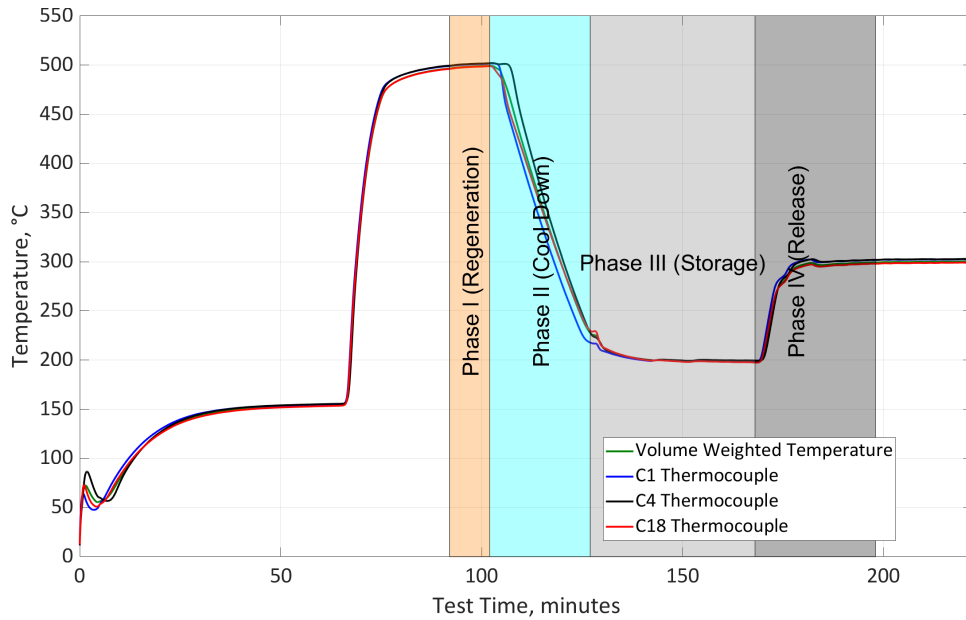
Figure 3.5 dCSC™ Exhaust Temperatures During a Control Test

3.4 Data Analysis Methods

The equations in this section were used in the postprocessing of the experimental data. The results from these equations were used to quantify the dCSC™ performance characteristics. Chapter 4 covers the results that were computed using these equations.

3.4.1 Adsorption and Desorption Calculations (Storage/Release)

The following equations were used to calculate the NOx storage and release, N_2O production, and NO_2 to NOx ratio at the dCSC™ outlet. Equation 3.1 is used to calculate the molar flow rate of the exhaust.

$$\dot{n}_{exhaust} = \frac{\dot{m}_{exhaust}}{M_{exhaust}} \qquad 3.1$$

35

Where, $\dot{n}_{exhaust}$ is the molar flow rate of the exhaust. $\dot{m}_{exhaust}$ is the mass flow rate of the exhaust which is equal to the measured $\dot{m}_{air}$ plus the $\dot{m}_{fuel}$. The $M_{exhaust}$ is the molecular weight of the exhaust. The molecular weight of the exhaust used was 28.97 per reference [25]. After calculating the molar flow rate of the exhaust, the molar flow rate of NOx in the exhaust is calculated using Equation 3.2.

$$\dot{n}_{NOx} = \dot{n}_{exhaust} * \frac{C_{NOx}}{1,000,000} \qquad 3.2$$

Where $\dot{n}_{NOx}$ is the molar flow rate of NOx, and C_{NOx} is the concentration of NOx in the exhaust. A more general form of Equation 3.2 is Equation 3.3, which can be used to calculate the molar flow rate of any exhaust gas constituent.

$$\dot{n}_X = \dot{n}_{exhaust} * \frac{C_X}{1,000,000} \qquad 3.3$$

Where $\dot{n}_X$ is the molar flow rate of any exhaust gas constituent x and C_X is the exhaust gas concentration of that constituent, x. Using the molar flow rate of a species in the exhaust, in this case it is NOx, the species' storage, release, or production can be calculated using Equation 3.4.

$$n_{NOx\,Stored} = \sum_{i=t_i}^{t_f} \left(\dot{n}_{NOx\,In\,(i)} - \dot{n}_{NOx\,Out\,(i)} \right) * \Delta t \qquad 3.4$$

Where, $n_{NOx\,Stored}$ is the moles of NOx stored. The sampling increment (Δt) is 0.5 seconds or 2 Hz. The summation for $n_{NOx\,Stored}$ is computed from the start of Phase III (t_i) to the time at which downstream dCSC™ NOx concentrations are equal to the upstream dCSC™ NOx concentrations (t_f). NOx storage in mass units can be computed by multiplying the moles of NOx stored ($n_{NOx\,Stored}$) by the molecular weight of NO_2 which is the definition of x = 2 (44.01). The molecular weight of NO_2 is used to calculate NOx stored because once NOx reaches the atmosphere the NO portion will be oxidized into NO_2. $\dot{n}_{NOx\,In\,(i)}$ is the molar flow rate of NOx into the dCSC™ and $\dot{n}_{NOx\,Out\,(i)}$ is

the molar flow rate of NOx out of the dCSC™. Equation 3.5 is used to calculate the moles of N_2O produced.

$$n_{N_2O\ Produced} = \sum_{i=t_i}^{t_f} \left(\dot{n}_{N_2O\ In\ (i)} - \dot{n}_{N_2O\ Out\ (i)}\right) * \Delta t \qquad 3.5$$

Where, $n_{N_2O\ Produced}$ is the moles of N_2O produced. $\dot{n}_{N_2O\ In}$ is the molar flow rate of N_2O into the dCSC™ and $\dot{n}_{N_2O\ Out}$ is the molar flow rate of N_2O out of the dCSC™. N_2O molar flow rate is calculated using Equation 3.3 and the N_2O concentration (C_{N_2O}).

During Phase III of the experiments, the downstream dCSC™ NOx concentration increases from 0 ppm NOx to the upstream dCSC™ NOx concentration. The point at which the downstream NOx concentration is exactly 50% of the upstream concentration (where the ratio is 0.5) is referred to as dCSC™ 50% NOx storage capacity. The ratio of the dCSC™ downstream NOx concentration to the upstream NOx concentration (dCSC™ NOx inlet to outlet ratio) is calculated using Equation 3.6.

$$\frac{NOx_{Out}}{NOx_{In}} = \frac{C_{NO_{x\ Out}}}{C_{NOx\ In}} \qquad 3.6$$

Where, $\frac{NOx_{Out}}{NOx_{In}}$ is the ratio of the dCSC™ downstream NOx concentration to the upstream concentration. $C_{NO_{x\ Out}}$ is the downstream dCSC™ NOx concentration and $C_{NOx\ In}$ is the upstream NOx concentration.

37

3.4.2 Calculation of NO₂ to NOx Ratio (NO Conversion Efficiency)

Equation 3.7 is used to calculate NO₂ to NOx ratio at the outlet of the dCSC™. This allows for the characterization of the NOx oxidation characteristics of the dCSC™ during the steady state portions of Phases III and IV.

$$\frac{NO_2}{NOx} = \frac{C_{NO_2\,Out}}{C_{NOx\,Out}} \qquad\qquad 3.7$$

Where $\frac{NO_2}{NOx}$ is the NO₂ to NOx ratio at the dCSC™ outlet, $C_{NO_2\,Out}$ is the concentration of NO₂ at the dCSC™ outlet, and $C_{NOx\,Out}$ is the concentration of NOx at the dCSC™ outlet. In Figure 3.6, the outlet concentration is greater for NO₂ than NO during Phase IV. This is because the substrate temperatures during these two phases are high enough to oxidize a large portion of the upstream NO to downstream NO₂.
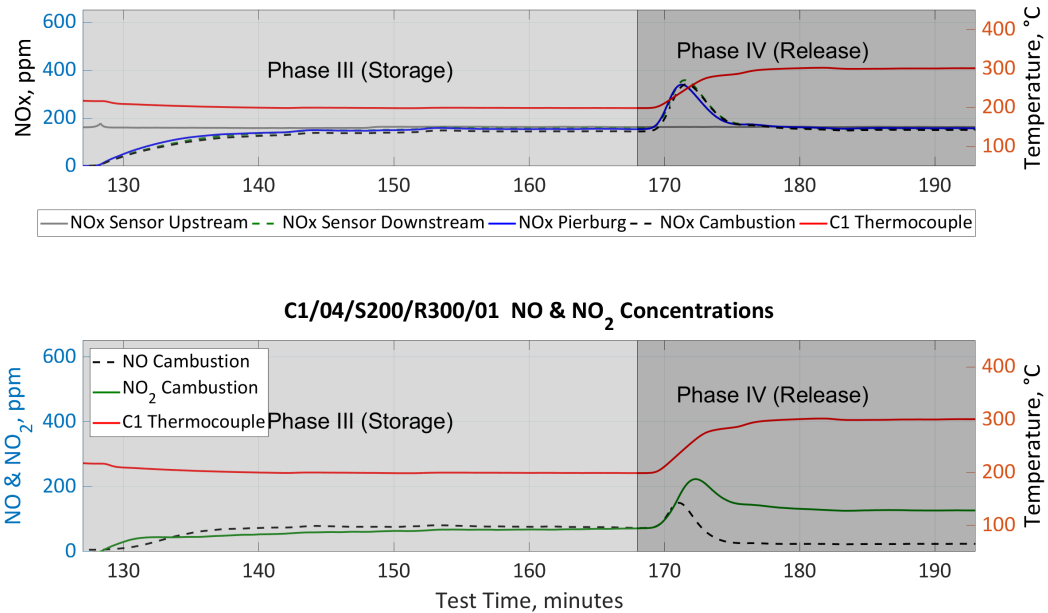

Figure 3.6 Downstream dCSC™ NO, NO₂, and NOx Concentrations during a 200 °C Phase III and 300 °C Phase IV

The NOx Storage is computed using the downstream NOx concentration versus time from the Pierburg CLD, Cambustion CLD, NOx sensor, and two upstream NOx concentrations from the Pierburg and NOx sensor.

3.4.3 Calculation of dCSC™ Volume Weighted Temperature

dCSC™ volume weighted temperature is calculated using Equation 3.8.

$$T_{V.W.} = \sum_{i=1}^{24} \left(W_{T.C.(i)} * T_{T.C. (i)} \right) \qquad 3.8$$

Where $T_{V.W.}$ is the dCSC™ volume weighted temperature, $W_{T.C.(i)}$ is the weight applied to each thermocouple, and $T_{T.C. (i)}$ is the thermocouple temperature reading. The weight applied to each thermocouple is calculated using Equation 3.9.

$$W_{T.C.} = \frac{V_{T.C.}}{V_{T.V.}} \qquad 3.9$$

Where, $W_{T.C.}$ is the weight applied to each thermocouple reading. $V_{T.C.}$ is the volume that each thermocouple represents and $V_{T.V.}$ is the total volume of instrumented dCSC™. Appendix E is a detailed explanation of the dCSC™ volume weighted temperature calculation.

3.4.4 dCSC™ 2D Temperature Distribution

The top half of the dCSC™ is instrumented with 32 K-type omega thermocouples, as shown in Figure 3.2. The temperature data from thermocouples C1 through C20 are used to plot a 2D temperature distribution of the top half of the dCSC™. This plot is then mirrored across the centerline of the dCSC™ to illustrate the entire substrate temperature distribution. Thermocouples C22, 23, and C24 are instrumented on the bottom half of the dCSC™. The RMS Error in the plot title is computed using the difference between these three thermocouples and the mirrored 2D temperature distribution. A MATLAB code

39

was written to plot the temperature distribution using the command 'contourf.' The 'contourf' command plots each thermocouple reading at its axial and radial location within the substrate. The resulting distribution assumes a linear temperature gradient in between the thermocouple readings. Thermocouples C13-C16 were not used to create the 2D temperature distributions. Because it was assumed a maldistribution in the exhaust flow upstream of the dCSC™ caused this row of thermocouples to be at a higher temperature than the thermocouples radially inward of this row. Figure 3.7 shows the dCSC™ 2D temperature distribution during Phase III of a test where the temperature setpoint was 200°C.

Figure 3.7 Control Test 15 at minute 115, dCSC™ Temperature 200°C, Phase III 2D Temperature Distribution

The numbers in red indicate the actual thermocouple readings in the dCSC™. Each *1's in red font indicates a location in the dCSC™ where there is no thermocouple.

40

4 Results

This chapter presents the experimental data results from Phases III and IV. These two Phases are the portions of the testing where emissions storage, release, and oxidation were observed and analyzed. Section 4.1 discusses the emissions time plots during experiment Phases III and IV. Appendix F shows the measured emissions concentrations, engine parameters, delta pressures, and temperatures vs. time during a test. Appendix G shows the control parameters measured for each test such as upstream dCSC™ emissions concentrations, exhaust mass flow rate, intake air mass flow rate, etc.

Section 4.2 discusses the NO, NO_2, and NOx storage/adsorption performance of the dCSC™ for a range of temperatures from 80 to 250 °C, during Phase III of the testing. Section 4.3 discusses the NO, NO_2, and NOx release/desorption performance of the dCSC™ for a range of temperatures from 200 to 450 °C, during Phase IV the of testing. Section 4.4 shows the dCSC™ NO to NO_2 oxidation characteristics. dCSC™ NO to NO_2 oxidation was calculated during Phases III and IV of testing, after the transient NOx storage or release event. During NOx release at the beginning of Phase IV, an N_2O concentration is observed downstream of the dCSC™ and section 4.5 discusses this production of N_2O. The dCSC™ CO storage/oxidation characteristics are discussed in section 4.6. Appendices H and I discuss the N_2O formulation and oxidation reactions in the dCSC™, respectively

dCSC™ 2D temperature distribution data were measured during Phases III and IV of testing and were plotted using the methodology described in 3.4.4. Section 4.7 presents the 2D temperature distribution plots of the dCSC™ temperatures. Throughout the figures in this chapter, the C1 thermocouple within the dCSC™ is referenced to represent the dCSC™ temperature. It was determined that additional thermocouples are needed to accurately capture the temperature gradient in the substrate, Appendix J discusses this.

Section 4.8 is the Summary and Conclusions of the results and Section 4.9 discusses recommendations for future work.

4.1   Test Phases III and IV Emissions Data

Figure 4.1 shows the NO, NO_2, NOx, CO, and N_2O concentrations at the outlet of the dCSC™ during a test with temperatures of 115 °C during Phase III and 300 °C during Phase IV. The NO and NOx are measured by the Cambustion Fast Response CLD analyzer. NO_2 is calculated by subtracting the measured NO from the measured NOx. CO is measured by the Pierburg 5-gas bench and N_2O is measured by the Thermo Fisher 46i N_2O analyzer. Before the start of Phase III, the dCSC™ has been controlled to 115 °C via the 25-kW electric heater. Once the temperature in the dCSC™ stabilizes at 115 °C, exhaust gas is routed to the dCSC™ and Phase III begins.

During Phase III, NO and NOx concentrations at the dCSC™ outlet start at 0 ppm and increase until they reach the upstream dCSC™ concentration of NO and NOx, indicating NO and NO_2 storage. At a temperature of 115 °C, there is zero NO to NO_2 oxidation occurring in the dCSC™ and the upstream NOx is comprised of 99% NO. Therefore, 0 ppm NO_2 is measured at the dCSC™ outlet. CO concentrations downstream of the dCSC™ start at 0 ppm and increase until they reach approximately 40 ppm. The upstream dCSC™ CO concentration during this test was approximately 85 ppm. This indicates a storage and oxidation of CO on the dCSC™. After the dCSC™ has finished storing emissions and the concentrations have reached steady state, steady state concentrations are recorded.

During Phase IV, dCSC™ temperature increases from 115 to 300 °C. As the temperature is increasing and reaches approximately 200 °C, the NO and NOx concentrations start increasing, indicating NOx release. The concentrations peak at approximately 450 ppm as the dCSC™ temperature reaches 250 °C and then decrease to a steady state concentration. Once the dCSC™ temperature reaches approximately 220 °C, the NO_2 concentration starts increasing, and the dCSC™ is now at a high enough temperature to oxidize some of the stored NO to NO_2 while releasing it. The NO_2 concentration peaks as the temperature reaches 265 °C and then decreases to a steady state concentration of approximately 110 ppm. The NOx concentration returns to its initial value of

42

approximately 150 ppm, and the NO concentration reaches a steady state concentration of about 40 ppm. The steady state NO_2 concentration is more than double the NO concentration, indicating over half of the NO entering the substrate is being oxidized to NO_2. These steady state concentrations from each test are used to compute the downstream dCSC™ NO_2/NOx ratio at each Phase IV temperature. As soon as the dCSC™ temperature starts increasing, the CO concentration downstream of the dCSC™ starts to decrease and reaches 0 ppm by the time the temperature reaches approximately 150 °C. The dCSC™ is then oxidizing all the upstream CO to downstream CO_2. A concentration of N_2O is observed at the dCSC™ outlet as the temperature approaches 200 °C. This concentration increases from 0 ppm to a peak of approximately 14 ppm as the dCSC™ reaches 230 °C and then decreases back to 0 ppm. The concentration of N_2O at the dCSC™ outlet is due to a small occurrence of HC lean NOx conversion occurring within the dCSC™, this is supported in reference [1].
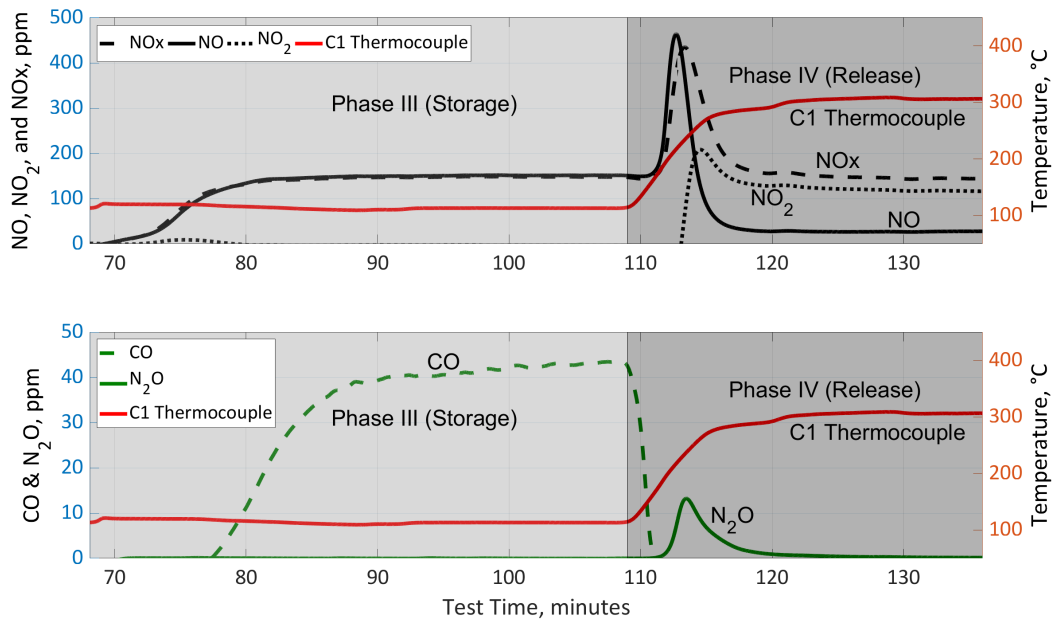
Figure 4.1 NO, NO_2, NOx, CO, and N_2O Concentrations Downstream of the dCSC™ during a 115 °C Phase III and a 300 °C Phase IV, at Engine Condition 1

43

4.2   NO, NO₂, and NOx Storage Performance

NOx concentrations upstream of the dCSC™ were measured using both the NOx sensor and the Pierburg CLD. NOx concentrations downstream of the dCSC™ were measured using the NOx sensor, Pierburg CLD, and a Cambustion CLD. Referring to Equation 3.4, a NOx concentration at the inlet (upstream) and outlet (downstream) of the dCSC™ is needed to compute the NOx stored. In this case there are two NOx concentration measurements made at the inlet (upstream) and three NOx concentration measurements made at the outlet (downstream). The upstream dCSC™ NOx concentration is constant throughout Phases III and IV of each of the tests as the engine condition remains constant. The NOx sensor monitors the upstream dCSC™ NOx concentration for the entire test. The Pierburg CLD measures the upstream dCSC™ NOx concentration at the conclusion of Phase IV of each of the tests.

The two upstream dCSC™ NOx concentrations (Pierburg and NOx Sensor) are compared in Figure 4.2. Figure 4.2 includes upstream dCSC™ NOx concentration data for all of the tests completed. Therefore, tests completed at all three engine conditions described in Chapter 3. The y-axis of the plot is NOx in ppm and the x-axis is the order in which each test was run. The upstream NOx concentration changes slightly from test to test due to factors such as test cell environmental conditions and engine condition. The Pierburg CLD measurement in Figure 4.2 is consistently slightly higher than the NOx sensor measurement. The Pierburg CLD upstream dCSC™ NOx concentration measurement is used to calculate NOx stored. During Phases III and IV of testing, dCSC™ NOx storage and release are calculated, respectively.
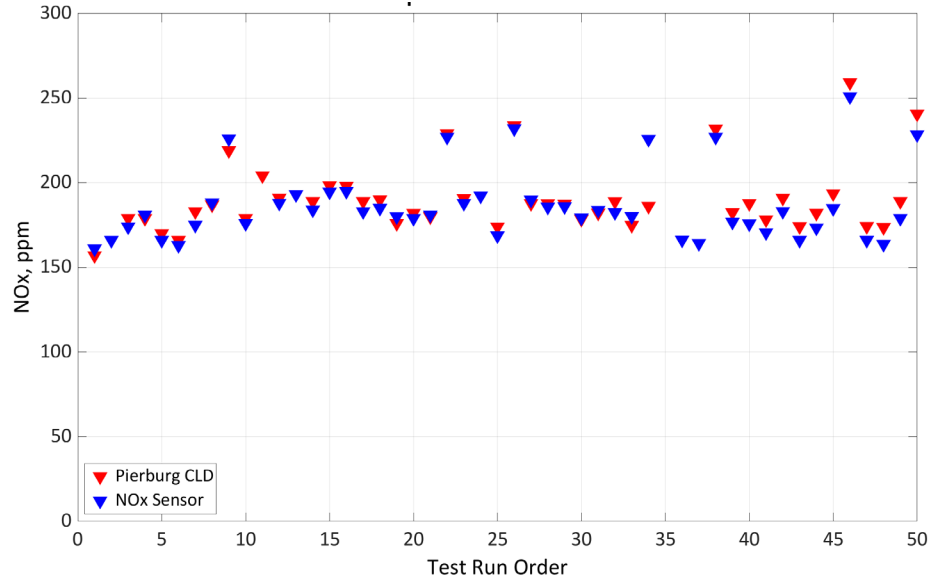
Figure 4.2 Upstream dCSC™ NOx Concentrations vs. Test Order

In order to calculate dCSC™ NOx storage and release, a downstream dCSC™ NOx concentration measurement is needed. Figure 4.3 shows the downstream dCSC™ NOx concentrations from the three different instruments during Phase III and IV of an experiment.

Before the start of Phase III, the dCSC™ temperature is controlled to 115 °C with a feed of room air that has been heated by the 25-kW Watlow heater. Once the dCSC™ temperature is stabilized at 115 °C, the feed is changed from heated ambient air to heated exhaust gas containing approximately 200 ppm of NOx. The exhaust gas temperature is also controlled by the 25-kW Watlow heater. The downstream dCSC™ NOx concentration starts at 0 ppm and increases to reach the upstream dCSC™ NOx concentration. The measured concentration of each of the three instruments measuring downstream dCSC™ NOx concentrations varies from instrument to instrument. The Pierburg NOx measurement increases first followed by the Cambustion CLD and NOx Sensor, respectively. Therefore, computing NOx stored with each of the three downstream NOx concentrations yields three different NOx stored values.

45

During Phase IV, the feed of exhaust gas is being heated from 115 to 300 °C. An increase in downstream dCSC™ NOx concentrations is not observed until the exhaust gas temperature reaches 200 °C. By the time the exhaust gas reaches 265 °C, the downstream dCSC™ NOx concentrations have peaked and are decreasing to reach the upstream dCSC™ NOx concentration. Therefore, the majority of the NOx release occurs from 200 to 265 °C.
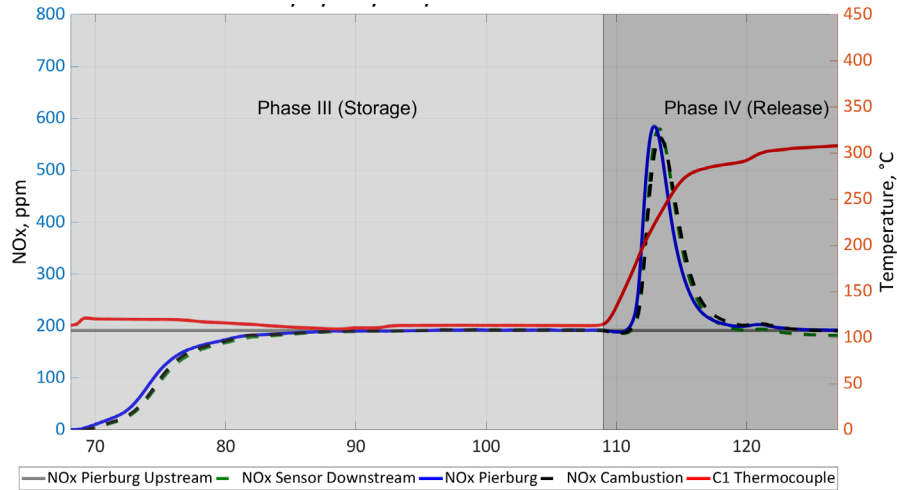
Figure 4.3 Downstream dCSC™ NOx Concentrations vs. Time during a 115 °C Phase III and 300 °C Phase IV, at Engine Condition 1

NOx storage was computed for each of the three NOx concentration measurements downstream of the dCSC™. Figure 4.4 shows total NOx storage for the tests with a 200 °C temperature during dCSC™ test Phase III from each downstream NOx measurement. Note that there is space between the points on the figure because these tests were not conducted with a 200 °C Phase III storage temperature.

The total NOx stored for the first eight control tests is approximately 0.6 g.NOx/L.Sub. During the last six control tests the total NOx stored was reduced to approximately 0.35 g.NOx/L.Sub. This is likely due to a decrease in the number of active NO storage sites on the dCSC™ substrate, or in the effectiveness of the sites, as more tests are completed.

46

Engine out NOx is composed of 90 to 95% NO, only a 5 to 10% of the NOx is NO_2. Therefore, most of the NOx stored by the dCSC™ is NO. The activity of the NO storage sites directly affects the total NOx storage. However, it is still possible for some NO_2 to be stored on the dCSC™.

From reference [19], H_2O can greatly inhibit NOx storage. Ambient air flows through the dCSC™ during Phase II of testing to control the dCSC™ to the Phase III temperature setpoint. It was investigated as to whether or not the relative humidity in the test cell had an effect on the NOx storage. During the first control test the relative humidity in the test cell was measured to be 36% and during the last test it was measured to be 28 %. From the first control test to the last control test total NOx stored decreased by 46%. The relative humidity during the last test was 8% lower than it was during the first test. This indicates that relative humidity of the test cell did not affect the total NOx storage. There was no trend showing that relative humidity in the test cell increased as NOx stored decreased. The relative humidity in the test cell was recorded for each test (Appendix G, Figure G.12) and the engine out H_2O concentrations are shown in Table 3.4.

There are significant reductions in control test total NOx storage from approximately 0.6 to 0.5 g.NOx/L.Sub. and 0.5 to 0.4 g.NOx/L.Sub. at the 15th test and the 35th test, respectively. These two transitions occur from control test 7 to 8 and control test 17 to 18 and have been labeled with a black dashed line in Figure 4.4. The time the dCSC™ was at 500 °C and exposed to engine exhaust while the engine was at 1660 rpm and 600 N-m was quantified at the start of the 15th and 35th tests. At the start of the 15th test the dCSC™ had been at 500 °C and exposed to exhaust gas from the diesel engine at 1660 rpm and 600 N-m for a total of 5 hours and 30 minutes. At the start of the 35th test the dCSC™ had been exposed to these conditions for 9 hours and 10 minutes. This high-temperature high load exposure is likely the reason for the reduced activity of the NO storage sites.

47
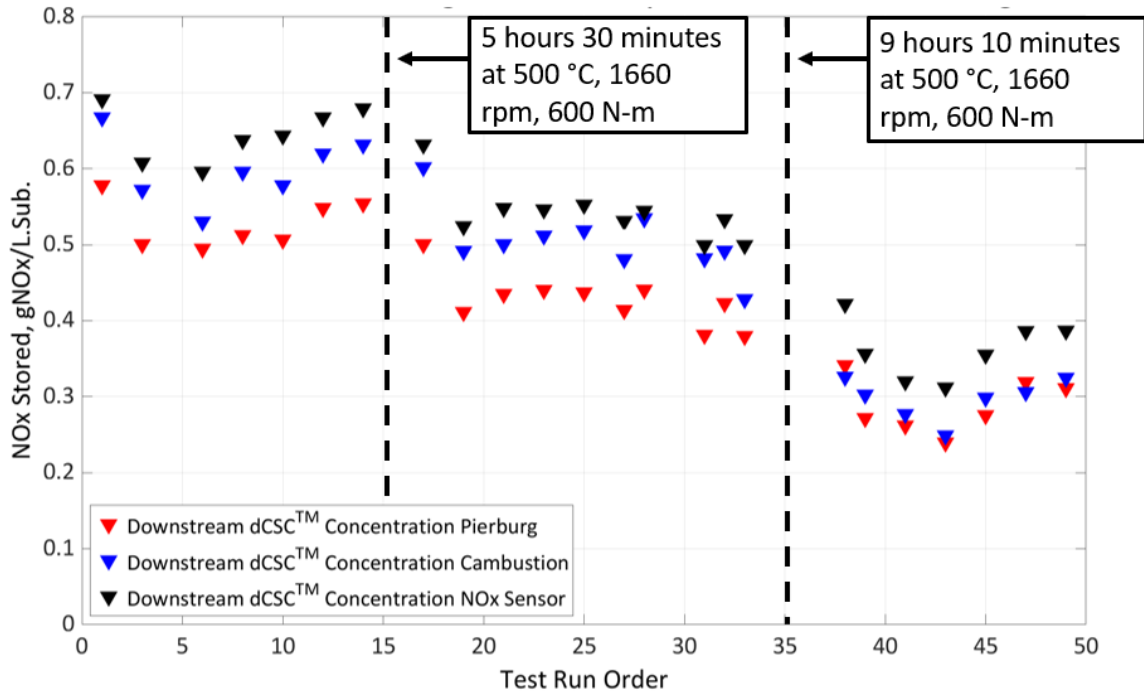
Figure 4.4 Control Test 200 °C Phase III dCSC™ Total NOx Stored vs. Test Order

Figure 4.5 shows the data from Phase III (storage) from two control tests, control test 7 and control test 23. Control test 7 was the 14th test to be run and control test 23 was the 48th test run. Figure 4.5 shows downstream dCSC™ NOx concentrations from the Pierburg CLD, during the 200 °C Phase III, for both tests. It also shows total NOx stored, computed from the downstream NOx concentrations. The total NOx stored from control test 23 is 0.32 g.NOx/L.Sub. while the total NOx stored from control test 7 is 0.55 g.NOx/L.Sub. This is a significant decrease in the total NOx storage capacity of the dCSC™ from the 14th to the 48th test run.

The initial rate of storage appears to be similar from 79-81 minutes, which refers to the initial bulk diffusion of reactants. Bulk diffusion of reactants is when the NO is reacting with the NO storage sites on the outer surfaces of the substrate, which are the easiest storage sites to reach, as discussed in reference [23]. The pore diffusion of reactants is when the NO in the feed gas has to diffuse through the substrate to reach active NO storage sites that are not as accessible as the bulk diffusion storage sites. Reactants go to

48

these sites after the easiest (bulk diffusion) NO storage sites have been saturated, as discussed in reference [23]. At a time of 81 minutes, the two NOx traces split and test 23's downstream dCSC™ NOx concentration increases more rapidly towards the upstream NOx concentration than test 7's. This indicates a decrease in the activity of the pore diffusion NO storage sites on the dCSC™, which causes the decrease in NOx storage capacity.
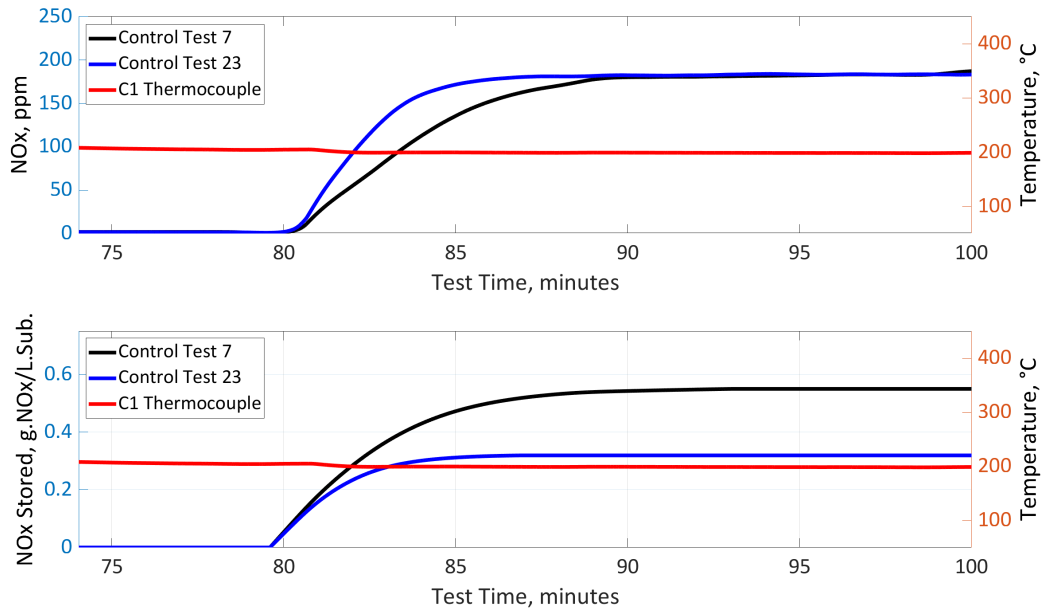
Figure 4.5 Control Test 200 °C Phase III NOx Storage Comparison, at Engine Condition 1

Over 200 hours of testing was completed on the dCSC™. The total NOx storage capacity of the dCSC™ appears to decrease over time due to a reduction of the active pore diffusion NO storage sites. However, the bulk diffusion NO storage sites appear to remain active. dCSC™ NOx storage capacity was computed for the first 200 seconds of each test. Figure 4.6 shows the total NOx stored during the first 200 seconds of the 200 °C Phase III control tests. The 200-second NOx storage capacity of the dCSC™ over the first 15 tests is roughly 0.35 g.NOx/L.Sub. The 200-second NOx storage capacity over

49

the last 15 tests is slightly less at 0.3 g.NOx/L.Sub. Indicating that the majority of the dCSC™ bulk diffusion NO storage sites remain active.
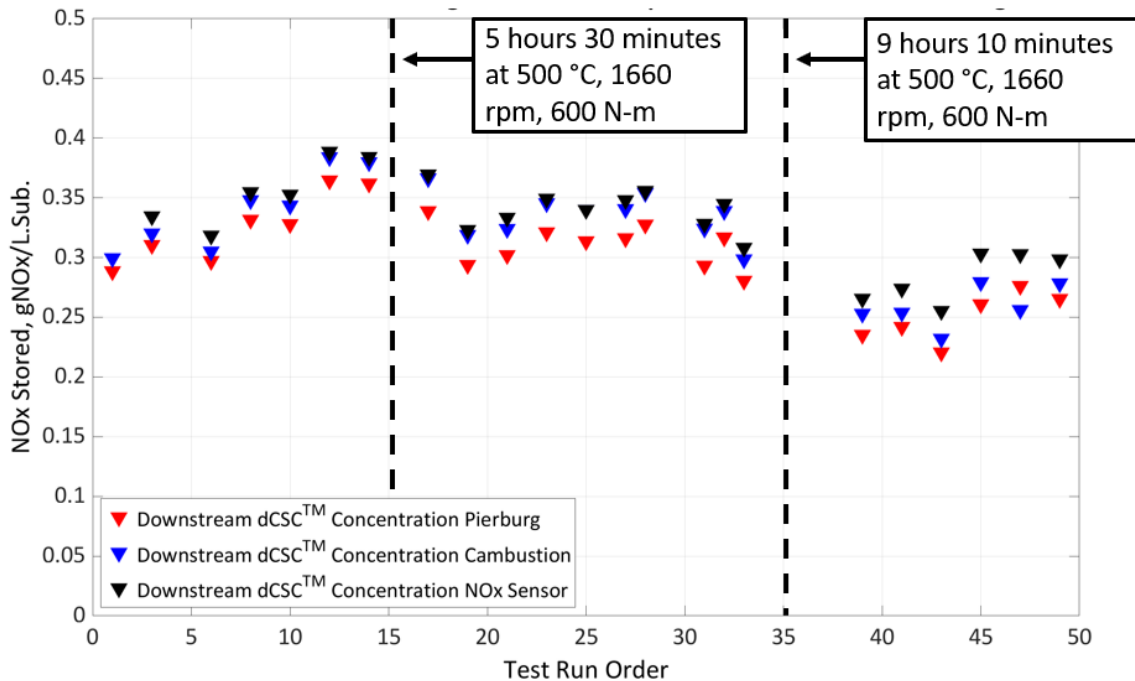
Figure 4.6 Control Test 200 °C Phase III 200-second dCSC™ NOx Storage Capacity vs. Test Order

The 200-second NOx storage capacity of the dCSC™ at Phase III test temperatures of 80 to 250 °C was computed. The NOx measurements used were the Pierburg CLD, upstream and downstream measurements. Figure 4.7 shows the 200 second NOx storage capacity of the dCSC™ versus the average volume weighted temperature calculated by the equations in section 3.4.3.

Consistent with references [1] and [8], the range of temperatures at which the dCSC™ stores the largest quantity of NOx is 125 to 150 °C. The storage capacity slightly decreases as the temperature decreases from 125 °C. This is because as the temperature is decreasing, the water concentration in the exhaust is increasing. The higher presence of water in the exhaust inhibits the ability of the NO storage sites on the dCSC™, as is

50

discussed in references [1, 8, 19]. At temperatures above 200 °C the NO storage sites on the dCSC™ become unstable and less able to store NOx [1, 8].

The black curve in Figure 4.7 is a 3rd order polynomial fit of the tests performed at engine condition 1. There are two points in Figure 4.7 at 150 °C and 0.65 g.NOx/L.Sub. that were performed at engine condition 2 (exhaust flow rate – 4.9 kg/min), where the exhaust flow rate is 1.5 kg/min more than engine condition 1 (exhaust flow rate – 3.5 kg/min). Therefore, during the 200-second period, the dCSC™ NO storage sites were exposed to a more molecules of NO than the tests at engine condition 1, and thus store a larger mass of NOx.
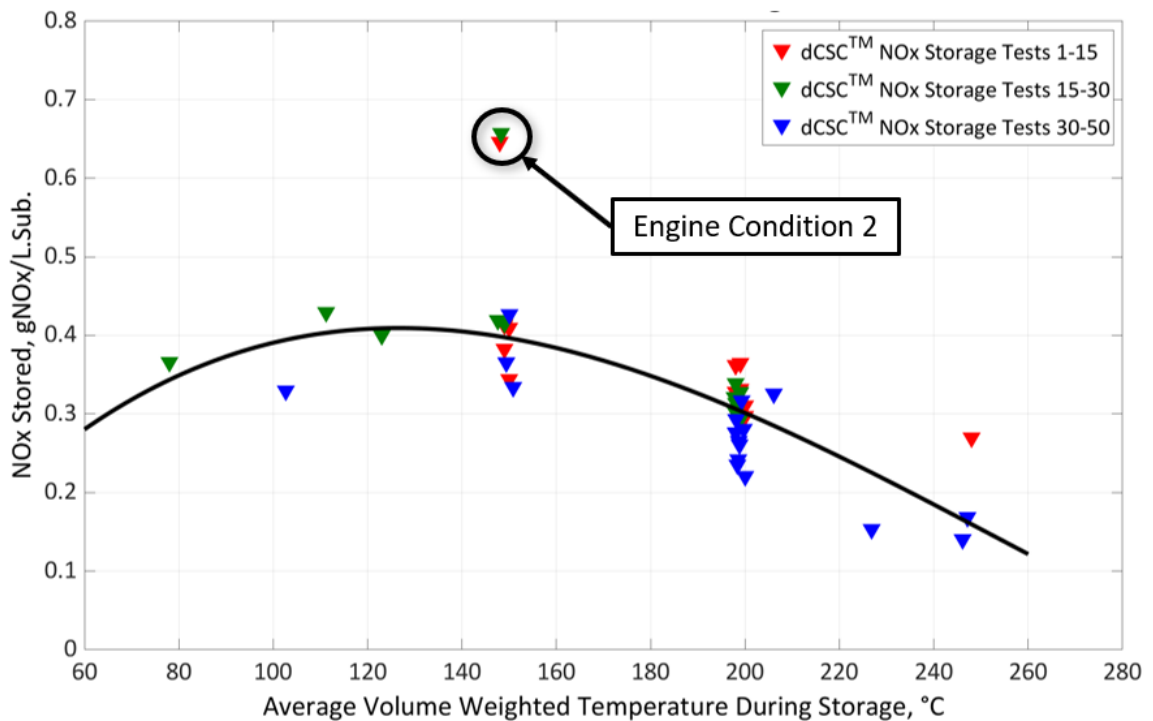
Figure 4.7 200-second dCSC™ NOx Storage Capacity vs. Temperature at all Engine Conditions

During Phase III of each test, the ratio of downstream dCSC™ NOx concentration to the upstream concentration (dCSC™ NOx inlet to outlet ratio) begins at 0 and increases to 1. The time it takes for the ratio to reach 0.5 (dCSC™ 50% NOx storage capacity) is

51

dependent upon the temperature of the dCSC™. Figure 4.8 shows time in minutes for the ratio to reach 0.5 at different dCSC™ temperatures.

The data in Figure 4.8 refers to the tests in three groups, tests 1-15, tests 15-30, and tests 30-50. The groups are arranged in chronological order in which the tests were run. Tests 1-15 show the largest amount of time before the dCSC™ 50% NOx storage capacity is reached, while tests 15-30 show a reduction in time and tests 30-50 show an even further reduction in time. The reduction in time to the 50% NOx storage capacity with increasing number of tests run is another indication that the pore diffusion NO storage sites are becoming less active.
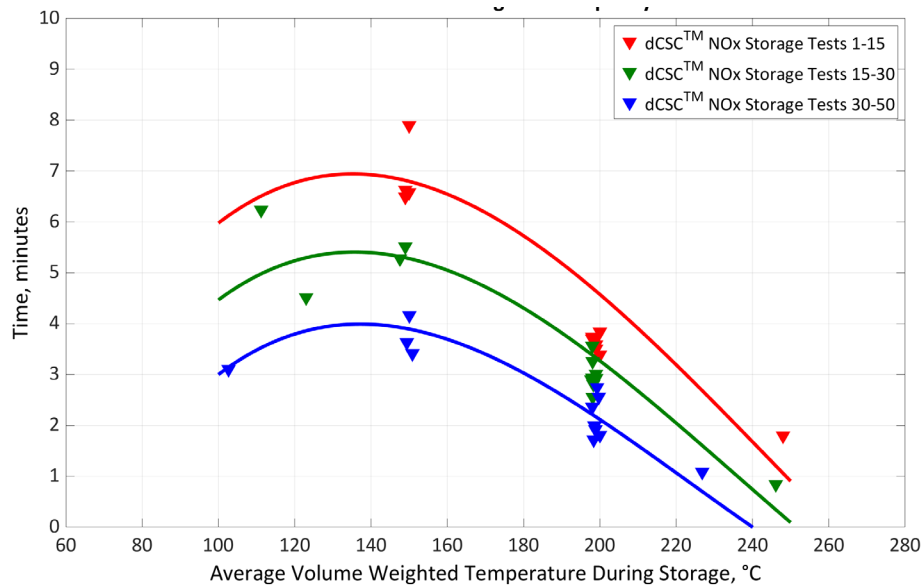
Figure 4.8 50% dCSC™ NOx Storage Capacity vs. Temperature

4.3   NO, NO₂, and NOx Release Performance

NOx release is calculated during Phase IV of each test. During this phase, the dCSC™ temperature increases from the temperature setpoint during Phase III to the temperature setpoint for Phase IV. As the dCSC™ temperature increases, the downstream dCSC™ NOx concentration increases from the initial value to a peak and then decreases to the

initial value, which indicates a NOx release. The NOx released in g.NOx/L.Sub. is calculated during this time using Equation 3.4.

Figure 4.9 shows the NOx released by the dCSC™ at different Phase IV (release) average volume weighted temperatures. The average volume weighted temperature of the dCSC™ is calculated using the equations in section 3.4.3. The dCSC™ NOx storage capacity is highest at Phase III (storage) temperatures of 125 to 150 °C and decreases as temperature increases from that range. Tests run with Phase III temperatures of 200 to 250 °C showed lower total NOx storage capacity. The dCSC™ can only release NOx that it has first adsorbed or stored. Therefore, the NOx released is dependent upon the NOx stored during Phase III, which is dependent upon the Phase III dCSC™ temperature. In addition, dCSC™ NOx storage capacity has shown to decrease with increasing number of tests run.
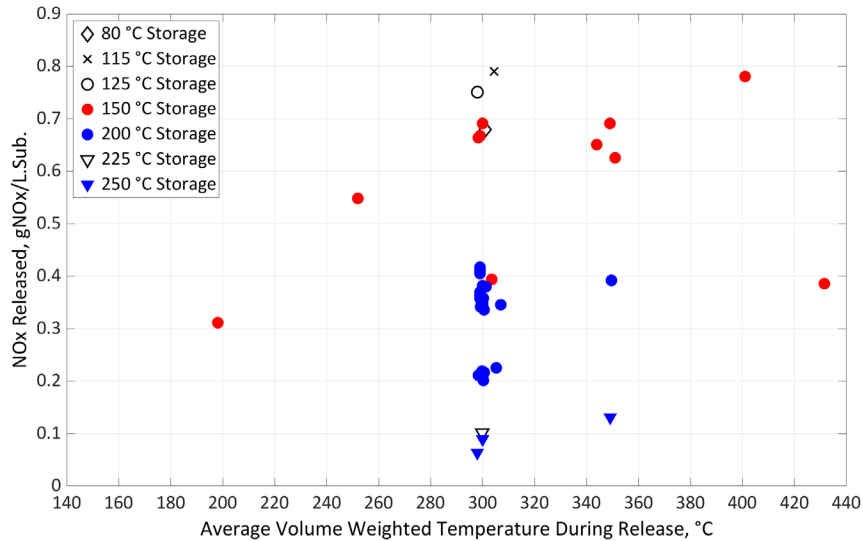
Figure 4.9 dCSC™ Total NOx Released vs. Temperature

The tests with 150 °C Phase III storage temperatures were followed by Phase IV release temperatures of 200 to 450 °C. This was done to determine the percentage of NOx stored that is released at different temperatures. Figure 4.10 shows the percentage of NOx stored during Phase III that is released during Phase IV. The black line is a curve fit through the percentage of stored NOx released points during the tests with a 150 °C Phase III

53

(storage) temperature. With a 150 °C Phase III temperature, as Phase IV (release) temperature increases, the percentage of NOx stored released also increases.

Two of the tests with a 300 °C average volume weighted release temperature, show a percentage of stored NOx released lower than 30%. These two tests had a storage temperature of 250 °C. Therefore, the temperature increase during Phase IV was from 250 to 300 °C. The rapid NOx release of the dCSC™ has been found to occur from 200 to 265 °C in reference [8]. Therefore, the NOx release event for these two tests, which occurs from 250 to 300 °C, does not pass through the rapid NOx release temperature range. However, there is a secondary rapid NOx release centered around 350 °C per reference [8]. A test was conducted with 250 °C Phase III storage temperature and a 350 °C Phase IV release temperature that shows over 90% of the stored NOx released. Therefore, in order to release a high percentage of the stored NOx, the release temperature ramp must ramp from 200-265 °C or reach at least 350 °C. The 250 to 350 °C temperature ramp is 60% more efficient at releasing NOx than the 250 to 300 °C temperature ramp.
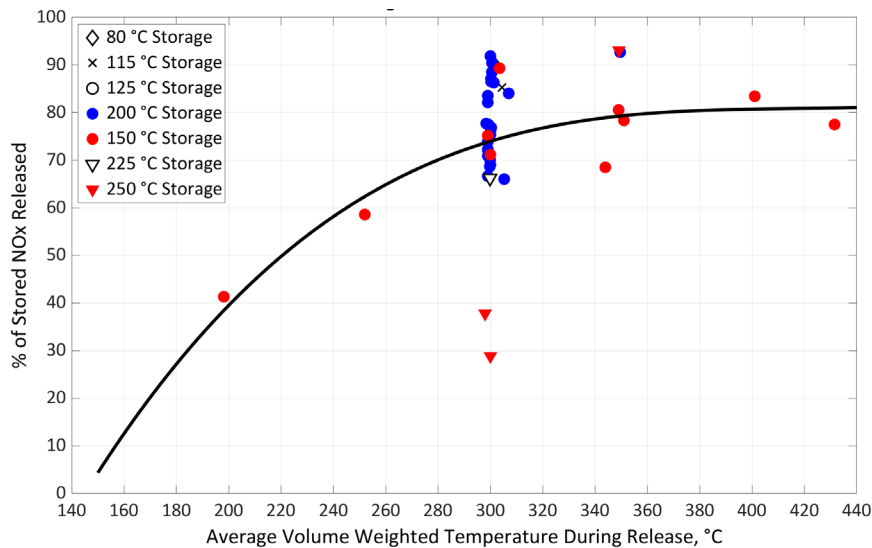
Figure 4.10 dCSC™ Percent of Stored NOx Released vs. Temperature

4.4   NO to NO$_2$ Oxidation Characteristics

The dCSC™ oxidizes NO to NO$_2$ through the catalytic oxidation reaction show in Equation 4.1 below.

$$2NO + O_2 \leftrightarrow 2NO_2 \qquad\qquad 4.1$$

During Phases III and IV of testing, after the transient NOx storage and release periods, steady state emissions are measured. The Cambustion CLD measures NO and NOx downstream of the dCSC™. Subtracting the NO from the NOx measurement yields NO$_2$. This NO$_2$ value and the Cambustion NOx value are used to calculate the NO$_2$ to NOx ratio at the dCSC™ outlet.

Figure 4.11 shows the NO to NO$_2$ oxidation performance of the dCSC™ at different temperatures. As temperature increases, the NO to NO$_2$ oxidation reaction rate increases and more of the NO passing through the substrate is oxidized to NO$_2$. Therefore, as the dCSC™ temperature increases from 100 to 300 °C, the NO$_2$/NOx ratio increases. Which indicates that the NO to NO$_2$ oxidation is increasing. At temperatures below 300 °C Equation 4.1 has an equilibrium towards the right side of the equation. From 300 to 450°C, the NO$_2$/NOx ratio decreases, meaning less of the NO passing through the substrate at these temperatures is oxidized to NO$_2$. This is because Equation 4.1 has an equilibrium which shifts to the left side of the equation at these higher temperatures which is discussed in reference [27]. Therefore, the dCSC™ NO to NO$_2$ ratio is decreasing as temperature increases beyond 300 °C.
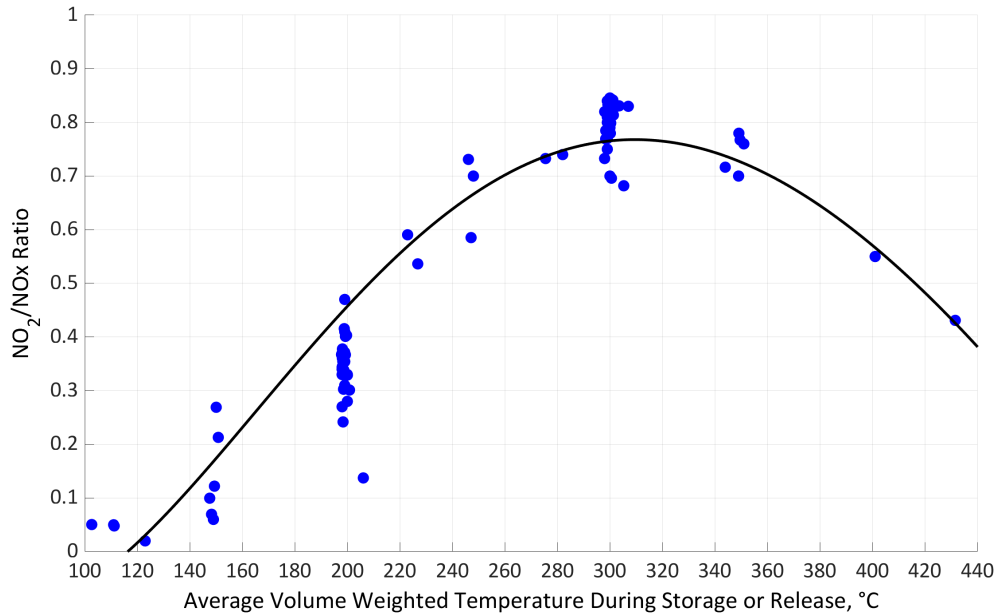
Figure 4.11 Downstream dCSC™ NO_2/NOx Ratio vs. Temperature

4.5 N_2O Production

N_2O concentrations were measured downstream of the dCSC™ substrate during Phases III and IV of testing. While the dCSC™ is releasing NOx, after a Phase III storage temperature of 150 °C or less, there is a low level of NOx conversion to N_2O observed. This production of N_2O in the dCSC™ is a result of the HC lean NOx reduction that occurs on the substrate, as discussed in reference [1]. The oxidation of adsorbed HC and NO, once the dCSC™ is approximately 200 °C and above, potentially results in the formation of N_2O [28]. Equation H.1 and H.2 in Appendix H describes the reactions that produce N_2O [28].

Figure 4.12 shows the N_2O concentration at the dCSC™ outlet during an 80 °C Phase III and a 300 °C Phase IV, at engine condition 3. At the beginning Phase IV, while the dCSC™ is releasing NOx and HC, there is N_2O production. The N_2O concentration increases to a peak of 12 ppm and then decreases to a constant concentration of 0 ppm at the 300 °C Phase IV temperature.

www.manaraa.com
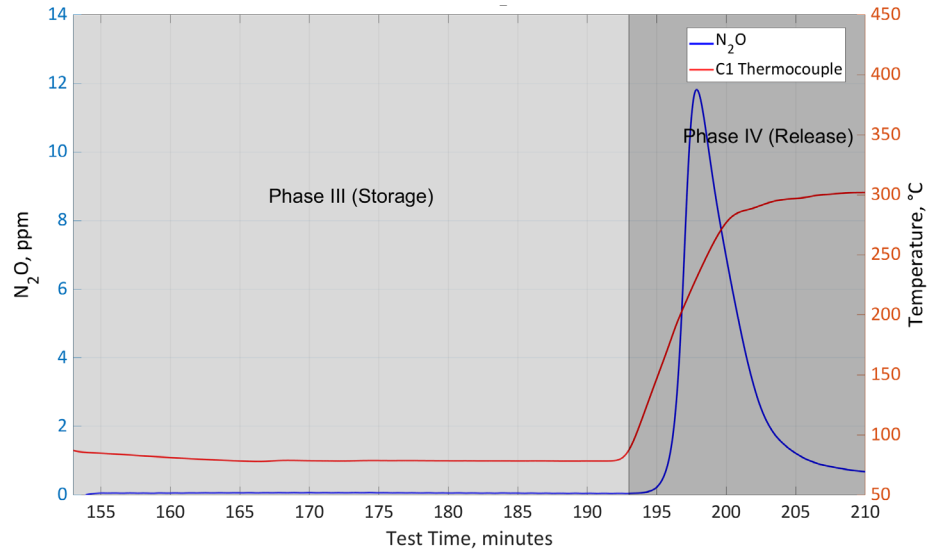
Figure 4.12 N_2O Concentration vs. Time during an 80 °C Phase III and a 300 °C Phase IV, at Engine Condition 3

4.6   CO Storage/Oxidation Performance

Figure 4.13 shows the CO concentration at the dCSC™ outlet, during a 125 °C Phase III and 300 °C Phase IV test at engine condition 1. During Phase III the downstream dCSC™ CO concentration increases from 0 ppm to a constant value of 35 ppm. The CO concentration upstream during this test is 85 ppm. The difference between the upstream 85 ppm CO concentration and downstream 35 ppm CO concentration is stored/oxidized by the dCSC™. During the start of Phase IV, as the dCSC™ temperature is increasing from 125 to 300 °C, the CO concentration decreases to 0 ppm. As the dCSC™ temperature increases, the CO oxidation capability of the dCSC™ increases and oxidizes all the CO to CO_2.

57
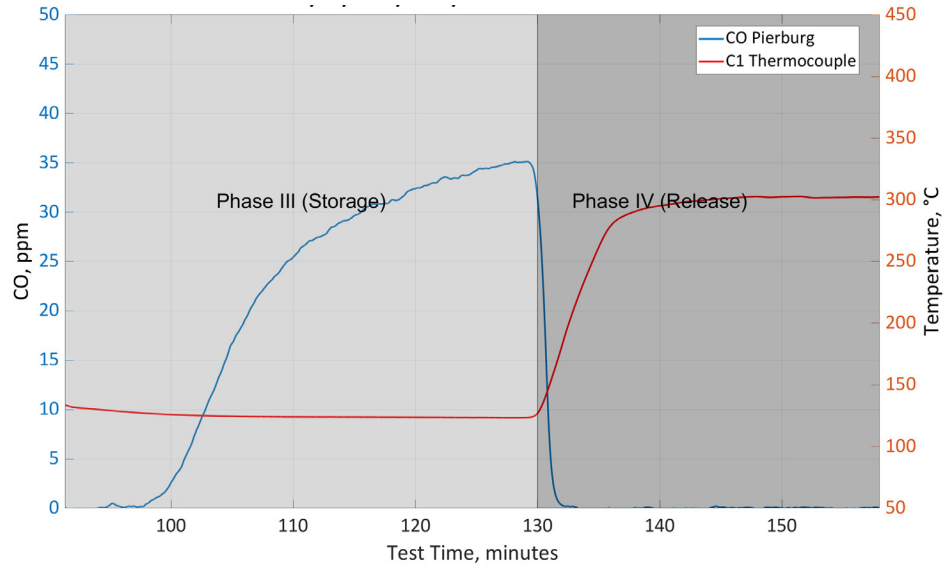
Figure 4.13 Downstream dCSC™ CO vs. Time during a 125 °C Phase III and 300 °C Phase IV, at Engine Condition 3

Figure 4.14 shows the dCSC™ CO storage/oxidation efficiency of the 125 °C Phase III and 300 °C Phase IV test, . During Phase III, the storage/oxidation efficiency starts at 100% and then decreases to 55% towards the end of Phase III. At the start of Phase IV the dCSC™ temperature increase from 125 to 300 °C. As dCSC™ temperature increases the CO storage/oxidation increases to 100%. As dCSC™ temperature increases all of the upstream CO is oxidized to downstream CO_2.

58
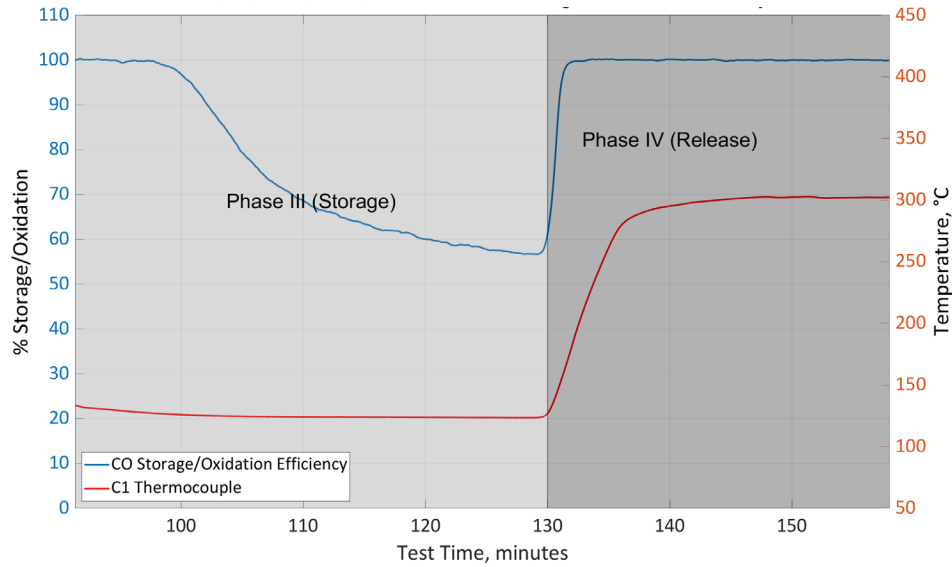
Figure 4.14 dCSC™ CO Storage/Oxidation Efficiency vs. Time during a 125 °C Phase III and 300 °C Phase IV, at Engine Condition 1

Figure 4.15 shows the steady state CO oxidation of the dCSC™ at different average volume weighted temperatures during Phases III and IV. The data in Figure 4.15 are from all the testing completed. At 150 °C, there is 100 % CO oxidation for the tests completed at engine condition 1. The 150 °C tests at engine condition 2 showed 90-99% CO oxidation. This is because at engine condition 2 (exhaust flow rate – 4.9 kg/min), the exhaust flow rate is 1.5 kg/min more than engine condition 1 (exhaust flow rate – 3.5 kg/min). Therefore, the dCSC™ is exposed to more molecules of CO at engine condition 2 than at engine condition 1. At temperatures above 150 °C the dCSC™ CO oxidation is 100%. The CO oxidation % decreases from 150 to 100 °C because the CO to CO_2 oxidation reaction rate is decreasing as temperature decreases. Also, the CO storage ability of the dCSC™ is being inhibited by H_2O in the exhaust at these low temperatures. However, from 100 to 80 °C the CO oxidation percentage increases. This is because the test at 80 °C was performed at engine condition 3 (exhaust flow rate – 2.6 kg/min) where the exhaust flow rate is 0.9 kg/min less than engine condition 1 (exhaust flow rate – 3.5 kg/min) where the 100 °C test was completed. Therefore, the dCSC™ is exposed to fewer molecules of CO at engine condition 3 than at engine condition 1. At temperatures

59

from 80 to 125 °C the dCSC™ showed 55 to 70% CO oxidation and 90 to 100% CO oxidation at temperatures from 150 to 400 °C.
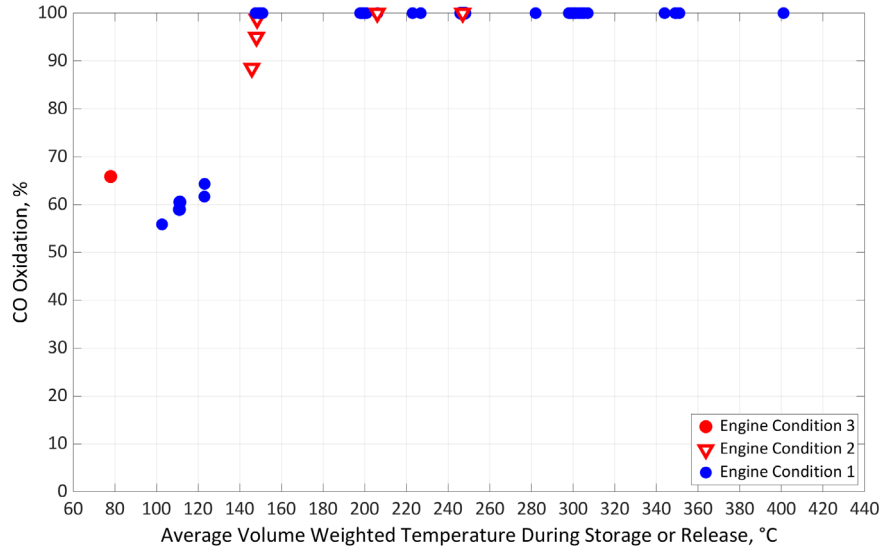
Figure 4.15 Downstream dCSC™ CO Oxidation % vs. Temperature

4.7   2D Temperature Distributions

Figure 4.16 shows the dCSC™ 2D temperature distribution for Phase III of control test 13 using the analysis methodology in Section 3.4.4. The temperature setpoint for the dCSC™ during Phase III of a control test is 200 °C. Each row of thermocouples (radial location) shows less than 6 °C temperature difference from the front to the back of the substrate. From the center of the dCSC™ to the outermost radius there is a 13 °C temperature difference between the furthest downstream thermocouple locations in each

60

row. The specific test name is shown in Figures 4.16 through 4.21, the names describe all the conditions for the test[1].
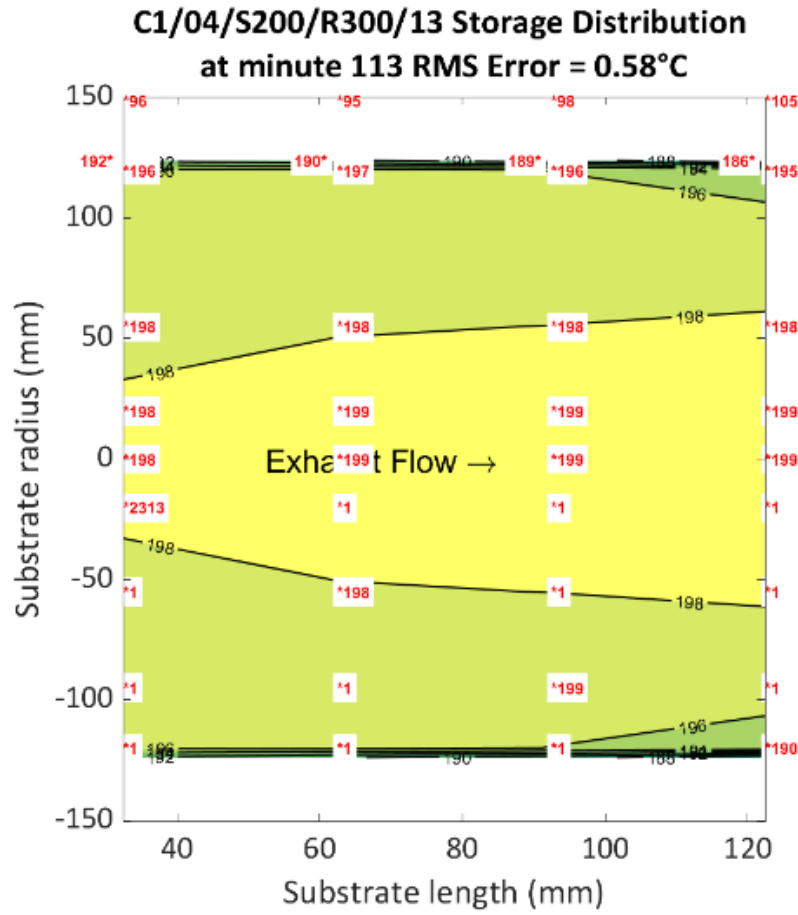
Figure 4.16 Control Test 13 at minute 113, dCSC™ Temperature 200 °C, Phase III 2D Temperature Distribution

[1] *Engine Condition/Test Number/Storage Temperature (°C)/Release Temperature (°C)/Indicates # of times the specific test has been run (02 = 2nd time running test). -TR1 indicates 20 °C/min ramp rate. -TR2 indicates

Figure 4.17 shows the dCSC™ 2D temperature distribution for a test with a 115 °C Phase III temperature. Differing from Figure 4.16, each row of thermocouples (radial location) shows less than 3 °C temperature difference from the front to the back of the substrate. From the center of the dCSC™ to the outermost radius there is a 6 °C temperature difference between the furthest downstream thermocouple locations in each row. Figure 4.16 showed larger temperature gradient's because the temperature setpoint was 200 °C, 75 °C higher than Figure 4.17, and room temperature is approximately the same.
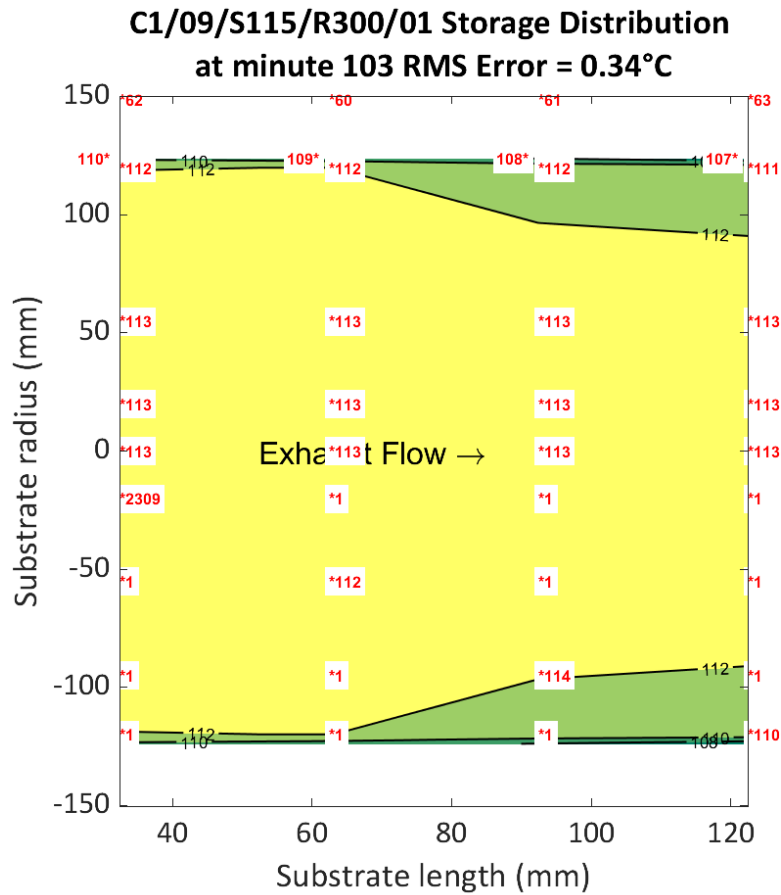
Figure 4.17 Test 9 minute 103, dCSC™ Temperature 115 °C, Phase III 2D Temperature Distribution

At the start of Phase IV, the dCSC™ temperature increases from the Phase III temperature setpoint to the Phase IV temperature setpoint. Figure 4.18 shows the dCSC™ 2D temperature distribution during this temperature increase. In this case it is plotted for

control test 13, where the temperature is increasing from 200 to 300 °C, at minute 119 when the dCSC™ temperature is approximately 250 °C. During this temperature increase there is a 20 °C temperature difference between the C1 and C4 thermocouples (front and back). There is also a 20 to 30 °C temperature difference from the center row of thermocouples to the outermost radius of the substrate.
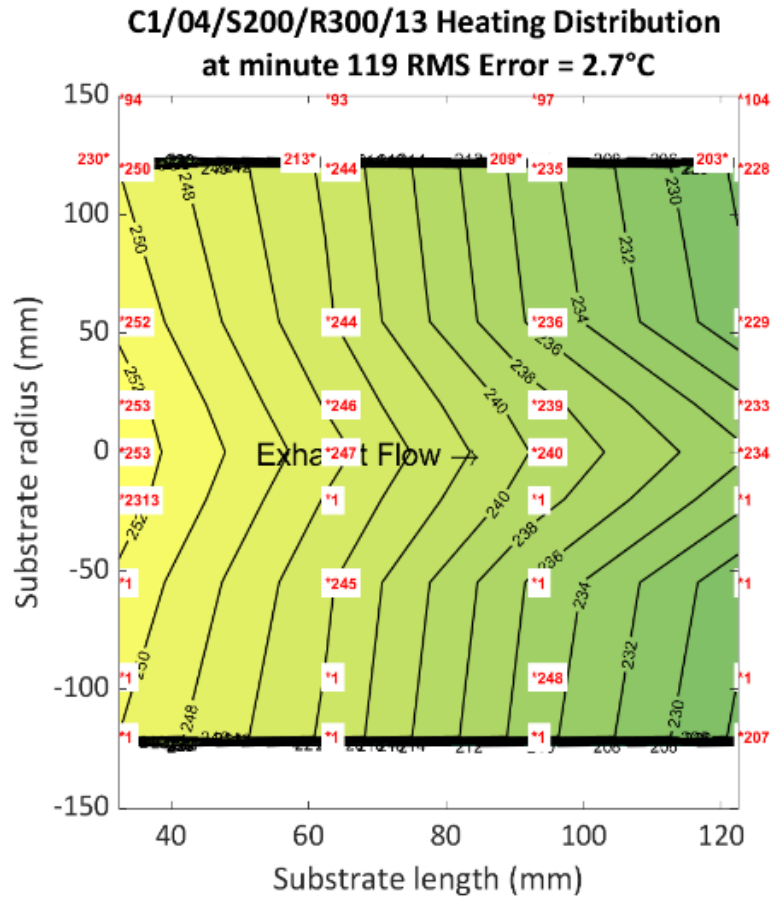
Figure 4.18 Control Test 13 at minute 119, dCSC™ Temperature Approximately 250°C, Phase IV Heating (from 200 to 300 °C) 2D Temperature Distribution

Figure 4.19 shows the dCSC™ 2D temperature distribution during a temperature increase from 115 to 300 °C during Phase IV. The 2D distribution is plotted at minute 119 when the temperature is approximately 250 °C. During this temperature increase within the dCSC™ there is a 30 °C temperature difference between the C1 and C4 thermocouples (front and back). This is 10 °C higher than in Figure 4.18 because the temperature ramp

63

starts at 115 °C in Figure 4.19 rather than 200 °C in Figure 4.18. Therefore, the dCSC™ temperature ramps an additional 75 °C in Figure 4.19 which makes the temperature gradient larger. There is also a 30 °C temperature difference from the center row of thermocouples to the outermost radius of the substrate, which is on the higher end of the same gradient in Figure 4.18.
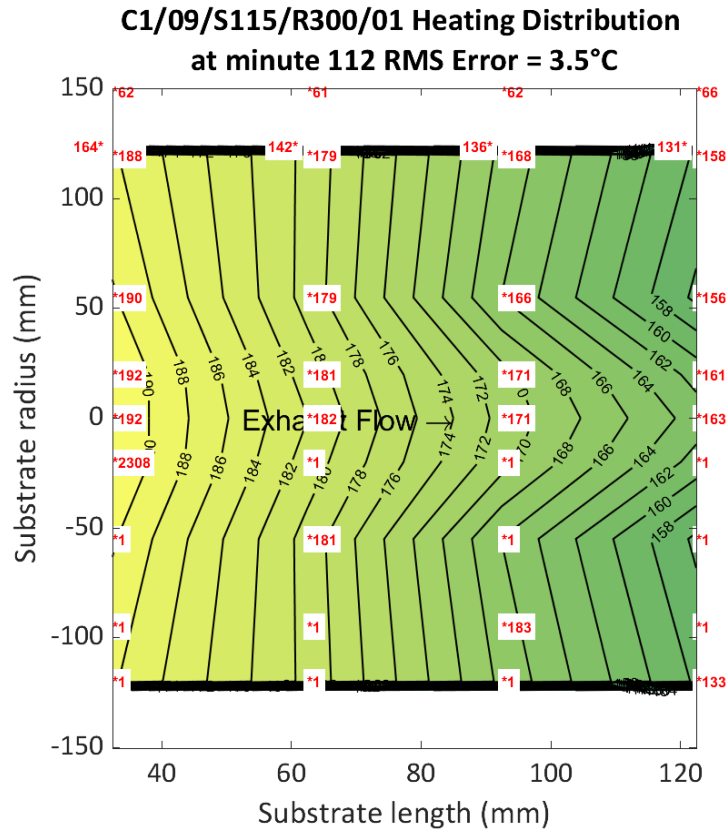
Figure 4.19 Test 9 minute 112, dCSC™ Temperature Approximately 175 °C, Phase IV Heating (from 115 to 300 °C) 2D Temperature Distribution

Figure 4.20 shows the dCSC™ 2D temperature distribution at test minute 149 of control test 13, when the dCSC™ has reached the 300 °C Phase IV temperature setpoint. Each row of thermocouples (radial location) shows less than 3 °C temperature difference from the front to the back of the substrate. From the center of the dCSC™ to the outermost radius there is a 26 °C temperature difference between the furthest downstream thermocouple locations in each row. This is twice the temperature difference from Figure

64

4.16. This is expected because the temperature setpoint is 100 °C higher in Figure 4.20 than 4.16, but the room temperature is approximately the same, providing a larger temperature gradient.
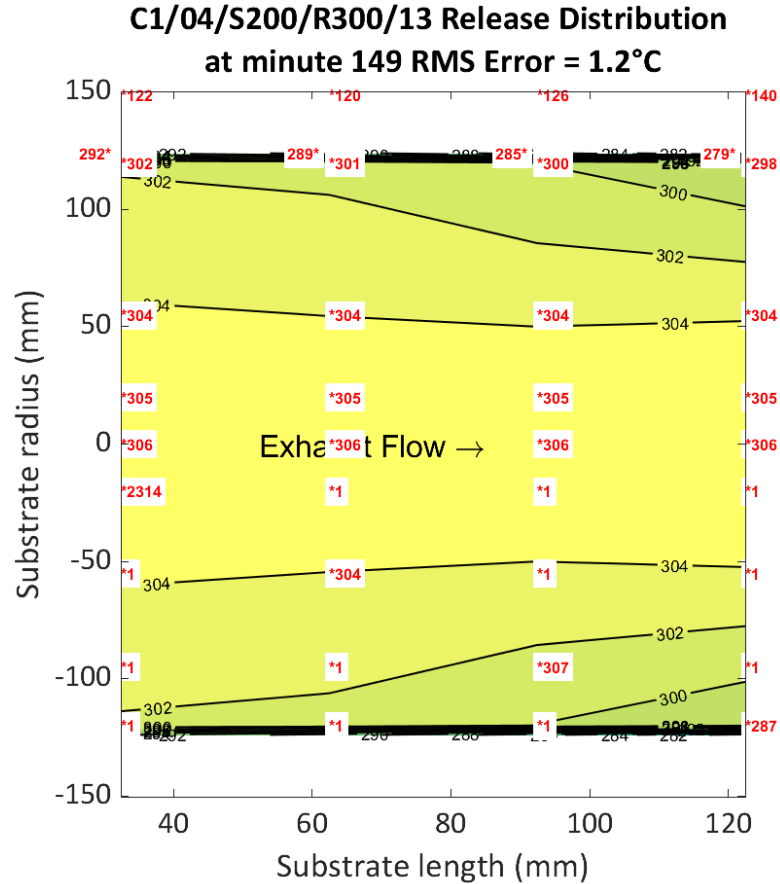
Figure 4.20 Control Test 13 at minute 149, dCSC™ Temperature 300 °C, Phase IV Release 2D Temperature Distribution

Figure 4.21 shows the dCSC™ 2D temperature distribution at test minute 140 of test 9, when the dCSC™ has reached the 300 °C Phase IV temperature setpoint. The temperature gradients between the thermocouples in each row, and between the rows, is within 1 °C of the temperature gradients in Figure 4.20. This is because the temperature setpoint is the same for Phase IV of both tests and test cell temperature is approximately the same. The RMS error for the dCSC™ 2D temperature distributions never exceeds 5 °C.

65
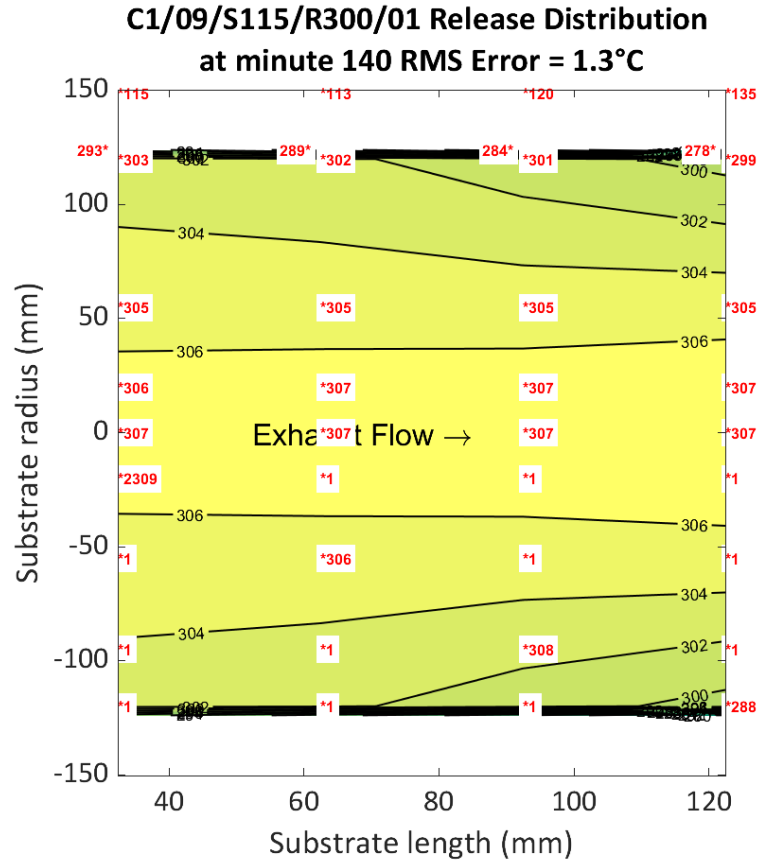
Figure 4.21 Test 9 minute 140, dCSC™ Temperature 300 °C, Phase IV Release 2D Temperature Distribution

4.8   Summary and Conclusions

A literature review was conducted to determine data and fundamentals of PNA devices that are available. An engine test cell and test procedure were developed as well as a statistical test matrix. The test cell instrumentation needed to acquire the data for the high-fidelity 2D flow through model of the dCSC™ was determined. Data analysis methods were developed to determine the dCSC™ performance characteristics from the experimental data. Over 200 hours of testing was completed on the Diesel Cold Start Concept Catalyst (dCSC™) with a 2013 Cummins ISB 6.7L 280 hp diesel engine.

The goal of the dCSC™ is to store NO, NO$_2$, CO, and HC emissions at temperatures below 200 °C where the current ATS is ineffective and release them at temperatures above 200 °C when the downstream ATS has increased its temperature. A list of conclusions from the experimental results are as follows.

1. Consistent with reference [8], the dCSC™ shows significant low temperature NOx storage capability, with peak NOx storage occurring from 125 to 150 °C.

2. Once the dCSC™ temperature has been at 500 °C while being exposed to exhaust gas from the diesel engine at 1660 rpm and 600 N-m for 5 hours and 30 minutes the 200 °C total NOx storage capacity reduces from approximately 0.6 to 0.5 g.NOx/L.Sub. After 9 hours and 10 minutes at these conditions the 200 °C dCSC™ total NOx storage capacity reduces from 0.5 to 0.4 g.NOx/L.Sub.

3. However, during the first 200-seconds of Phase III of testing, the 200 °C dCSC™ NOx storage capacity remained nearly constant at 0.3 g.NOx/L.Sub.

4. The ability of the dCSC™ to regain NOx storage capacity is dependent upon the release temperatures. If the dCSC™ temperature ramped through the 200 to 265 °C range, rapid NOx release was observed and the substrate released over 70% of the NOx stored on the substrate. At a release temperature of 350 °C, another rapid NOx release temperature range was observed and 70 to 90% of the NOx stored was released. This conclusion is supported by the data in reference [8].

5. The 250 to 350 °C temperature ramp is 60% more efficient at releasing NOx than the 250 to 300 °C temperature ramp.

6. The rapid NOx release temperature range of the dCSC™ occurs at temperatures above 200 °C. This is well within the operating temperature range of the aftertreatment system after the cold start period.

7. N$_2$O production was measured as a result of the HC lean NO reduction that occurs on the dCSC™, this is supported by the data in reference [1]. A peak N$_2$O concentration of 12 ppm was measured during a dCSC™ temperature ramp from an 80 °C Phase III to a 300 °C Phase IV. This indicates the upstream NO is

converted to downstream N_2O during the temperature ramp at the beginning of Phase IV, where NOx release is observed.

8. At temperatures from 200 to 400 °C, the dCSC™ shows 50% or greater NO to NO_2 oxidation. NO to NO_2 oxidation peaks at approximately 75% at 300 °C.

9. The dCSC™ also showed 50 to 70% CO oxidation at temperatures of 125 °C and below. At temperatures of 150 °C and above the dCSC™ oxidizes 90 to 100% of the CO emissions entering the substrate.

10. The RMS error of the dCSC™ 2D temperature distributions is less than 5 °C.

4.9 Future Work

Modeling of the dCSC™ substrate will take place now that the experimental data has been acquired. This model will be used to predict downstream dCSC™ emissions concentrations at specified conditions. In conjunction with the species model an accurate thermal model of the device will be developed from all of the temperature data acquired herein.

In order to improve the temperature measurements, it is recommended that an additional row of thermocouples be instrumented within the dCSC™ substrate. Details of this recommendation are in Appendix J.

Additional experimental research with accurate methods to measure upstream and downstream dCSC™ HC is needed. This needs to be done in order to calibrate the HC storage, release, and oxidation performance of the dCSC™.

The NOx storage capacity of the dCSC™ is finite, therefore, the faster the more robust downstream ATS reaches its operating temperature of over 200 °C, the better. Experimental research must be done to determine a reliable method for increasing the ATS temperature downstream of the dCSC™ as quickly as possible. Electric heaters, fuel burners, engine calibration, engine hardware, etc. have all been brought up as viable options [5, 11, 12, 13].

References

1. Chen, H., Mulla, S., Weigert, E., Camm, K. et al., "Cold Start Concept (CSC™): A Novel Catalyst for Cold Start Emission Control," *SAE Int. J. Fuels Lubr.* 6(2):2013, doi:10.4271/2013-01-0535. (2013)

2. "Modular Aftertreatment System," *Cummins Inc.* [Online]. Available: https://www.cummins.com/components/aftertreatment/modular-aftertreatment-system. [Accessed: 09-Nov-2019].

3. CARB, "California Air Resources Board Staff Current Assessment of the Technical Feasibility of Lower NOx Standards and Associated Test Procedures for 2022 and Subsequent Model Year Medium-Duty and Heavy-Duty Diesel Engines," CARB staff white paper, (2019).

4. "Cleaner Trucks Initiative," *EPA*, 21-Feb-2019. [Online]. Available: https://www.epa.gov/regulations-emissions-vehicles-and-engines/cleaner-trucks-initiative. [Accessed: 10-Nov-2019]. (2019)

5. Sharp, C., Webb, C., Neely, G., Sarlashkar, J. et al., "Achieving Ultra Low NOx Emissions Levels with a 2017 Heavy-Duty On-Highway TC Diesel Engine and an Advanced Technology Emissions System - NOx Management Strategies," SAE Int. J. Engines 10(4):2017, doi:10.4271/2017-01-0958. (2017)

6. Emission Standards, Available from: www.dieselnet.com.

7. "Low Load Cycle (LLC)," Emission Test Cycles: Low Load Cycle (LLC). [Online]. Available: https://www.dieselnet.com/standards/cycles/llc.php. [Accessed: 12-Nov-2019]. (2019)

8. Chen, H., Liu, D., Weigert, E., Cumaranatunge, L. et al., "Durability Assessment of Diesel Cold Start Concept (dCSC™) Technologies," SAE Int. J. Engines 10(4):2017, doi:10.4271/2017-01-0955. (2017)

9. Alissa Recker, "Fuel Contaminants, Effects on Aftertreatment, and Their Limits on NOx Stringency and Extended Useful Life", *presentation, University of Wisconsin Madison symposium on technologies to meet ultra-low NOx standards*. https://www.erc.wisc.edu/symposium2019.php. (2019)

10. Naseri, M., Aydin, C., Mulla, S., Conway, R. et al., "Development of Emission Control Systems to Enable High NOx Conversion on Heavy Duty Diesel Engines," SAE Int. J. Engines 8(3):2015, doi:10.4271/2015-01-0992. (2015)

11. Culbertson, D., Pradun, J., Khair, M., and Diestelmeier, J., "Development of Robust Electric Heating System for Medium Duty Diesel Vehicles," SAE Technical Paper 2017-01-0937, doi:10.4271/2017-01-0937. (2017)

12. Magee, Mark E. "Exhaust Thermal Management Using Cylinder Deactivation and Late Intake Valve Closing." MS Thesis, Purdue University, May, (2014)

13. Sharp, C., Webb, C., Neely, G., Carter, M. et al., "Achieving Ultra Low NOX Emissions Levels with a 2017 Heavy-Duty On-Highway TC Diesel Engine and an Advanced Technology Emissions System - Thermal Management Strategies," SAE Int. J. Engines 10(4):2017, doi:10.4271/2017-01-0954. (2017)

14. J. M. S. E. Control, "Ammonia slip catalysts," *JM Stationary Emissions Control*. [Online]. Available: https://www.jmsec.com/air-pollution-solutions/selective-catalytic-reduction-scr/ammonia-slip-catalysts/?L=0. [Accessed: 10-Nov-2019].

15. W. A. Majewski, "Selective Catalytic Reduction," *Selective Catalytic Reduction* [Online]. Available: https://www.dieselnet.com/tech/cat_scr.php. [Accessed: 10-Nov-2019]. (2005)

16. Sharp, C., Webb, C., Yoon, S., Carter, M. et al., "Achieving Ultra Low NOX Emissions Levels with a 2017 Heavy-Duty On-Highway TC Diesel Engine - Comparison of Advanced Technology Approaches," SAE Int. J. Engines 10(4):2017, doi:10.4271/2017-01-0956. (2017)

17. Zheng, Y., "Low-Temperature Pd/Zeolite Passive NOx Adsorbers: Structure, Performance, and Adsorption Chemistry." The Journal of Physical Chemistry C **121**(29): 15793-15803. (2017)

18. Chen, H. Y.; Collier, J. E.; Liu, D. X.; Mantarosie, L.; Duran-Martin, D.; Novak, V.; Rajaram, R. R.; Thompsett, D. Low Temperature NO Storage of Zeolite Supported Pd for Low Temperature Diesel Engine Emission Control. Catal. Lett. 2016, 146, 1706−1711. (2016)

19. S. Malamis, M.P. Harold, W.S. Epling, "Coupled NO and C3H6 Trapping, Release and Conversion on Pd-BEA: Evaluation of The Lean Hydrocarbon NO¬x Trap," in press, Ind. Eng. Chem. Res. (2019)

20. Vu, A.; Luo J.; Li, J.; Epling, W.S.; Effects of CO on Pd/BEA Passive NO_x Adsorbers. Catal. Lett. 2017, 147, 745-750. (2017)

21. "An Experimental Investigation of the Effect of Temperature and Space Velocity on the Performance of a Cu-Zeolite Flow-through SCR and a SCR Catalyst on a DPF with and without PM Loading," Vaibhav Kadam, MS Thesis, Michigan Technological University, (2016)

22. "An Experimental Investigation into NO2 Assisted Particulate Oxidation With and Without Urea and Active Regeneration of Particulate Matter in a SCR Catalyst on a DPF," Erik Gustafson, MS Thesis, Michigan Technological University, (2016)

23. "Catalyst Fundamentals," Catalyst Fundamentals. [Online]. Available: https://www.dieselnet.com/tech/cat_fund.php#rate. [Accessed: 11-Nov-2019].

24. Pihl, J., Majumdar, S.S., NO adsorption and desorption phenomena on a Pd-exchanged zeolite passive NOx adsorber, CLEERS Workshop, September 19, (2018)

25. Heywood, John B., Internal Combustion Engine Fundamentals. New York: McGraw-Hill, (1988)

26. James Sanchez, "EPA's Cleaner Trucks Initiative", *presentation, University of Wisconsin Madison symposium on technologies to meet ultra-low NOx systems.* https://www.erc.wisc.edu/symposium2019.php *(2019)*

27. W.A. Majewski, "Diesel Oxidation Catalyst," *Diesel Oxidation Catalyst* [Online]. Available: https://www.dieselnet.com/tech/cat_doc.php. [Accessed: 6-Dec-2019]. (2018)

28. Malamis, S., Ambast, M., Harold, M.P., Epling, Coupled NO and C3H6 trapping, release and conversion on Pd-BEA, W., CLEERS Workshop, September 19, (2018)

Appendix A.   Heater PID Tuning

Tuning of the heater PID controller was needed in order to achieve zero steady state temperature error. 10 °C temperature oscillations were observed when attempting to hold the temperature constant, as shown in Figure A.1. The C1, C2, C3, and C4 thermocouples are on the centerline of the dCSC™ substrate spaced evenly from front to back, respectively.
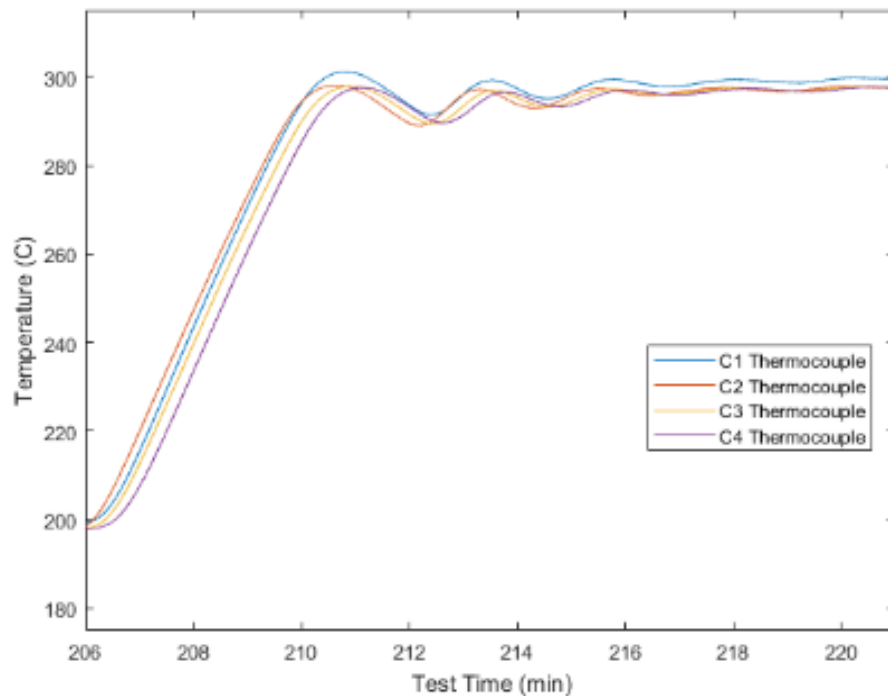
A.1 Watlow Heater Temperature Data Showing Oscillating Response

By tuning the heater controller all temperature oscillations were eliminated. As shown in Figure A.2, the dCSC™ thermocouple data achieve steady state readings.
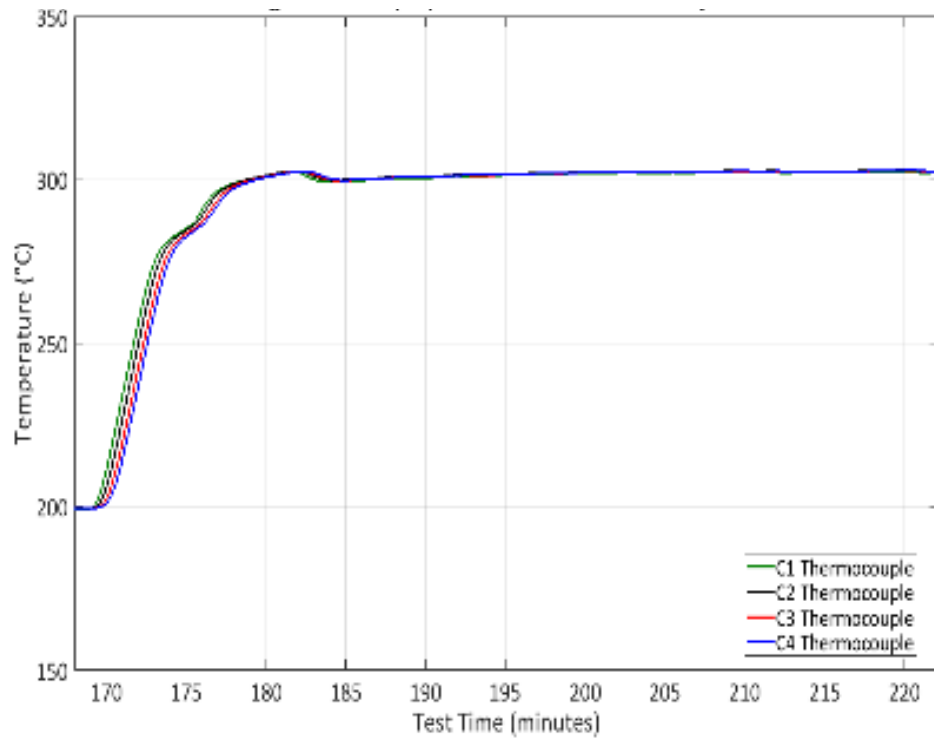
A.2 Watlow Heater Temperature Response Data After Tuning

Appendix B.　　　　Emissions Instrumentation

B.1　　　Pierburg 5-Gas Bench

The Pierburg 5-Gas bench was utilized to measure exhaust gas concentrations of CO, CO_2, NO, NO_2, and O_2. In addition, the bench is setup to measure exhaust gas concentrations from two different locations within the ATS. With the control of solenoid valves, air pressure regulates one-way valves open or closed. By opening one valve and closing another, it is possible to switch from upstream dCSC™ sampling to downstream sampling in seconds. A list of the measuring methods for each exhaust gas constituent is in Table B.1.

Table B.1 Pierburg 5-Gas Bench Analyzer Types

Exhaust Gas Constituent	Detection Method	Notes:
O_2	Paramagnetic	
CO_2	IRD	
CO	IRD	
NO	Chemiluminescence	
NO_2	NO_2 to NO converter, Chemiluminescence	
Total Hydrocarbons	Flame Ionization (FID)	Not able to measure with current sampling system.

NO_2 is not directly measured, it is first converted from NO_2 to NO and then measured with the Pierburg Chemiluminescence detection system. Due to the long lengths of sample line from the ATS, total hydrocarbons could not be measured with the Pierburg FID.

74

B.2   Cambustion Fast NO and NOx CLD

Cambustion's fNO400 CLD Fast Response NO measuring system was used to measure NO and NOx downstream of the dCSC™. In order to measure total NOx, a NO_2 to NO converter was placed in line with channel 2 of the fNO400 system. Figures B.1 and B.2 illustrate the Cambustion sampling system. Figure B.1 shows the sampling locations of both Cambustion channels (Fast NO and Fast NOx), a production NOx sensor, and the downstream sample location for the Pierburg 5-gas bench and Thermo Fisher N_2O analyzer.
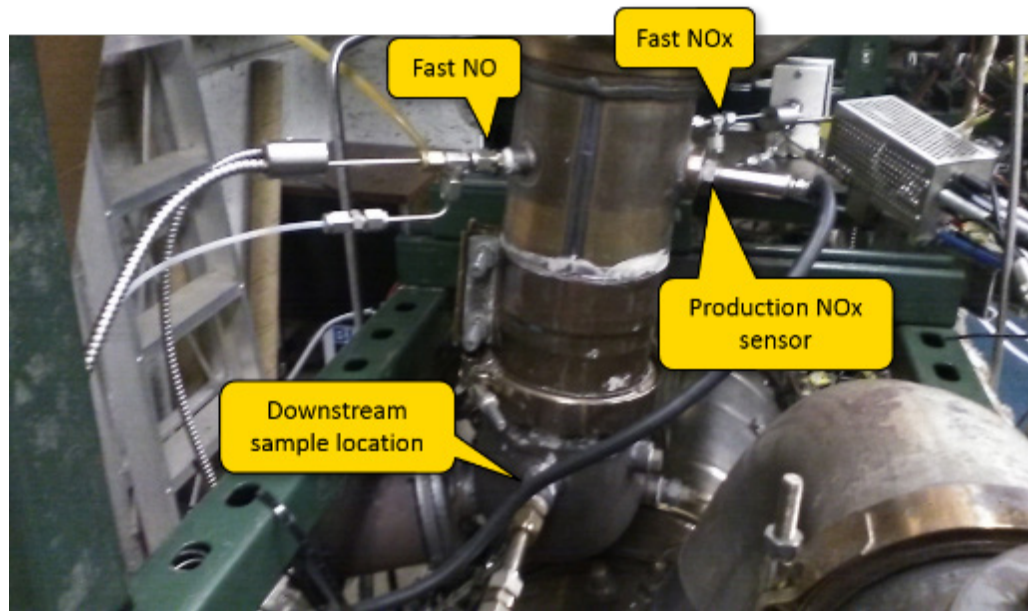
B.1 Downstream dCSC™ NOx Sample Locations.

Figure B.2 shows the NO_2 to NO converter placed directly in line with the Cambustion fNO400 channel 2 sampling system. Fittings were fabricated in order to allow the converter to be mounted in between the sample probe and sample head.
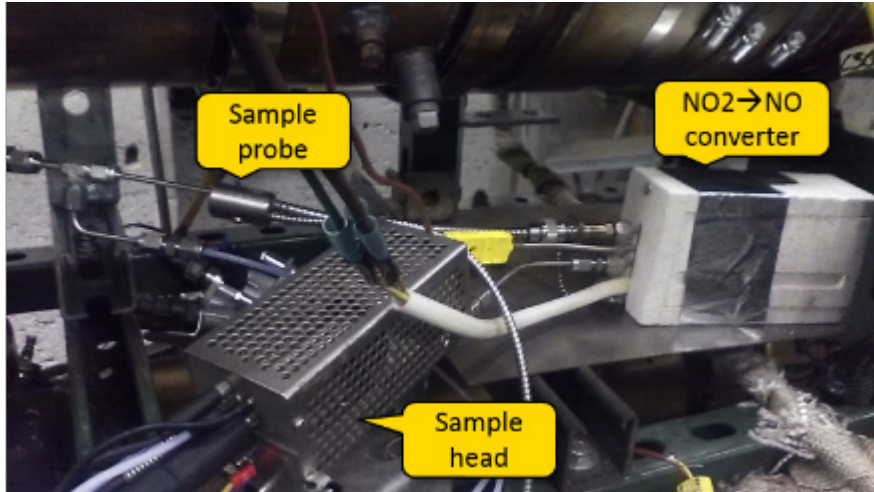
B.2 Cambustion fNO400 CLD NOx Channel Setup

The Cambustion fNO400 CLD Fast Response system has a 4 ms response time of the CLD output from 90% to 10% NO concentration. This is in response to a step input at the sample source. Insitu calibration is achieved via flooding the entire sampling system with calibration gas.

B.3   Cambustion HFR 400 Fast FID

A Cambustion HFR 400 Fast FID measured total hydrocarbon concentrations in the exhaust. Similar to the fNO400 CLD system the HFR 400 has two measuring channels, insitu calibration, and a 4 ms 10-90% response time of the FID output for a step input at the source. The FID fuel is pure hydrogen (H_2).

B.4   Thermo Fisher 46i N_2O IRD

The range of this analyzer is 0 to 50 ppm with a 60 s 10-90% response time to a step input. This system samples in parallel with the Pierburg 5-gas bench. It was initially a concern that CO_2 might cause and interference while measuring N_2O. In Figure B.3, it is shown that the N_2O analyzer does measure a concentration of N_2O when exposed to a constant CO_2 concentration. However, the CO_2 concentration during testing is constant, therefore the interference is constant. By taking an upstream dCSC™ measurement with

the N_2O analyzer, the constant CO_2 interference can be accounted for. The N_2O measurement upstream of the dCSC™ is subtracted from the N_2O measurements downstream of the dCSC™. The N_2O analyzer was logged in LabVIEW.
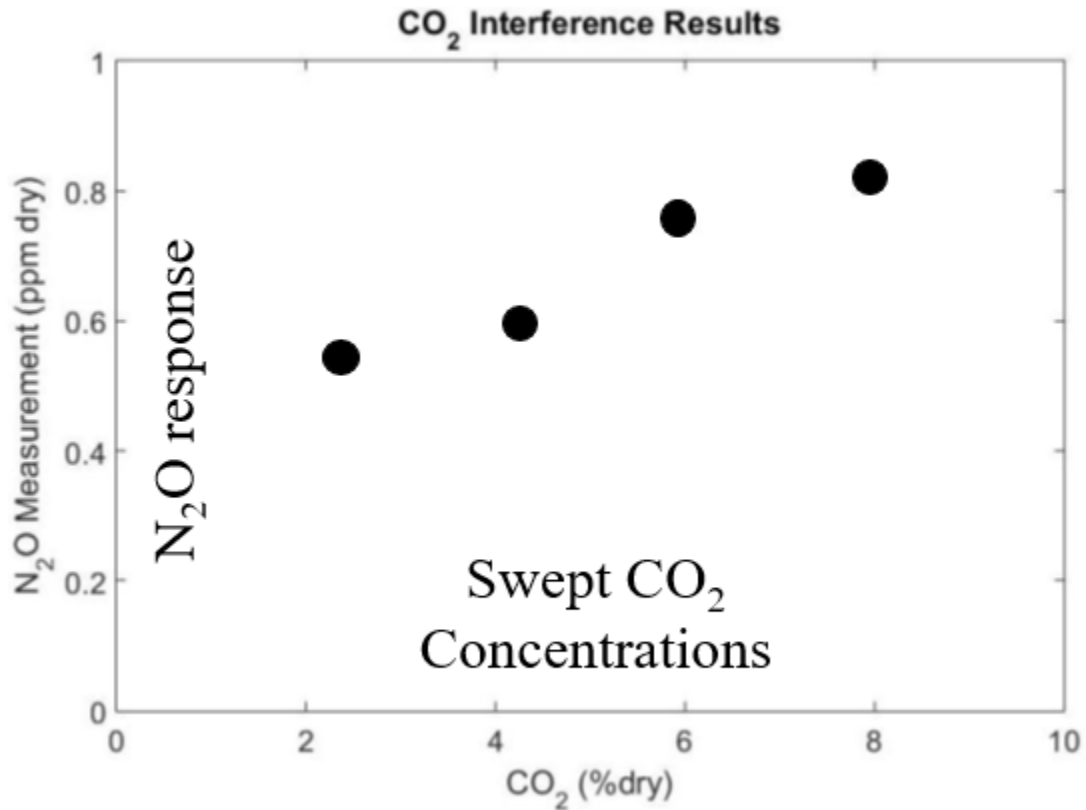
B.3 N_2O Analyzer CO_2 Concentration Interference

B.5   NOx Sensors

Two production NOx sensors are setup to measure engine out NOx and downstream dCSC™ NOx concentrations. The error of these sensors is +- 10 ppm or 10%, whichever is greater. The sensors' output were logged using Cummins Calterm Software. In order to ensure the NOx sensors were on at all times, the ATS temperature sensors were clamped in a heater to keep them above 200 °C during testing. If these sensors dropped below 200 °C, the NOx sensors would shut off to protect them from condensation.

77

Appendix C. Paragon ULSD #2 Fuel Analysis Results

Table C.1 Paragon ULSD #2 Fuel Analysis Results

ANALYTICAL RESULTS

Workorder: 224870 MICH TECH-080618

Lab ID:	2248700001		Date Collected: 11/27/2017 00:00		Matrix: Diesel
Sample ID:	#2 ULSD		Date Received: 8/6/2018 15:42		
Sample Desc:			PO: CC ON FILE		

Parameters	Qualifier	Result Units	Dilution Factor	Reporting Limit	Result Qualifier Min	Result Qualifier Max	Analyzed	By
Elemental Analysis								
Analytical Method: ASTM D5291 D [A]								
Carbon (Wt%)		86.55 % m/m	1	0.05			8/10/2018 15:01	PRS
Hydrogen (Wt%)		13.45 % m/m	1	0.05			8/10/2018 15:01	PRS
Individual Parameters								
Analytical Method: ASTM D4052 [A]								
API Gravity at 15.56°C		34.5 °API	1	0.1			8/13/2018 10:28	VUA
Density at 15.56°C		0.8516 g/mL	1	0.0001			8/13/2018 10:28	VUA
Spec. Grav. at 15.56°C/15.56°C		0.8524	1	0.0001			8/13/2018 10:28	VUA
Analytical Method: ASTM D240 [A]								
Gross Heating Value (BTU/lb)		19669 BTU/lb	1	175			8/8/2018 09:54	AJB2
Gross Heating Value (MJ/kg)		45.749 MJ/kg	1				8/8/2018 09:54	AJB2
Net Heating Value (BTU/lb)		18442 BTU/lb	1	175			8/8/2018 09:54	AJB2
Net Heating Value(MJ/kg)		42.895 MJ/kg	1				8/8/2018 09:54	AJB2
Analytical Method: ASTM D613 [A]								
Cetane No.		51.7	1				8/9/2018 13:08	PRS
Stoichiometric Ratios								
Analytical Method: SAE J1829								
Air/Fuel Ratio (CH-based)		14.58	1	0.01			8/13/2018 12:46	PRS
H/C Atomic Ratio		1.852	1	0.001			8/13/2018 12:46	PRS

78

Appendix D.   Experimental Testing Matrix

Table D.1 Experimental Testing Matrix

Run Order	Test Name	Engine Condition	Phase III Storage Temp. (°C)	Phase IV Release Temp. (°C)	Temp. Ramp (°C/minute)
22	C1/01/S100/R300	1	100	300	N/A
6	C1/02/S125/R300	1	125	300	N/A
3	C1/03/S150/R300	1	150	300	N/A
16	C1/04/S200/R300	1	200	300	N/A
11	C1/05/S225/R300	1	225	300	N/A
7	C1/06/S250/R300	1	250	300	N/A
17	C1/07/S200/R350	1	200	350	N/A
14	C1/08/S250/R350	1	250	350	N/A
8	C2/09/S115/R300	2	115	300	N/A
5	C2/10/S150/R300	2	150	300	N/A
21	C2/11/S200/R300	2	200	300	N/A
19	C2/12/S250/R300	2	250	300	N/A
15	C1/13/S150/R200	1	150	200	N/A
1	C1/14/S150/R250	1	150	250	N/A
23	C1/15/S150/R300	1	150	300	N/A
2	C1/16/S150/R350	1	150	350	N/A
4	C1/17/S150/R400	1	150	400	N/A
18	C2/18/S150/R300	2	150	300	N/A
13	C2/19/S150/R350	2	150	350	N/A
9	C1/20/S125/R300	1	125	300	N/A
20	C1/21/S200/R300	1	200	300	N/A
10	C1/22/S150/R350 - TR1	1	150	350	20
12	C1/23/S150/R350 - TR2	1	150	350	40
24	C3/24/S080/R300	3	80	300	N/A
25	C1/25/S150/R450	1	150	450	N/A

*Engine Condition/Test Number/ Phase III Storage Temperature (°C)/Phase IV Release
Temperature (°C)/Indicates # of times the specific test has been run (02 = 2nd time
running test). -TR1 indicates 20 °C/min ramp rate. -TR2 indicates

79

Appendix E.   Calculation of dCSC™ Volume Weighted Temperature

First, the total volume of instrumented dCSC™ is calculated using Equation D.1.

$$V_{T.V.} = \pi * r_{T.V.}{}^2 * L_{T.V.}$$ E.1

Where $V_{T.V.}$ is the instrumented dCSC™ total volume, $r_{T.V.}$ is the outermost radius of the instrumented dCSC™, and $L_{T.V.}$ is the total length of the instrumented dCSC™. The radius of cylindrical volume that each thermocouple represents is calculated by Equation D.2.

$$r_W = \sqrt{\frac{r_{O.T.}{}^2 + r_{T.C.}{}^2}{2}}$$ E.2

Where r_W is the radius of cylindrical volume that the thermocouple represents. $r_{O.T.}$ is the radial location of the next outer thermocouple and $r_{T.C.}$ is the radial location of the thermocouple being weighted. The axial length of dCSC™ substrate each thermocouple represents is calculated using Equation D.3.

$$L_{T.C.} = \frac{L_U}{2} - \frac{L_D}{2}$$ E.3

$L_{T.C.}$ is the axial length of substrate that the thermocouple represents. L_U is the axial length of substrate to the next thermocouple or dCSC™ edge upstream and L_D is the axial length of substrate to the next thermocouple or dCSC™ edge downstream. Equation D.4 is then used to calculate the dCSC™ volume that each thermocouple represents.

$$V_{T.C.} = (\pi * r_W{}^2 * L_{T.C.}) - V_{I.T.C.}$$ E.4

$V_{T.C.}$ is the dCSC™ volume each thermocouple represents and $V_{I.T.C.}$ is the volume represented by the next inner radial thermocouple. Equation D.5 is used to calculate the weight applied to each thermocouple reading.

$$W_{T.C.} = \frac{V_{T.C.}}{V_{T.V.}} \qquad\qquad \text{E.5}$$

$W_{T.C.}$ is the weight applied to each thermocouple reading. $V_{T.C.}$ is the volume that each thermocouple represents and $V_{T.V.}$ is the total volume of instrumented dCSC™. From Equation D.5 and the thermocouple readings, Equation D.6 was developed to calculate the dCSC™ volume weighted temperature.

$$T_{V.W.} = \sum_{i=1}^{24} \left(W_{T.C.(i)} * T_{T.C.\ (i)} \right) \qquad\qquad \text{E.6}$$

Where $T_{V.W.}$, is the volume weighted temperature of the dCSC™ substrate and $T_{T.C.\ (i)}$ is the reading of each thermocouple used in the calculation. $W_{T.C.(i)}$ is the weight applied to each corresponding thermocouple reading. The thermocouples' used in Equation D.6 are C1-20 and C25 – C28.

Appendix F. Emissions Timeplots During Testing
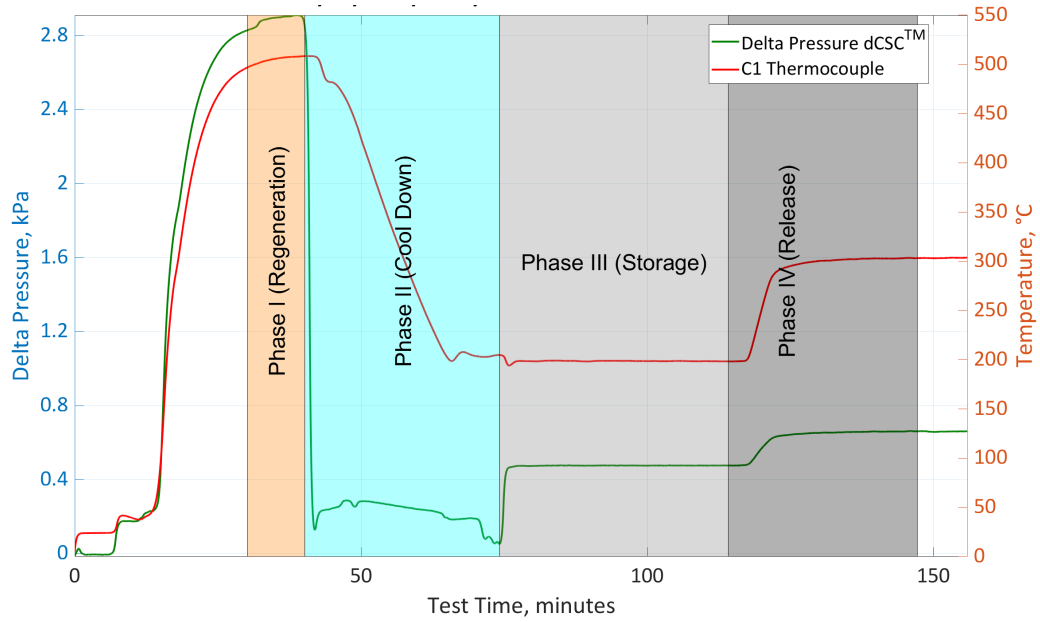
F.1 Control Test dCSC™ Delta Pressure during Test Phases I-IV
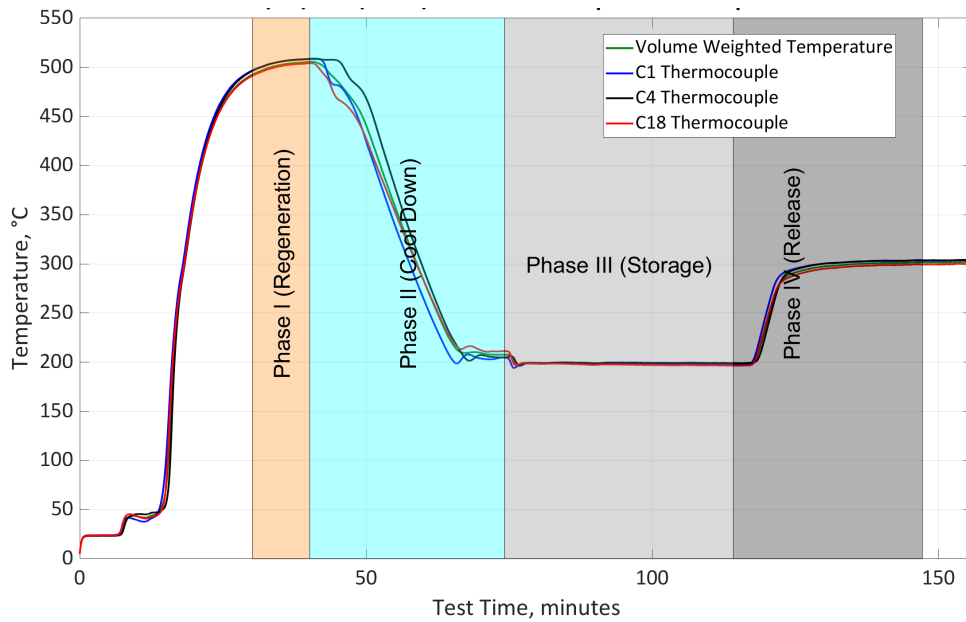
F.2 Control Test dCSC™ Temperature during Test Phases I-IV

82
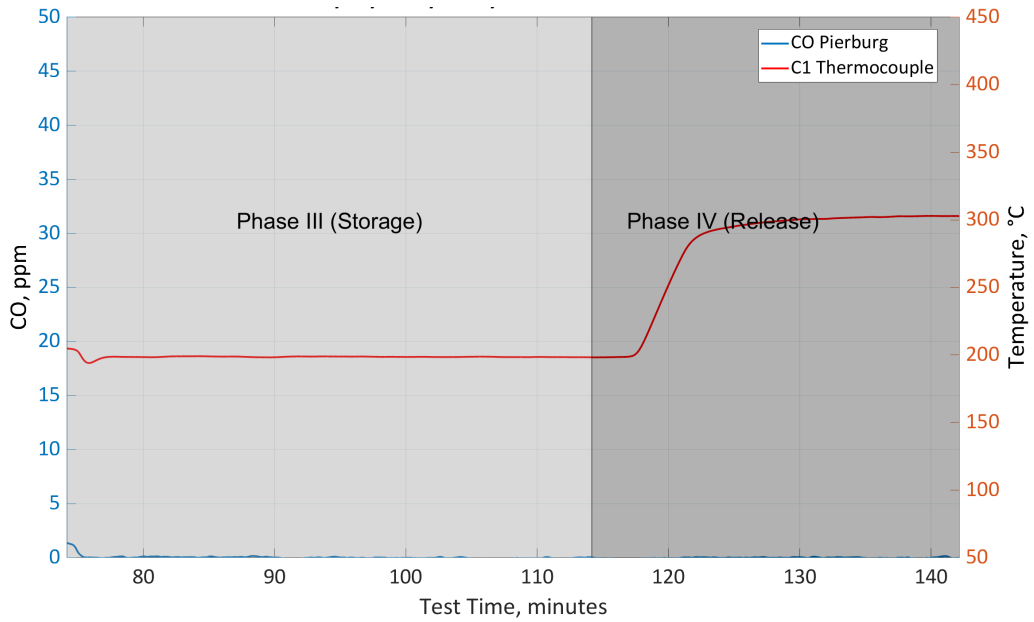
F.3 Downstream dCSC™ CO Concentration during a 200 °C Test Phase III and 300 °C Phase IV, at Engine Condition 1
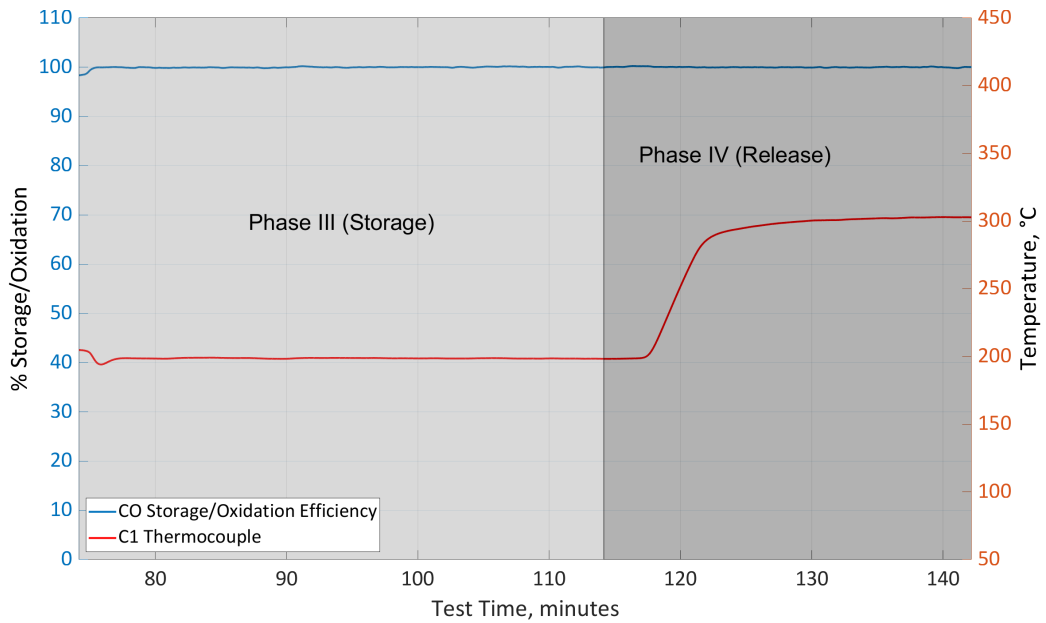
F.4 dCSC™ CO Storage/Oxidation Efficiency during a 200 °C Test Phase III and 300 °C Phase IV, at Engine Condition 1
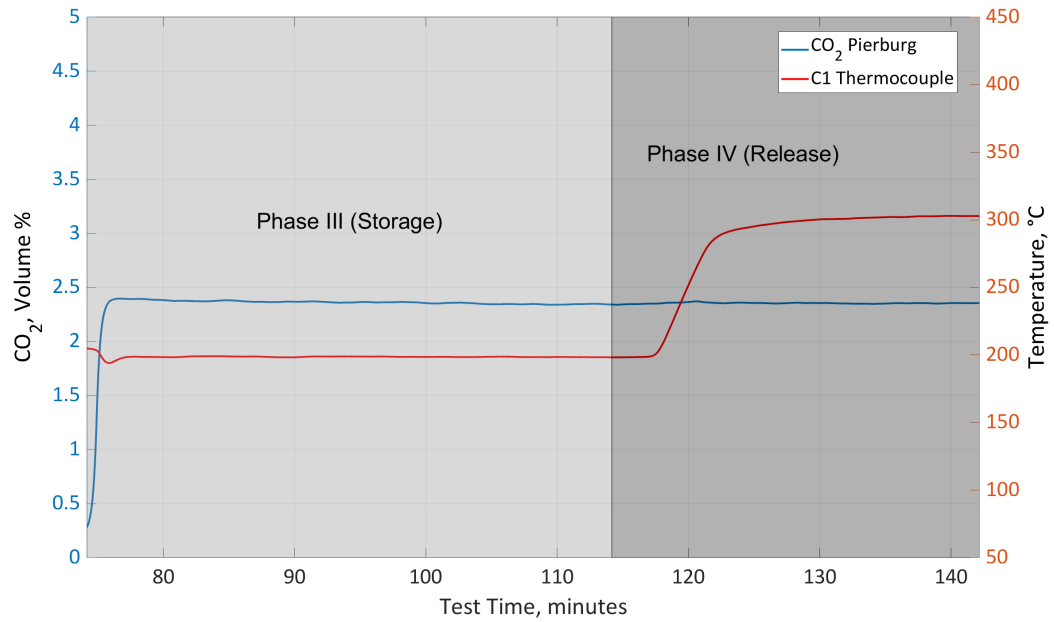
F.5 Downstream dCSC™ CO_2 Concentration during a 200 °C Test Phase III and 300 °C Phase IV, at Engine Condition 1
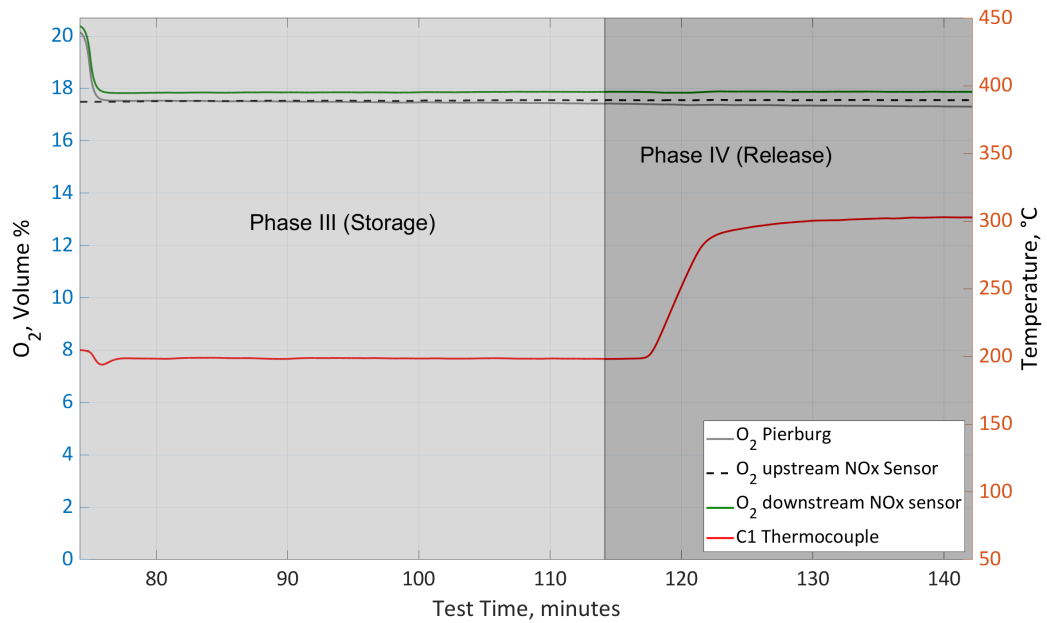
F.6 Downstream dCSC™ CO_2 Concentration during a 200 °C Test Phase III and 300 °C Phase IV, at Engine Condition 1
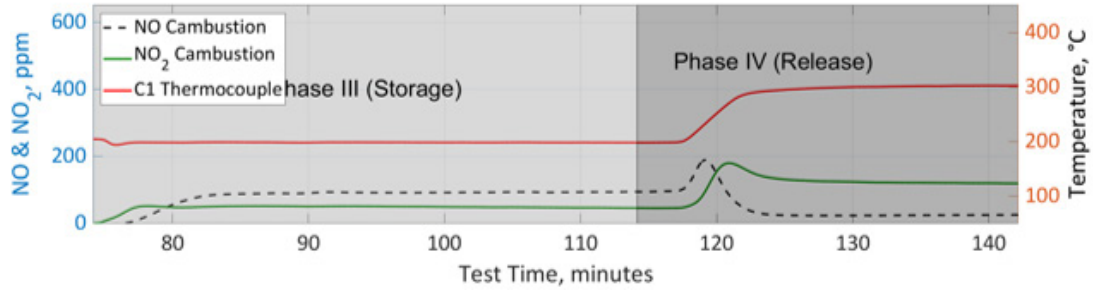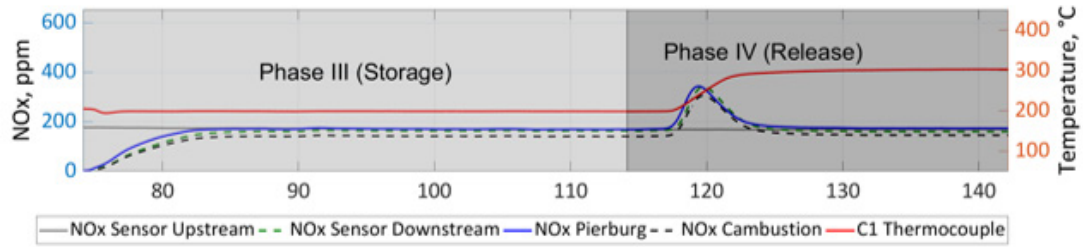
F.7 Downstream dCSC™ NO, NO$_2$, and NOx Concentrations during a 200 °C Test Phase III and 300 °C Phase IV, at Engine Condition 1
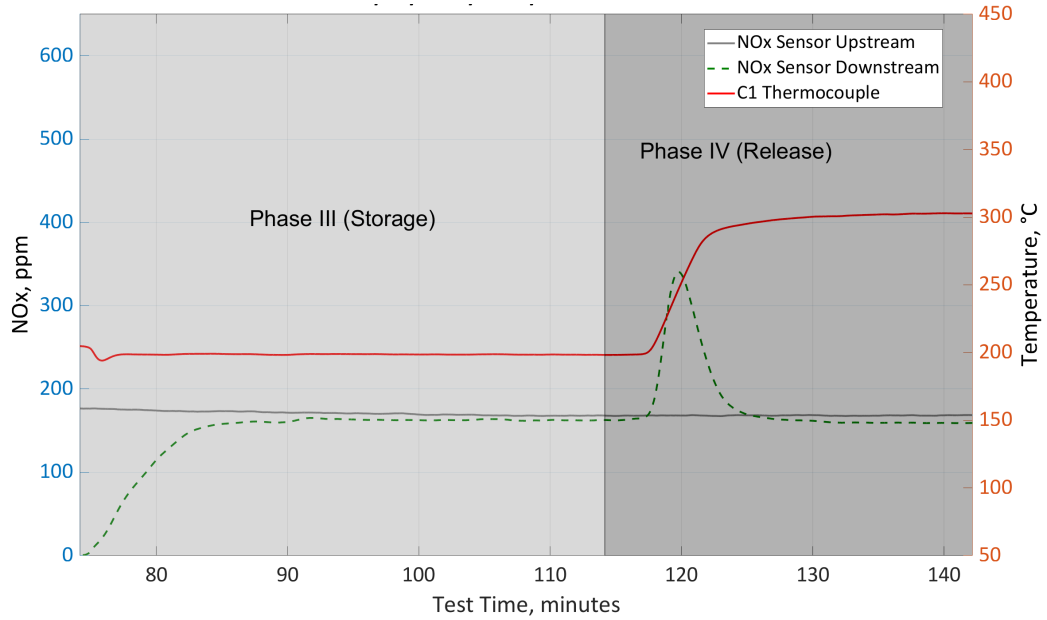
F.8 Downstream dCSC™ NOx Sensor Concentrations during a 200 °C Test Phase III and 300 °C Phase IV, at Engine Condition 1

85
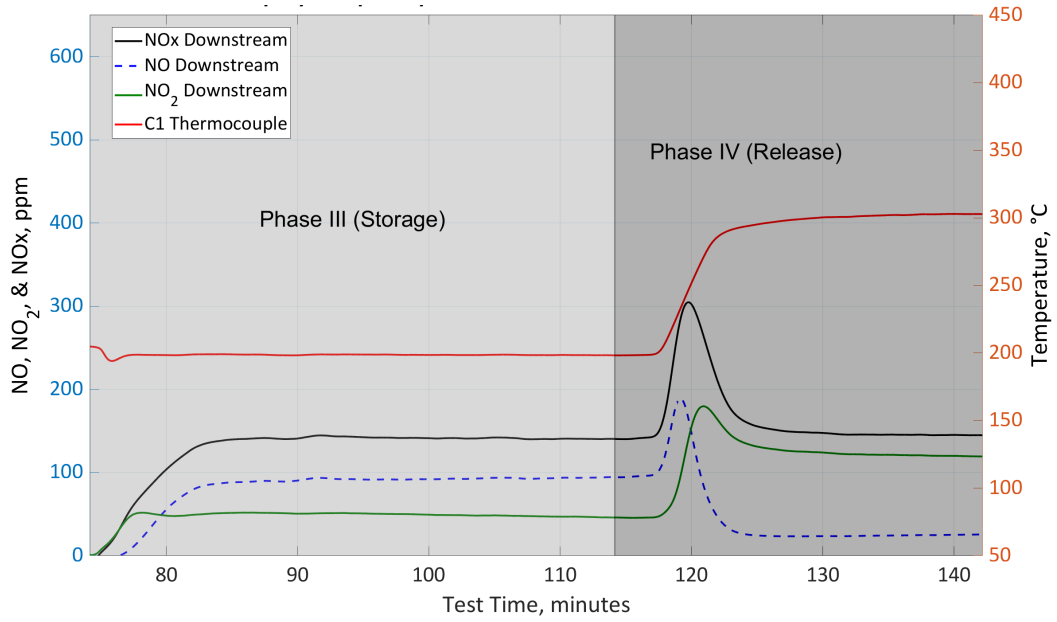
F.9 Downstream dCSC™ Cambustion CLD NO, NO$_2$, and NOx Concentrations during a 200 °C Test Phase III and 300 °C Phase IV, at Engine Condition 1
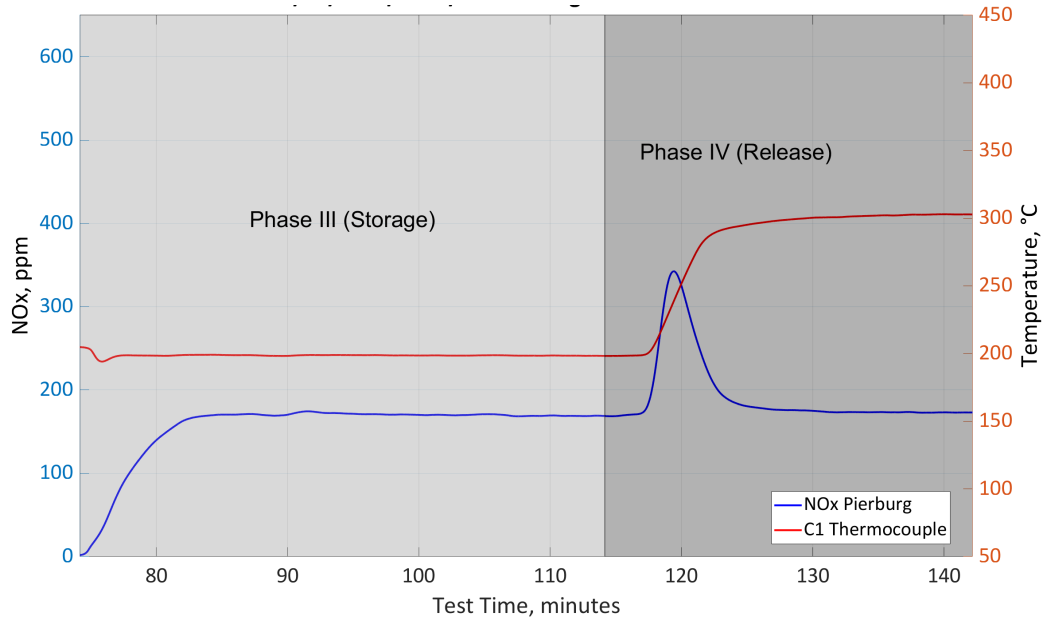
F.10 Downstream dCSC™ NOx Concentrations during a 200 °C Test Phase III and 300 °C Phase IV, at Engine Condition 1

86
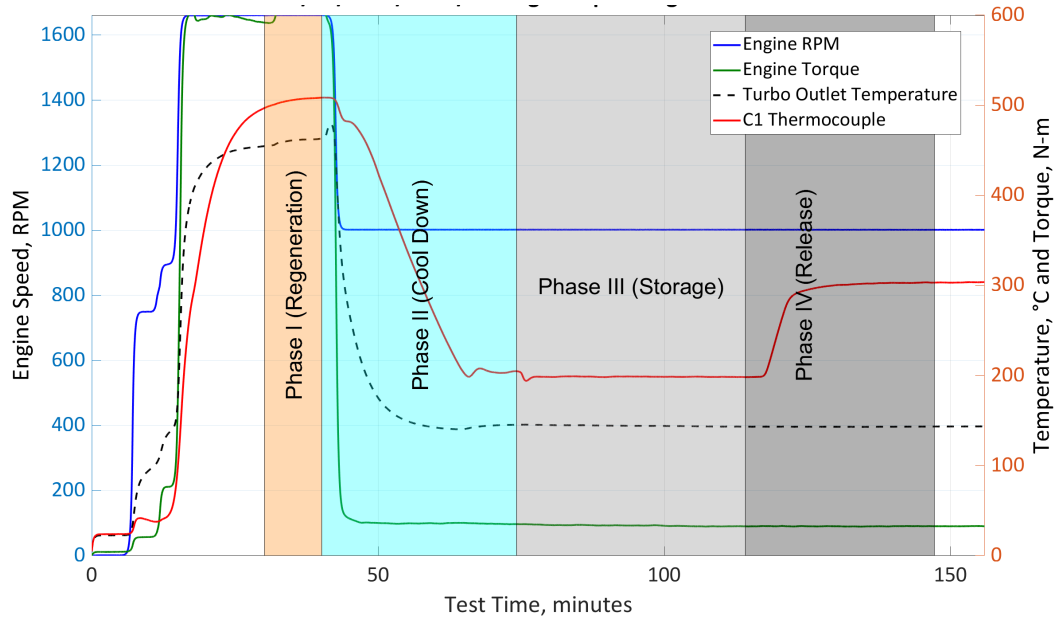
F.11 Engine Load and Speed, Turbo Outlet Temperature, and C1 Thermocouple Temperature during a 200 °C Test Phase III and 300 °C Phase IV, at Engine Condition 1
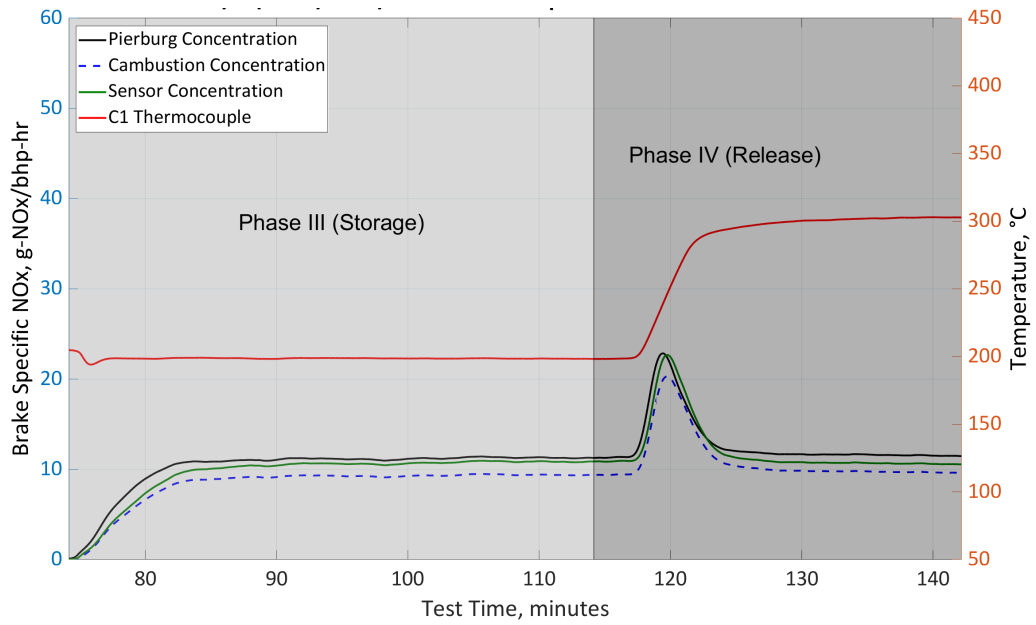
F.12 Downstream dCSC™ Brake Specific NOx during a 200 °C Test Phase III and 300 °C Phase IV, at Engine Condition 1

87

Appendix G.   Control Plots

Appendix G shows control plots for the various lab instrumentation and testing conditions monitored during testing. Test run order refers to the order in which the tests were run. Certain engine and test cell conditions were measured with lab instrumentation and are also measured with sensors on the engine or calculated by the Cummins Calterm calibration tool. The values measured with lab instrumentation were logged with NI LabVIEW DAQ hardware and software. These values are referred to in the plot legend as LabVIEW. The values measured with sensors on the engine or calculated by Calterm are referred to in the plot legend as Calterm.
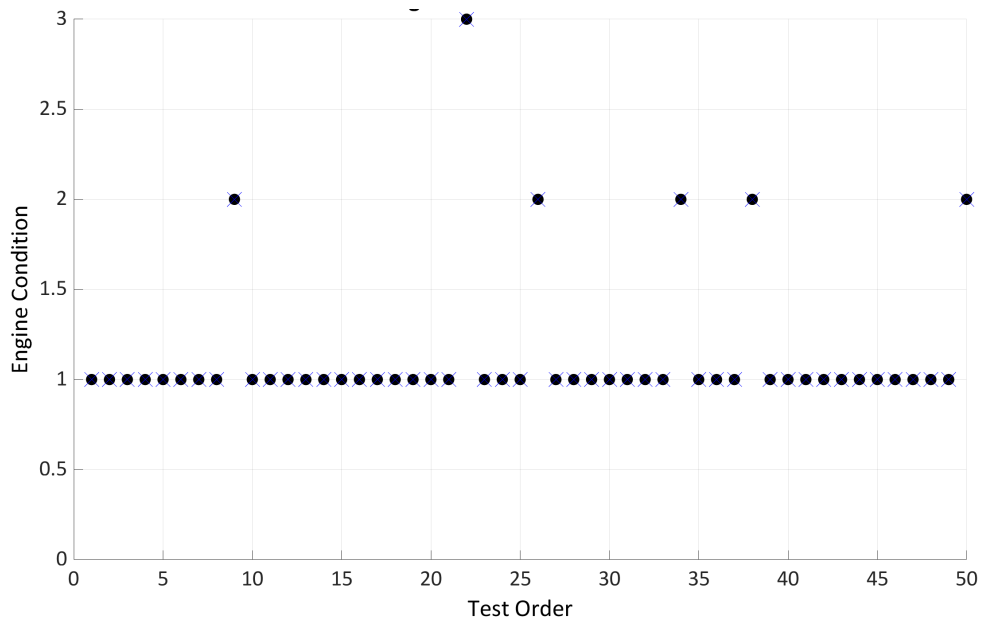
G.1 Engine Condition vs. Test Order
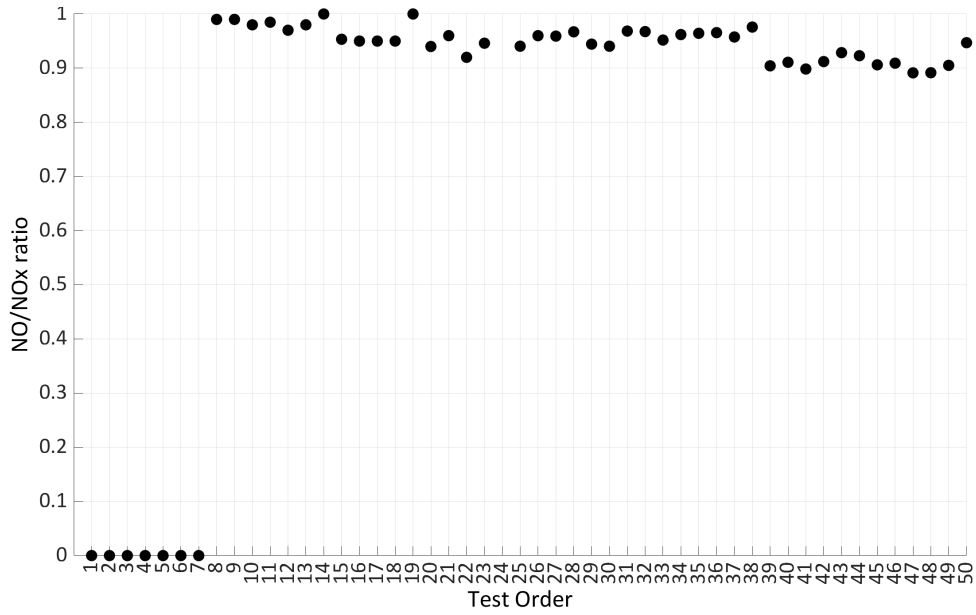
G.2 Upstream dCSC™ NO/NOx Ratio vs. Test Order
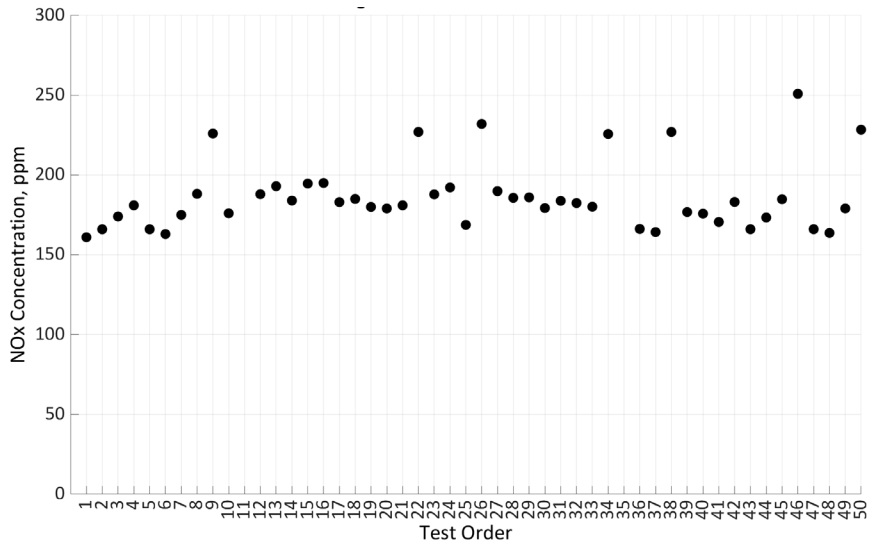
G.3 Upstream dCSC™ NOx Sensor NOx Concentration vs. Test Order

89
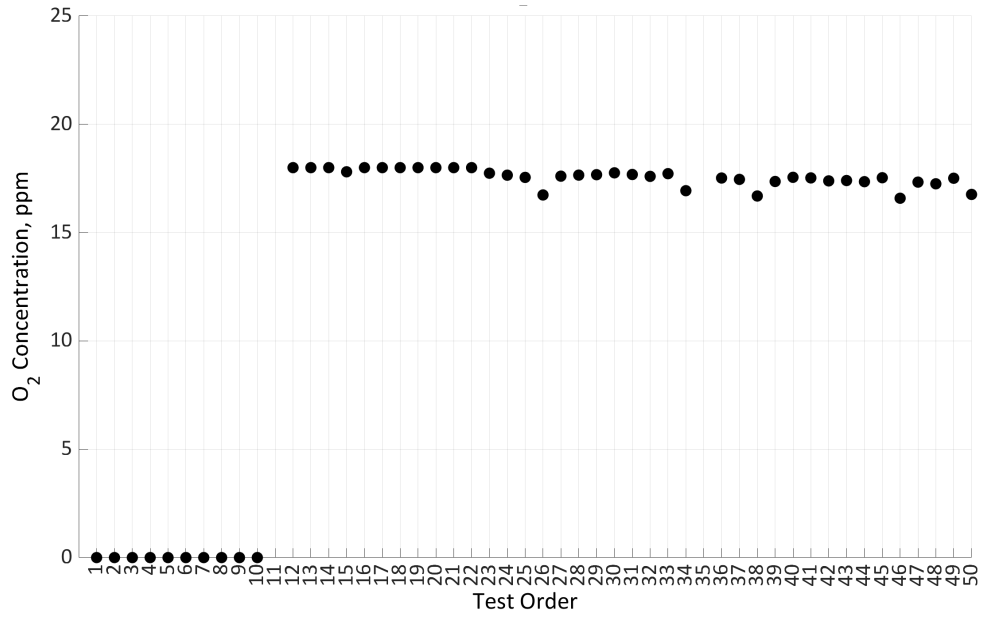
G.4 Upstream dCSC™ NOx Sensor O_2 Concentration vs. Test Order
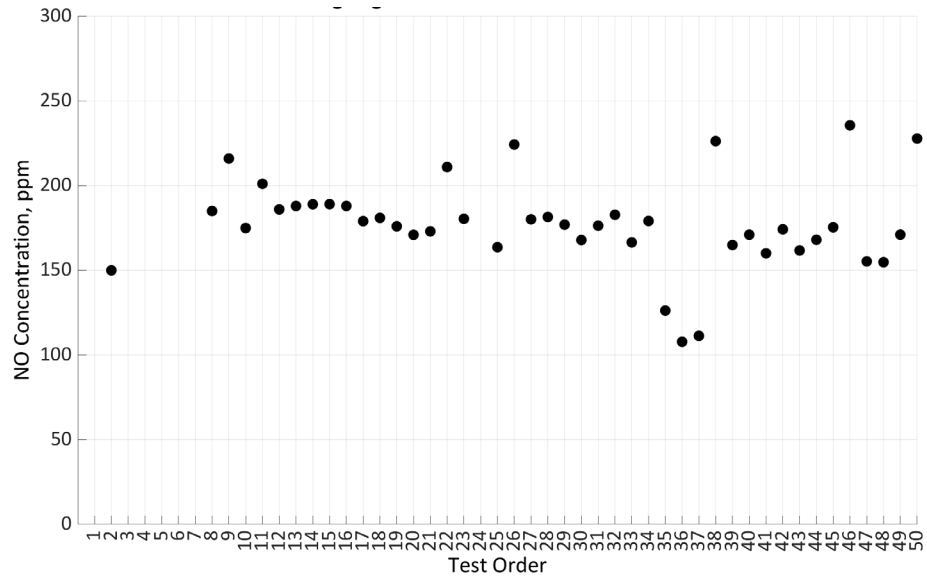
G.5 Upstream dCSC™ Pierburg NO Concentration vs. Test Order

90
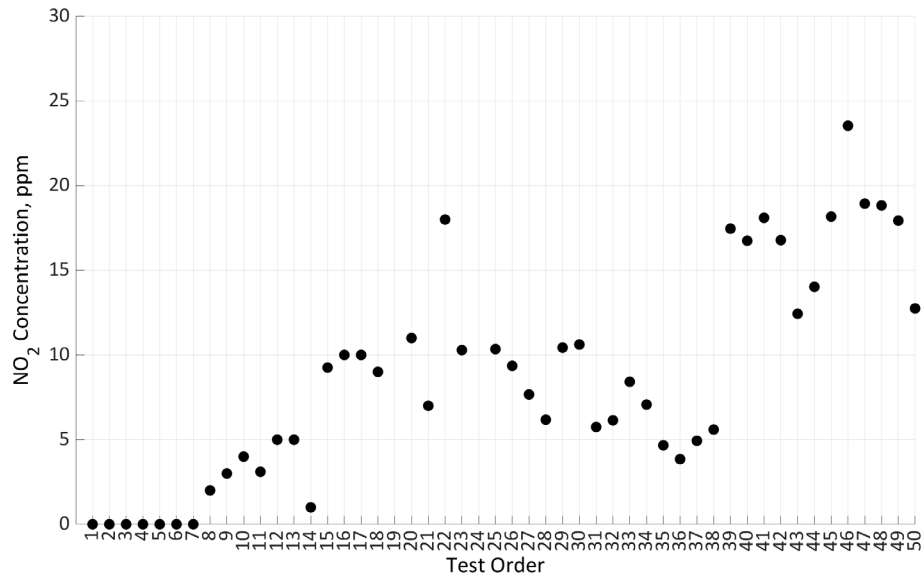
G.6 Upstream dCSC™ Pierburg NO_2 Concentration vs. Test Order
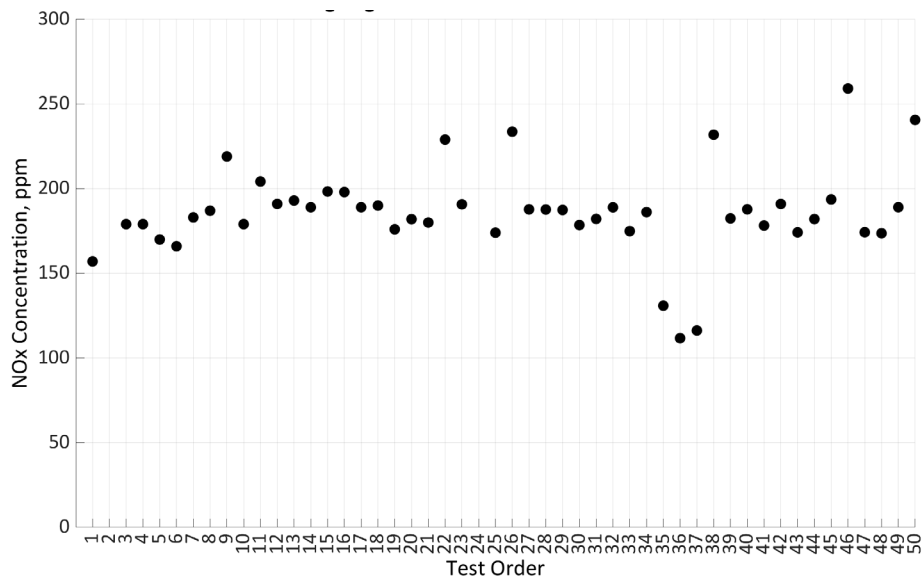
G.7 Upstream dCSC™ Pierburg NOx Concentration vs. Test Order

91
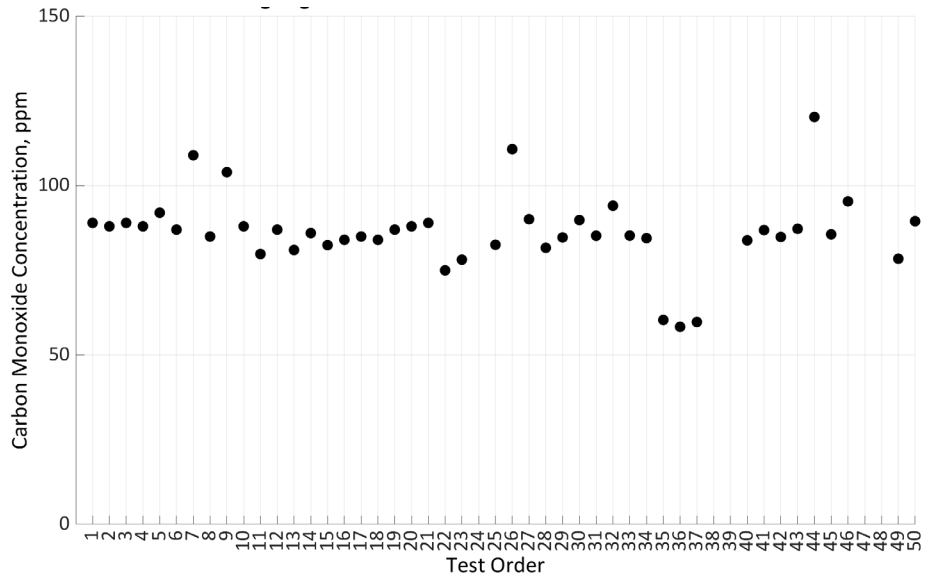
G.8 Upstream dCSC™ Pierburg CO Concentration vs. Test Order
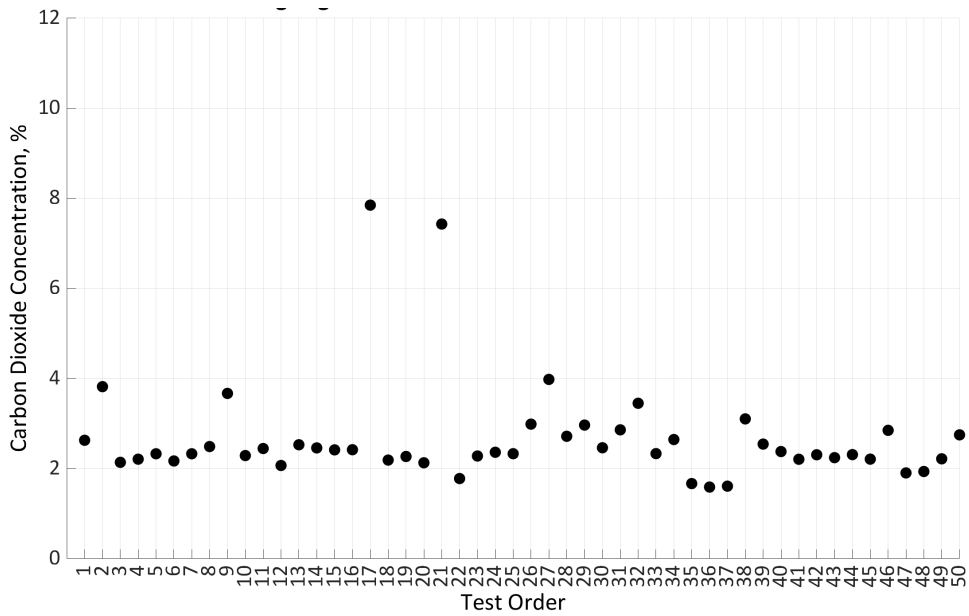
G.9 Upstream dCSC™ Pierburg CO_2 Concentration vs. Test Order

92
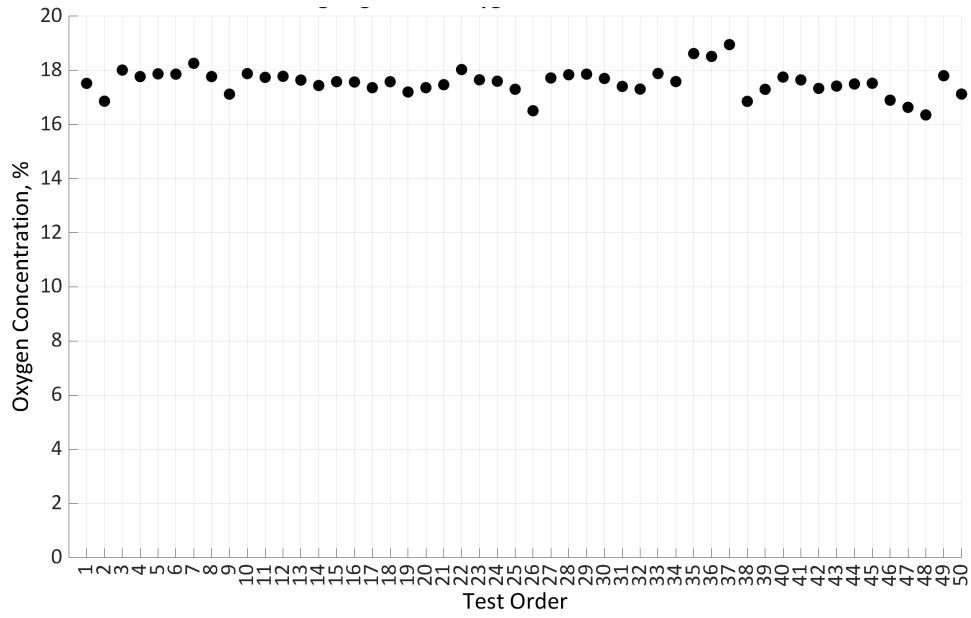
G.10 Upstream dCSC™ Pierburg O_2 Concentration vs. Test Order
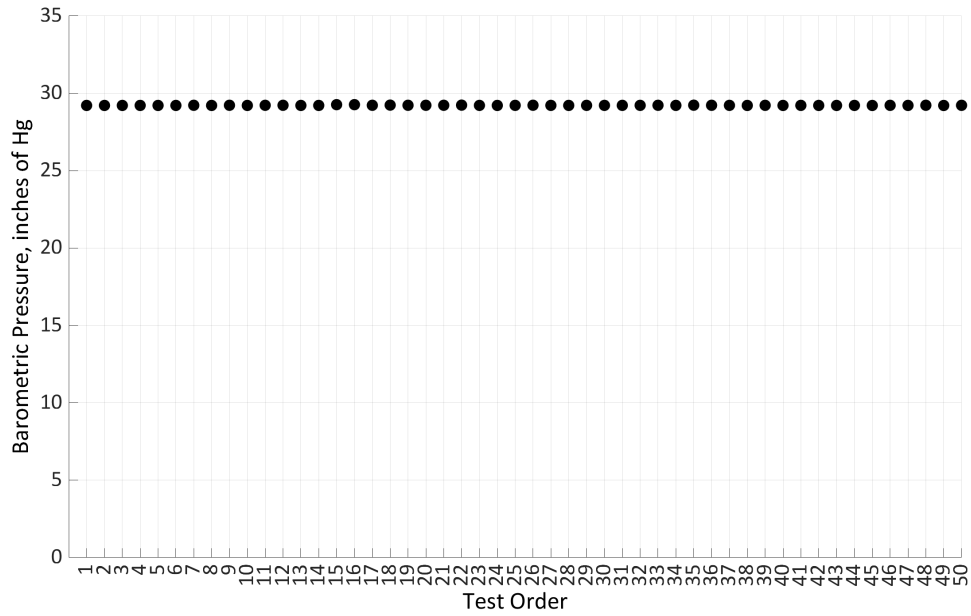
G.11 Test Cell Barometric Pressure vs. Test Order

93
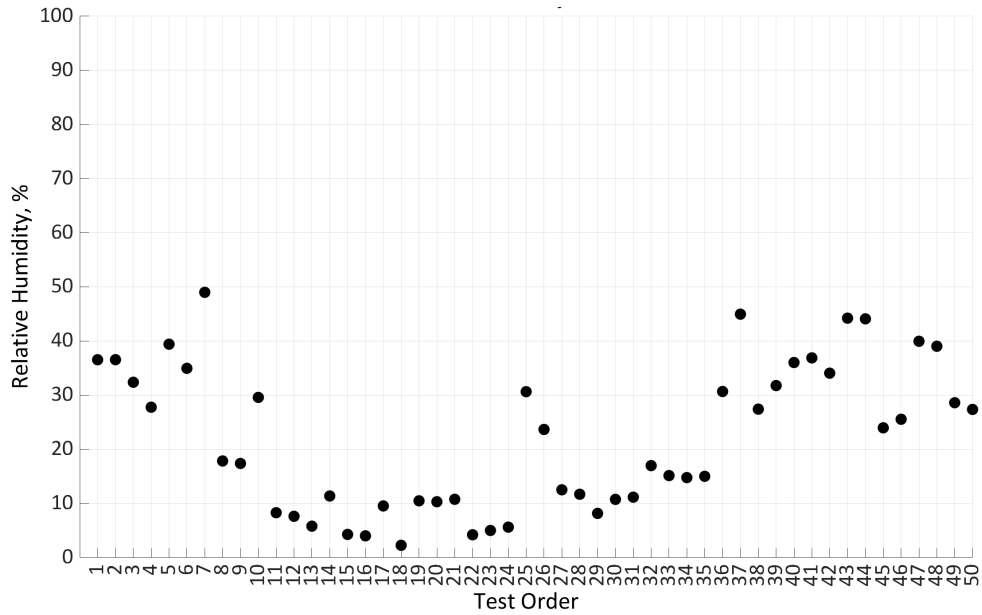
G.12 Test Cell Relative Humidity vs. Test Order
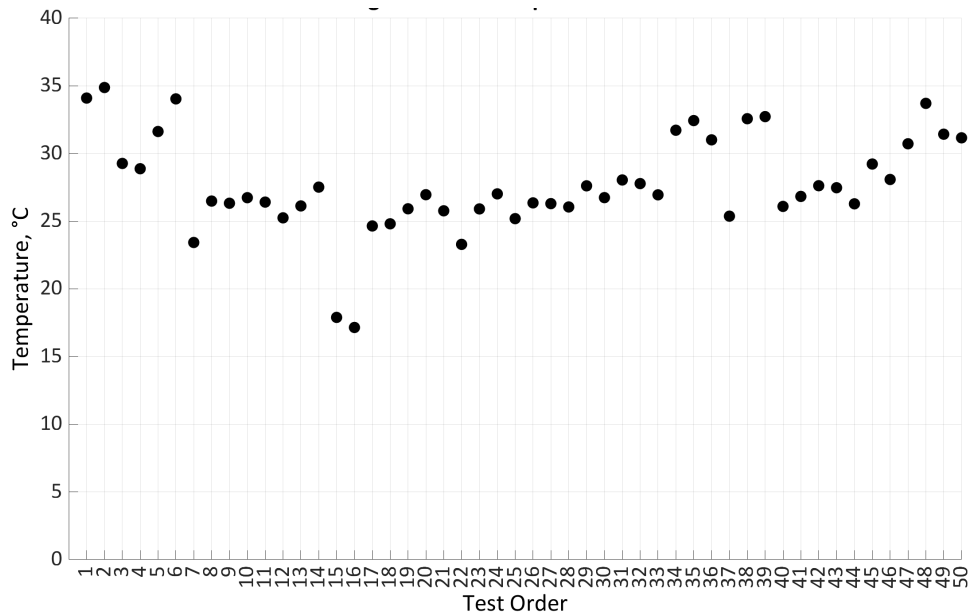
G.13 Average Test Cell Temperature during Test vs. Test Order

94
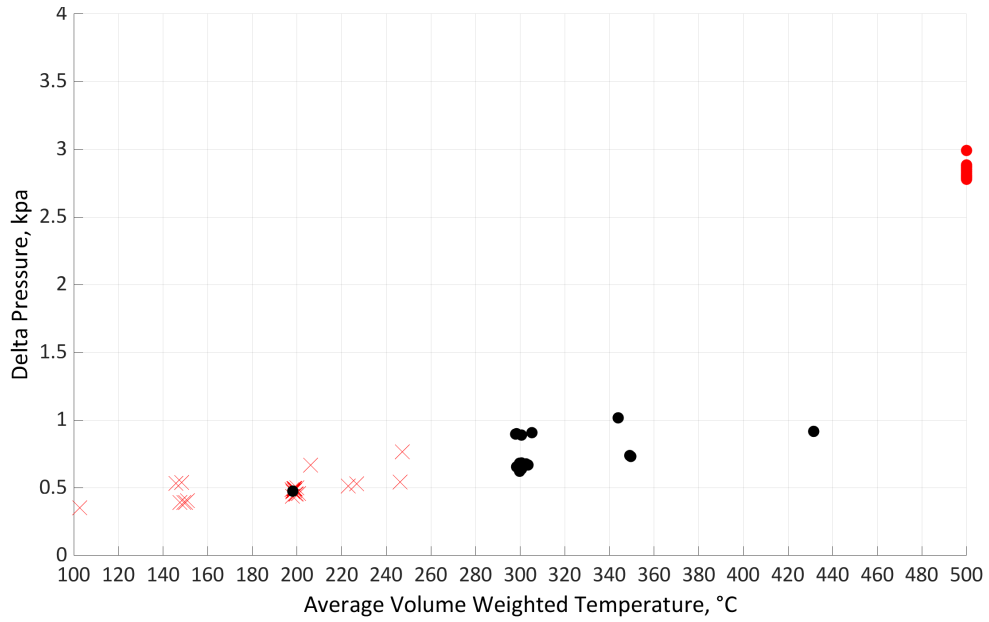
G.14 dCSC™ Delta Pressure vs. Average Volume Weighted Temperature
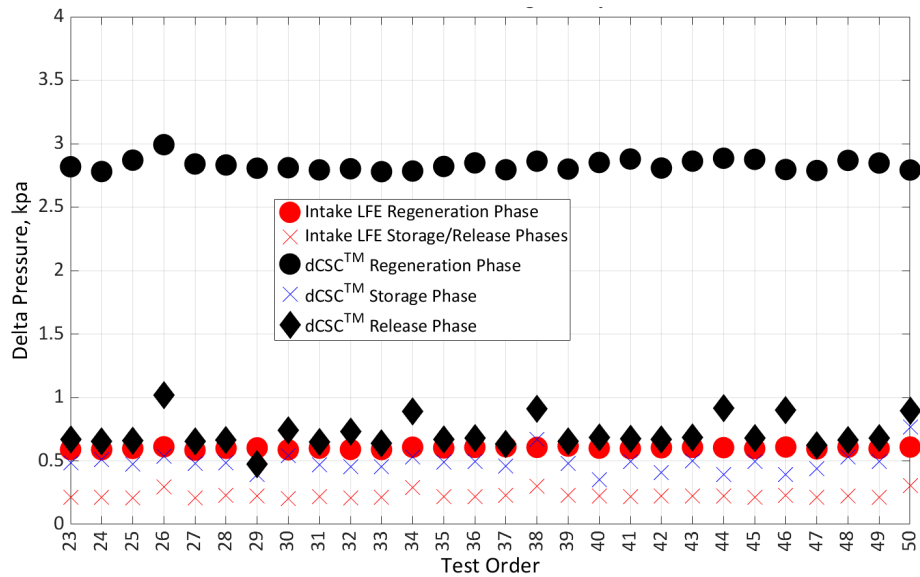
G.15 Engine Intake and dCSC™ Delta Pressures vs. Test Order

95
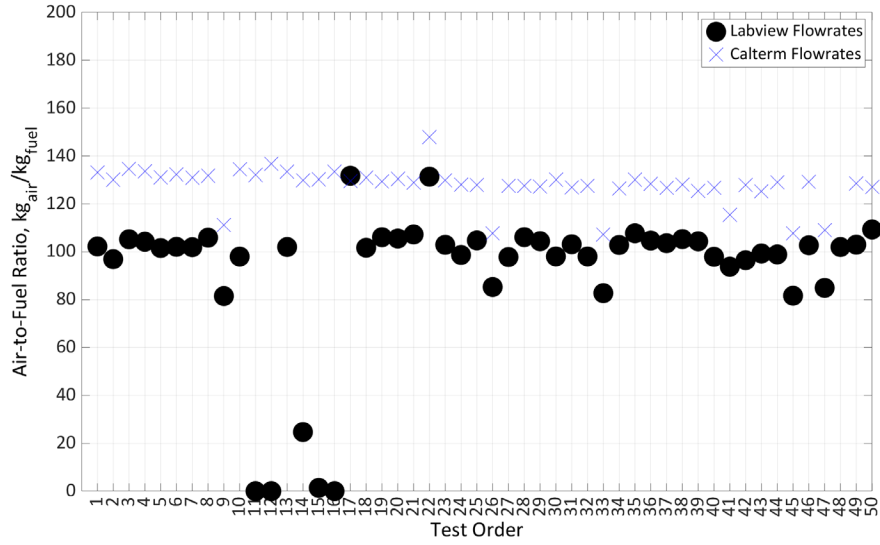
G.16 AFR Calculated from Fuel and Air Flow Rates vs. Test Order
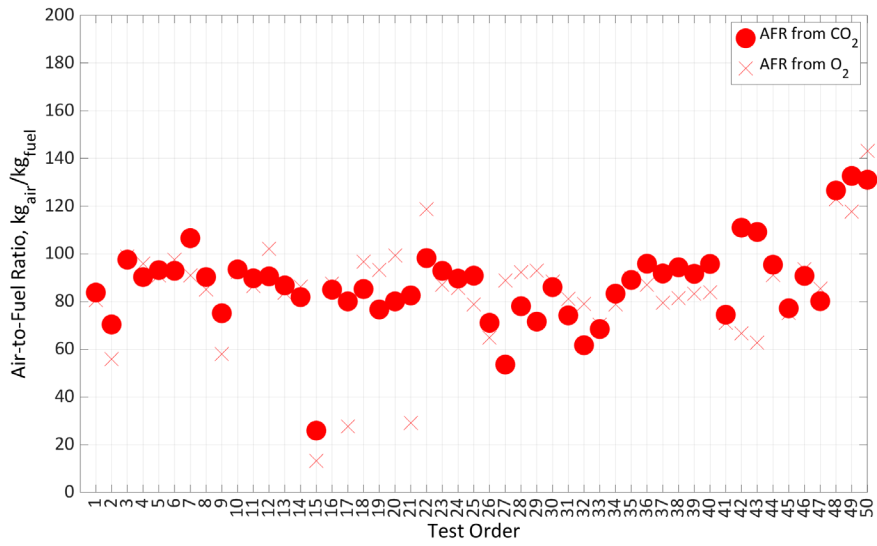
G.17 AFR Calculated from O_2 and CO_2 vs. Test Order

96
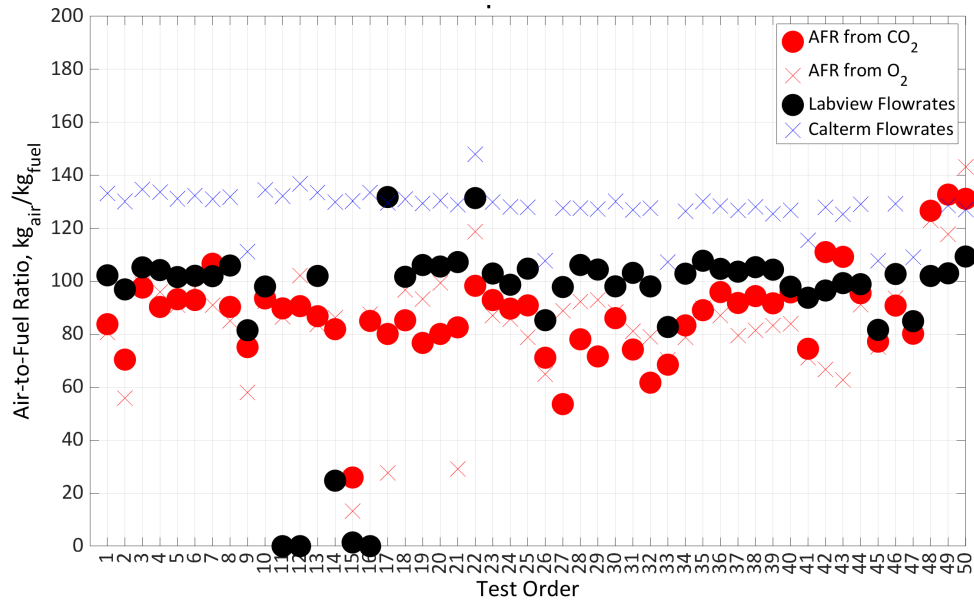
G.18 Comparison of all AFR Calculations vs. Test Order
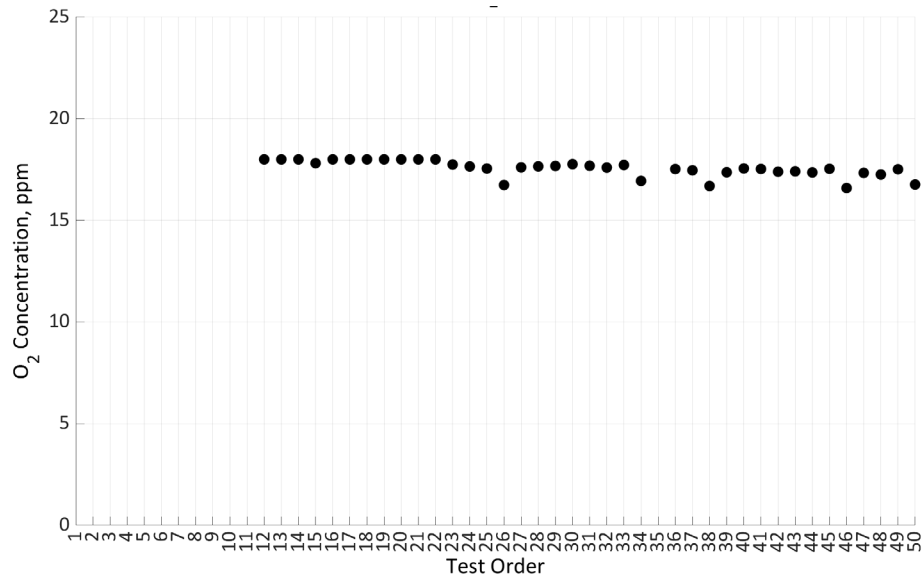
G.19 Upstream dCSC™ NOx Sensor O_2 Concentration vs. Test Order

97
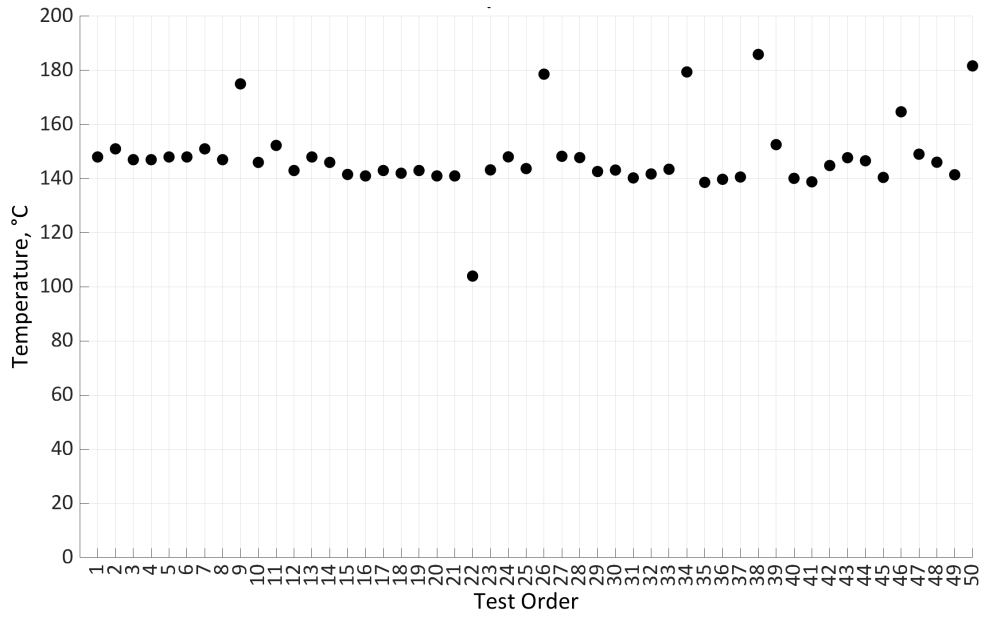
G.20 Engine Turbo Outlet Temperature vs. Test Order
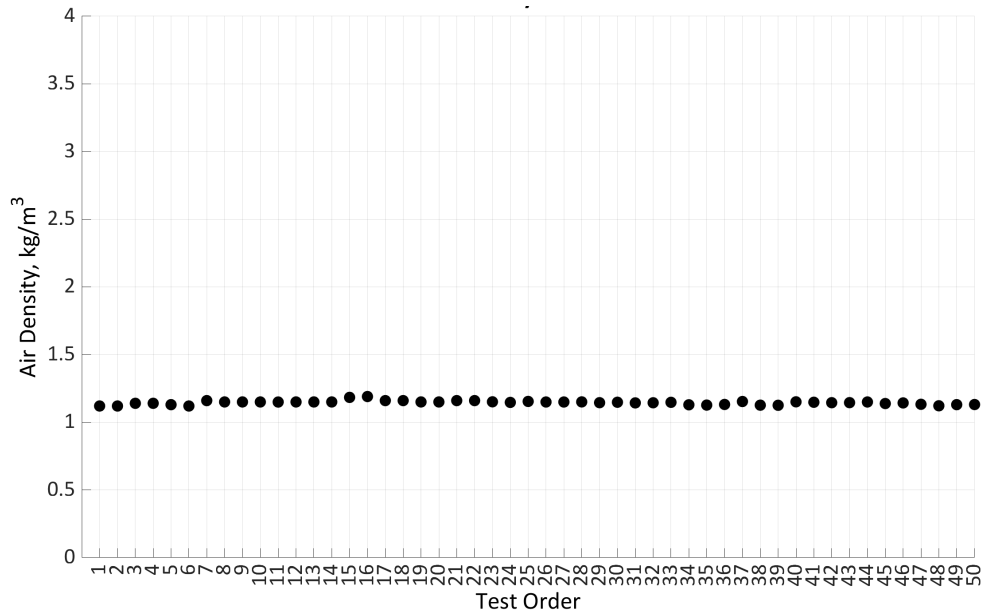
G.21 Engine Inlet Air Density vs. Test Order

98
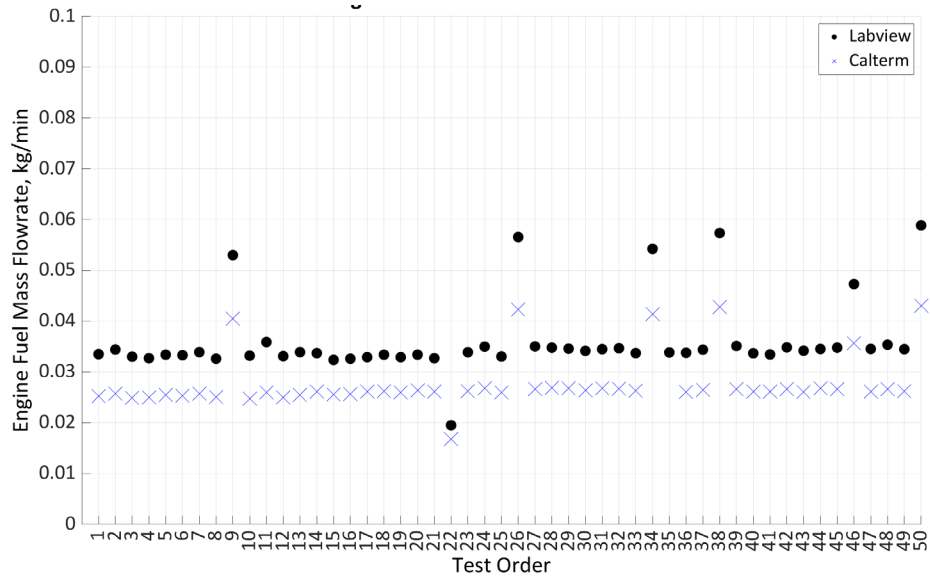
G.22 Coriolis Fuel Flow Meter (LabVIEW) and Calculated (Calterm) Fuel Flow Rate vs.

Test Order
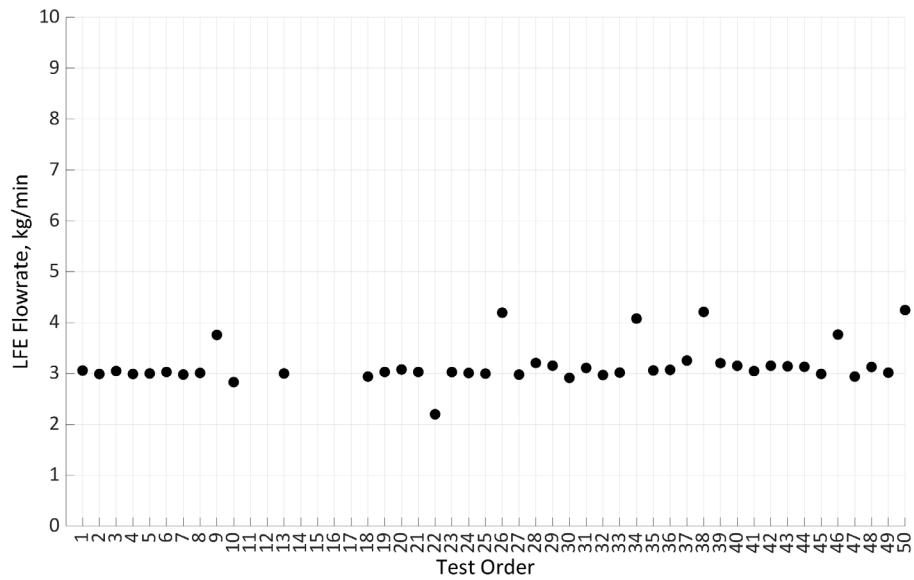
G.23 Laminar Flow Element Engine Intake Air Mass Flow Rate vs. Test Order

99
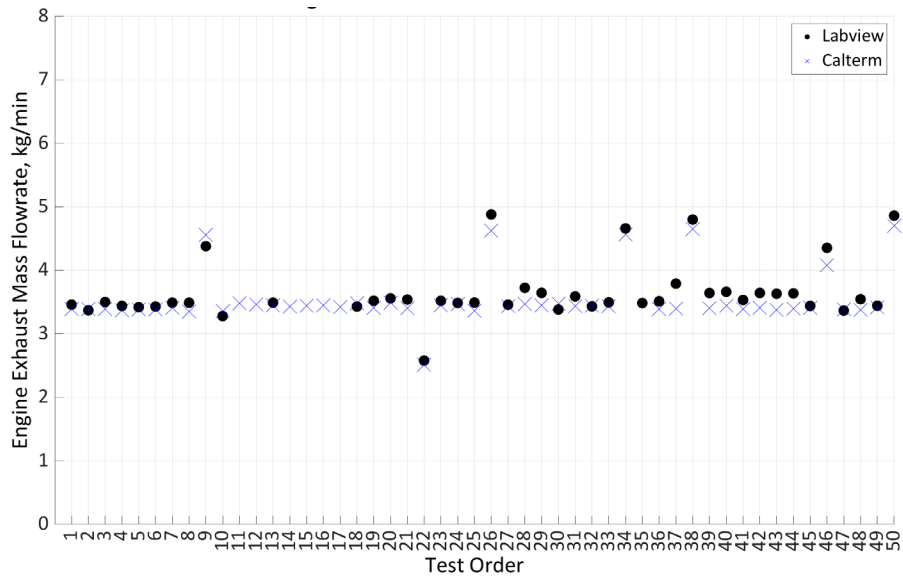
G.24 Engine Exhaust Mass Flow Rate Measured (LabVIEW) and Calculated (Calterm) vs. Test Order
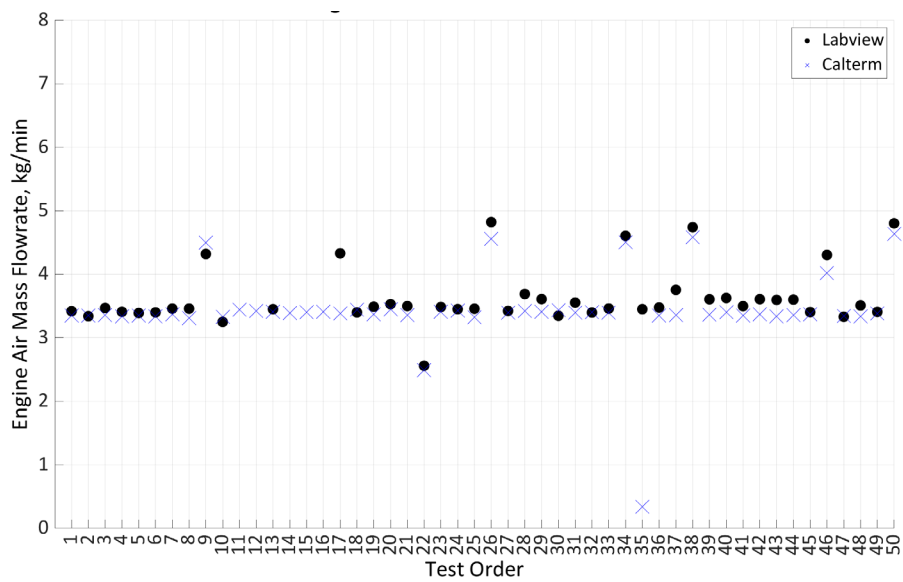
G.25 Engine Air Mass Flow Rate Measured (LabVIEW) and Calculated (Calterm) vs. Test Order
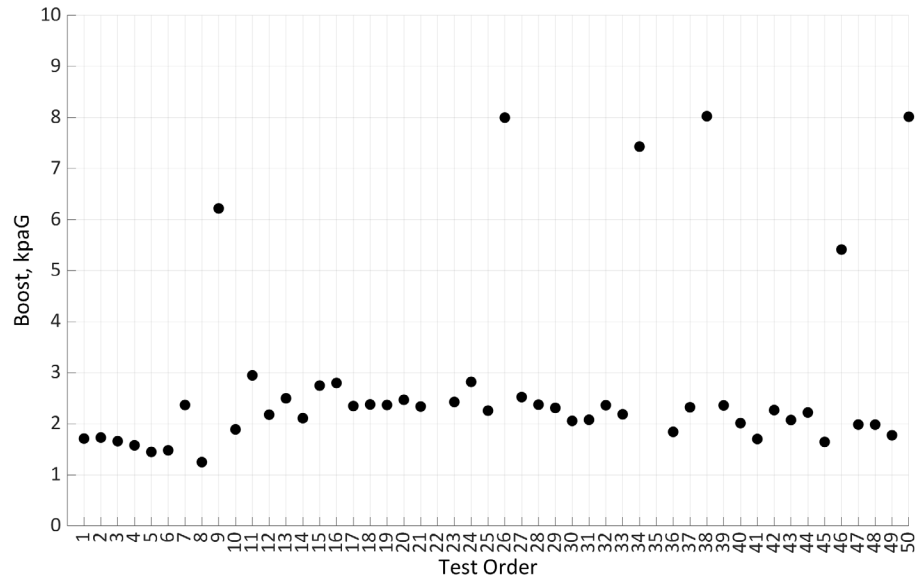
G.26 Engine Intake Boost (Calterm) vs. Test Order
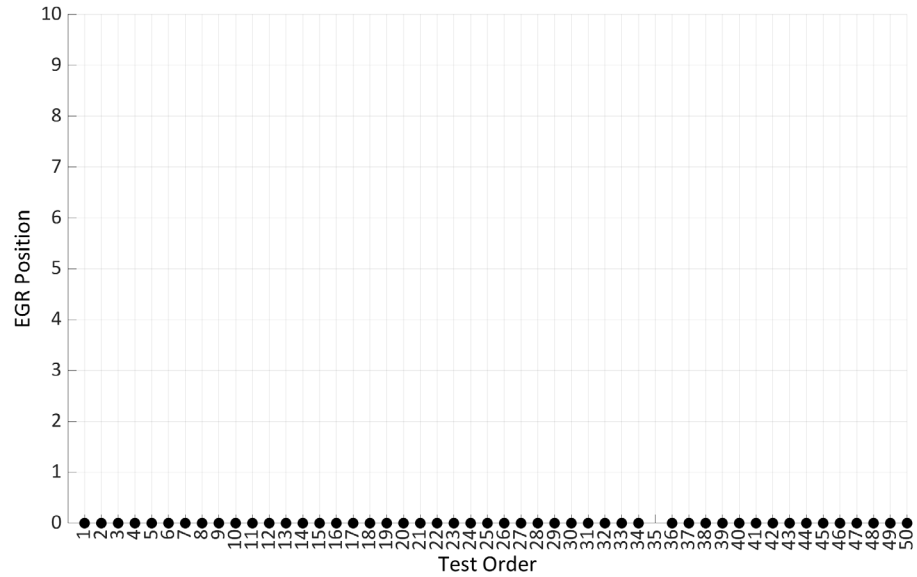
G.27 Engine EGR Position (Calterm) vs. Test Order

101
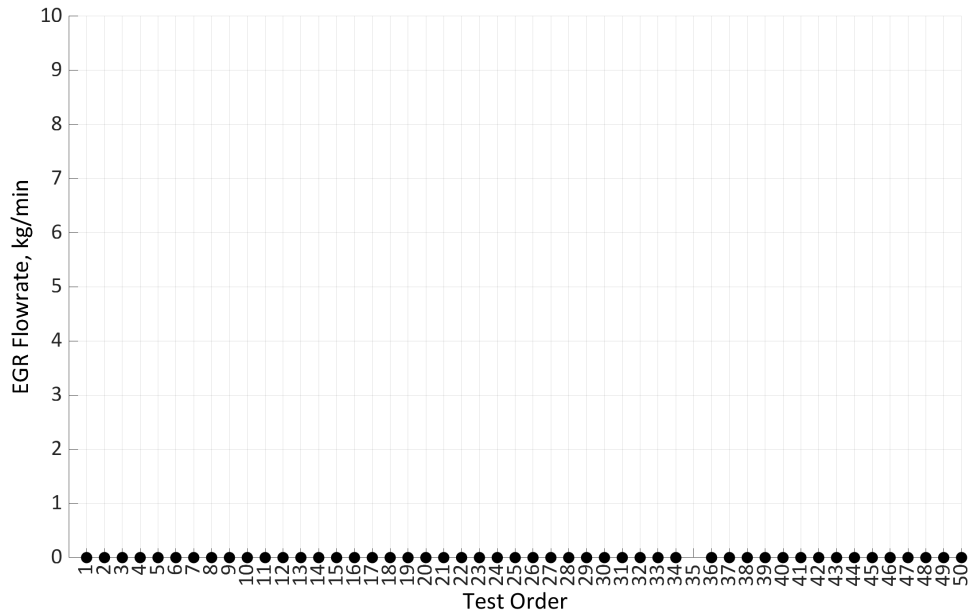
G.28 Engine EGR Flow Rate (Calterm) vs. Test Order
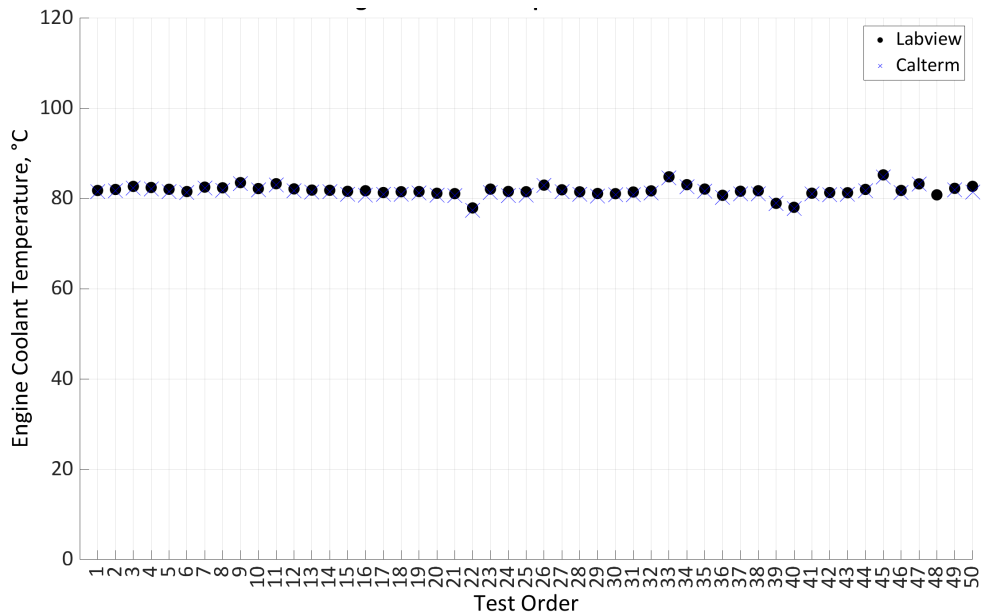
G.29 Engine Coolant Temperature (LabVIEW and Calterm) vs. Test Order

102
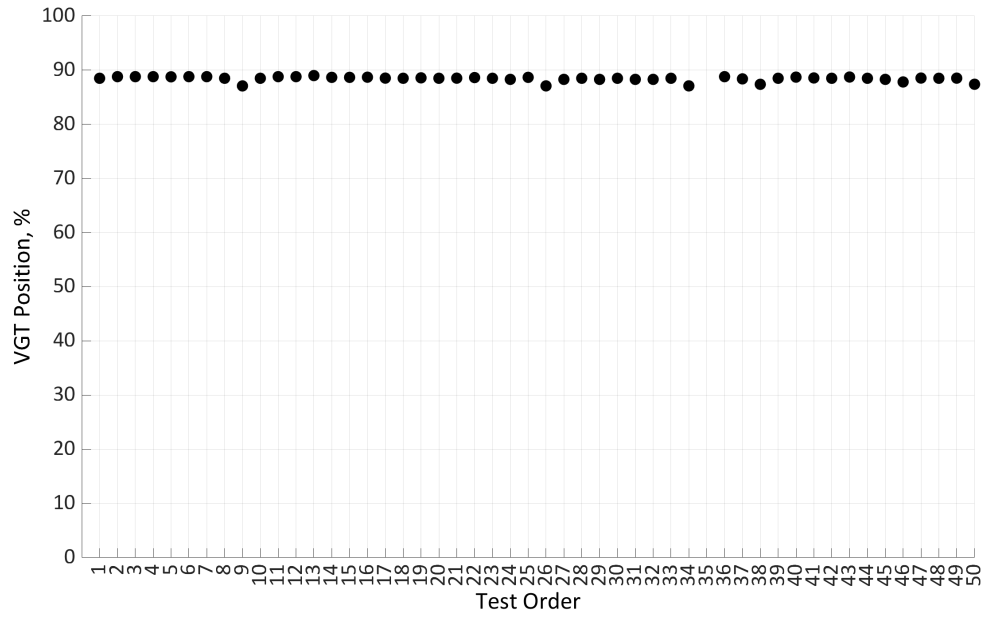
G.30 Engine Variable Geometry Turbo Position (Calterm) vs. Test Order
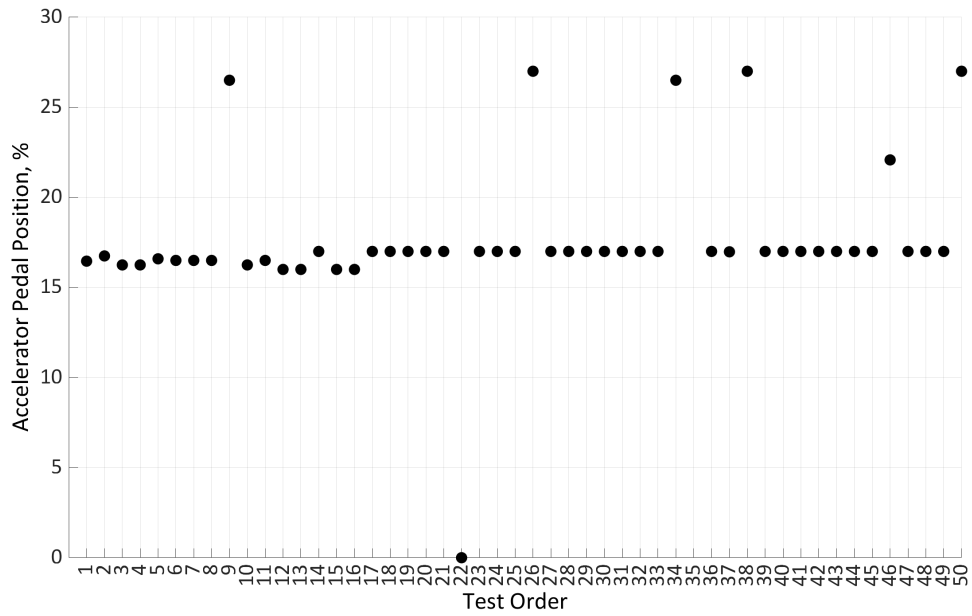
G.31 Engine Accelerator Pedal Position (Calterm) vs. Test Order

103
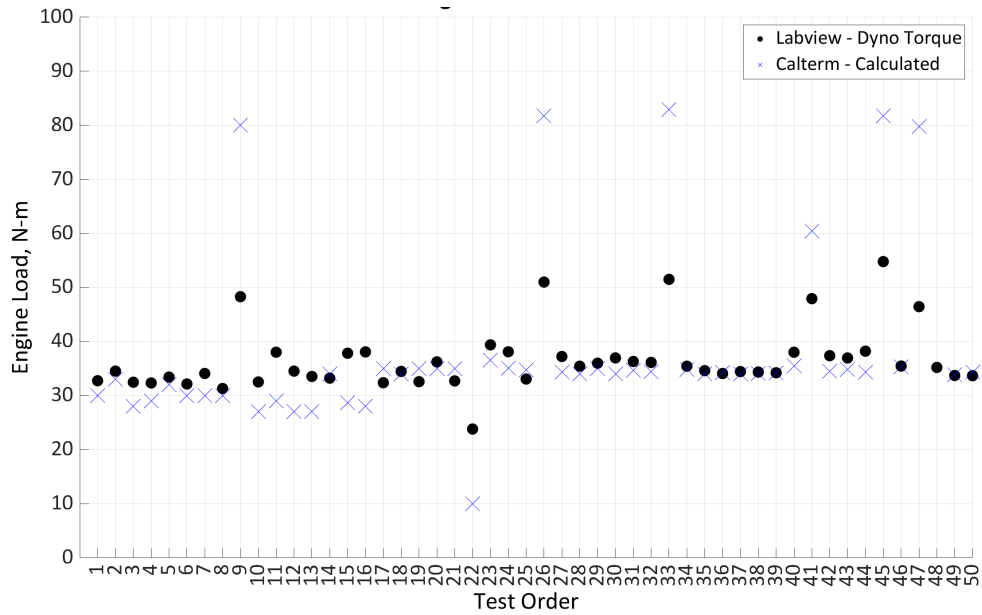
G.32 Engine Load vs. Test Order
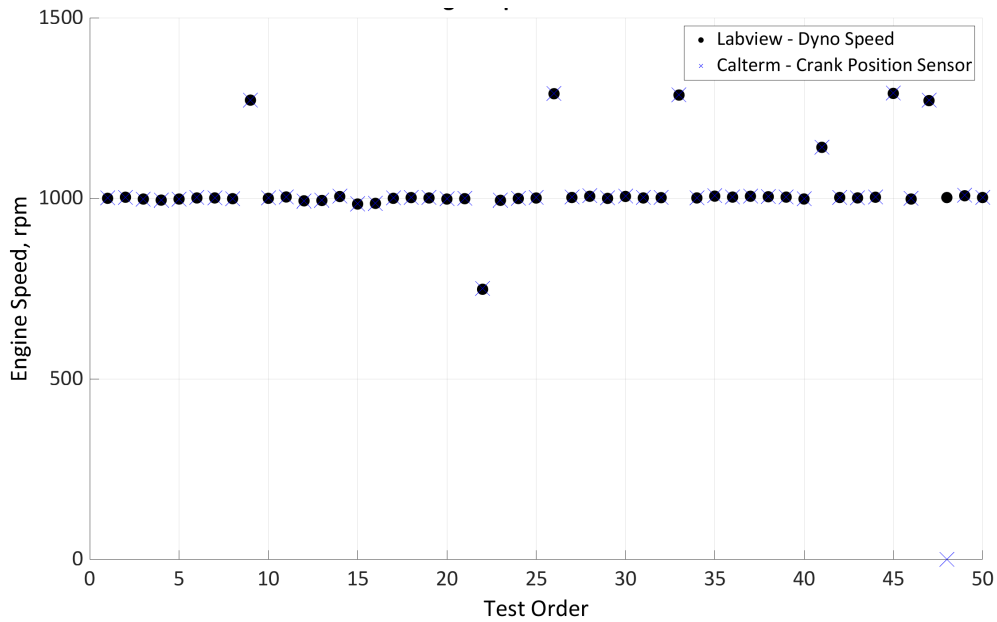
G.33 Engine Speed vs. Test Order

104

www.manaraa.com
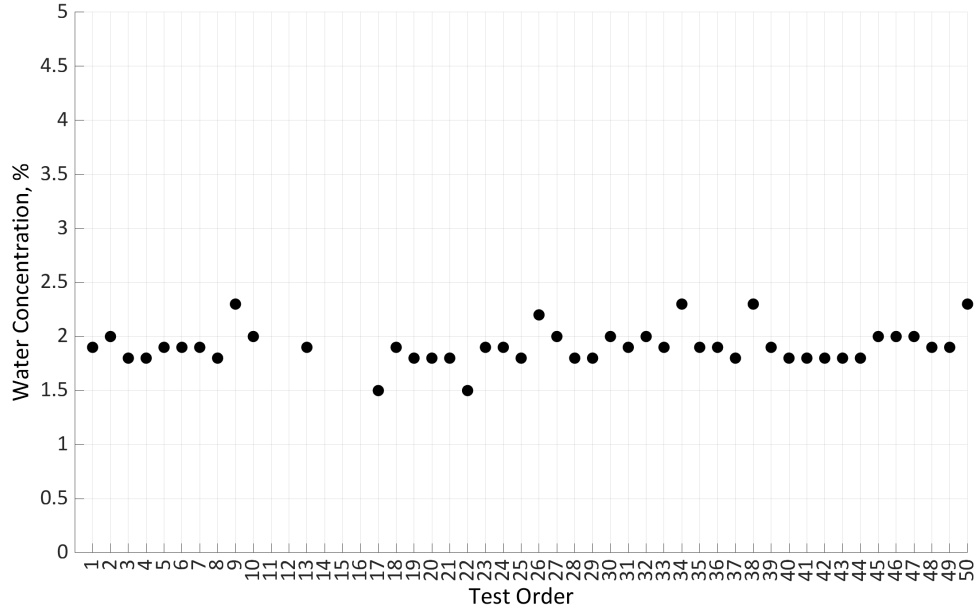
G.34 Engine Out H_2O Concentration Calculated from LabVIEW Flowrate AFR vs. Test
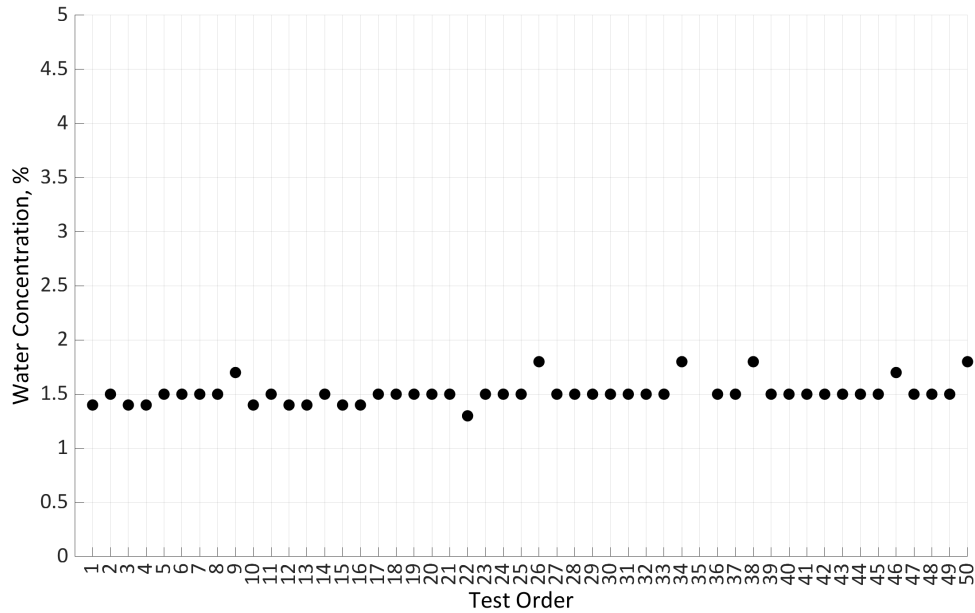
Order

G.35 Engine Out H_2O Concentration Calculated from Calterm Flowrate AFR vs. Test

Order

105
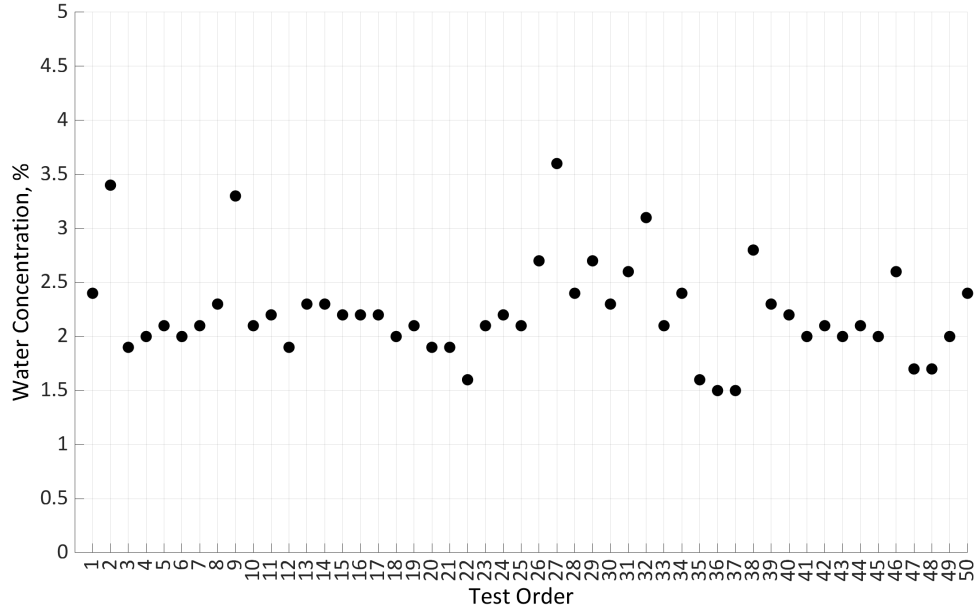
G.36 Engine Out H_2O Concentration Calculated from Pierburg Engine Out CO_2 Concentration vs. Test Order
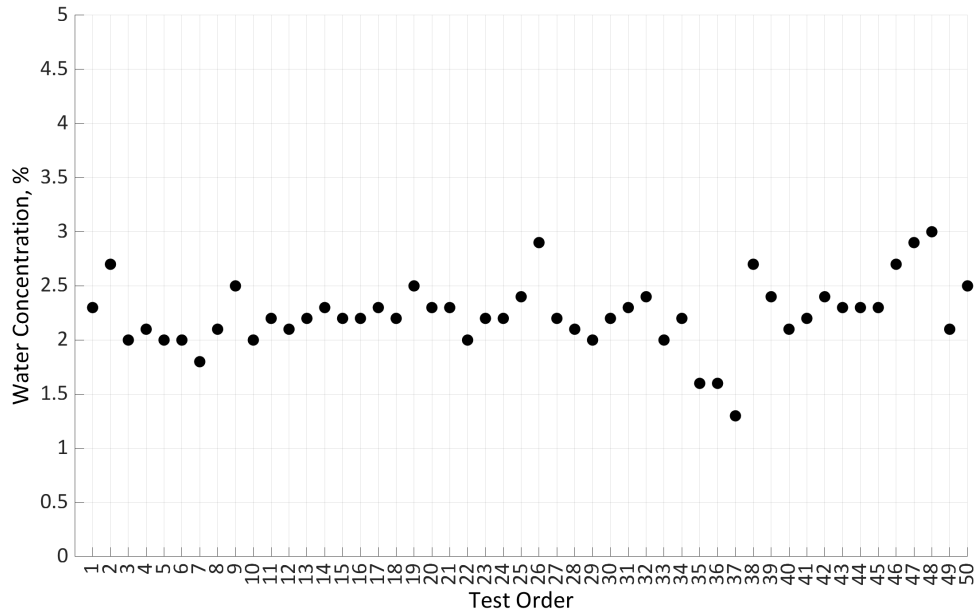
G.37 Engine Out H_2O Concentration Calculated from Pierburg Engine Out O_2 Concentration vs. Test Order

106

Appendix H. N₂O Formulation Reactions

The following equations are used to describe the N$_2$O formulation reactions within the dCSC™ per reference [19, 28]. Equation H.1 describes the NO reduction reaction that results in N$_2$O production.

$$2NO \rightarrow 0.5O_2 + N_2O \qquad \text{H.1}$$

Where NO forms N$_2$O and O$_2$. Equation H.2 describes the reaction between C$_3$H$_6$ and NO$_2$ causing a formulation of CO, H$_2$O, and N$_2$O.

$$C_3H_6 + 4NO_2 \leftrightarrow 3CO + 3H_2O + 2N_2O \qquad \text{H.2}$$
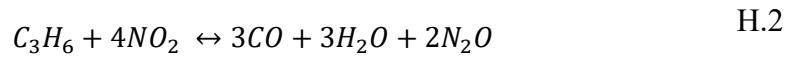
Appendix I.   CO, HC, and NO Oxidation Reactions

The following equations describe the oxidation reactions within the dCSC™. The equations were found in reference [27]. Equation H.1 defines the HC oxidation reaction.

$$HC + O_2 \rightarrow CO_2 + H_2O \qquad\qquad\qquad I.1$$

Where 1 HC atom is oxidized with 1 O_2 atom to form carbon dioxide, CO_2, and water vapor, H_2O. Equation H.2 describes the oxidation reaction of CO.

$$CO + O_2 \rightarrow 2CO_2 \qquad\qquad\qquad I.2$$

Where 2 CO atoms are oxidized with 1 O_2 to form 2 CO_2 atoms. Equation H.3 describes the oxidation reaction of NO.

$$NO + \frac{1}{2}O_2 \leftrightarrow NO_2 \qquad\qquad\qquad I.3$$

Where 1 NO atom is oxidized with ½ of an O_2 atom to form 1 NO_2 atom.

Appendix J. Additional Substrate Thermocouples

Additional substrate temperature instrumentation is needed in order to capture temperature gradient. Figure H.1 shows the dCSC™ radial temperature gradient measured during a steady state temperature condition of 250 °C. It is recommended for future testing to add rows of thermocouples at the locations indicated in Figure I.1.
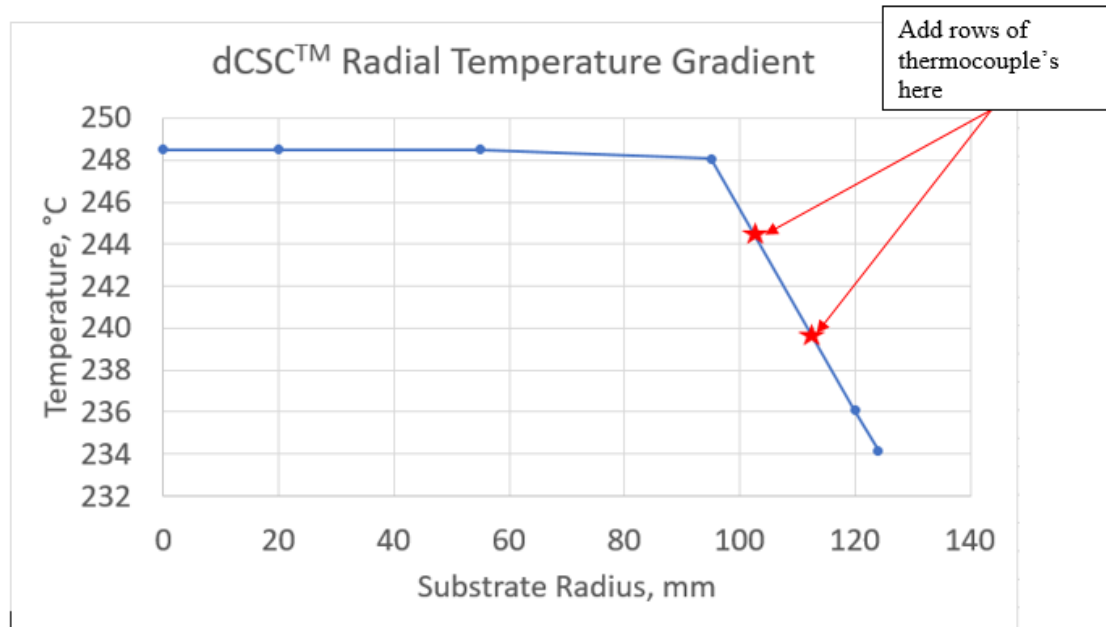
J.1 Recommended Additional Thermocouples to Measure Temperature

Appendix K.　　　Copyright Documentation

K.1.　　　Figure 1.1 Possible ULN ATS Compared to Current ATS

Conor Berndt <ctberndt@mtu.edu>　　　　　　　　Tue, Oct 29, 2019 at 4:33 PM

To: alissa.recker@daimler.com

Dear Alissa,

I am writing to request permission to reference a figure from your presentation "Fuel contaminants, effects on aftertreatment, and their limits on NOx stringency and extended useful life" - from the UW Symposium. The figure is shown below.

The figure would appear in my thesis titled: "AN EXPERIMENTAL STUDY OF A PASSIVE NOX ADSORBER (PNA) FOR THE REDUCTION OF COLD START DIESEL EMISSIONS."

Is there a paper this figure appears in? Otherwise I would reference the presentation in the figure caption and text.

Thank you for your time,

Conor Berndt

Mechanical Engineering - Graduate Student

Michigan Technological University

Email: ctberndt@mtu.edu

Phone: (906) 221-6485

MEEM B008

Conor Berndt <ctberndt@mtu.edu>   Wed, Nov 6, 2019 at 1:12 PM

To: alissa.recker@daimler.com

Hi Alissa,

I was wondering if you received my first email? Please let me know if you have any questions.

Thanks,

Conor Berndt

Mechanical Engineering - Graduate Student

Michigan Technological University

Email: ctberndt@mtu.edu

Phone: (906) 221-6485

MEEM B008

111

---

alissa.recker@daimler.com <alissa.recker@daimler.com>

Thu, Nov 7, 2019 at 1:06 PM

To: ctberndt@mtu.edu

Hi Conor,

Sorry for the delayed response. Yes, you can use it. It's really just a simple schematic of some of the proposals we've been seeing from CARB and Southweast Research. You can find more of them in the CARB White Paper:

https://ww3.arb.ca.gov/msprog/hdlownox/white_paper_04182019a.pdf

Thanks,

Alissa Recker

Catalyst Kit Engineer

ATS Performance TP/PNF

Daimler Trucks Powertrain Engineering NAFTA

Cell: +1 313 452-3926

Desk: +1 313 592-5689

[Quoted text hidden]

K.2.   Copyright Permission for Thesis Figure 1.2 Turbine Outlet Temperature vs. AFR

Conor Berndt <ctberndt@mtu.edu> Tue, Oct 29, 2019 at 3:31 PM

To: gshaver@purdue.edu

Dear Dr. Shaver,

I am writing to request permission to use Figure 2.2 from Mark Magee's masters thesis "Exhaust Thermal Management

Using Cylinder Deactivation and Late Intake Valve Closing" as a reference for my own masters thesis at Michigan

Technological University.

My thesis will be titled "AN EXPERIMENTAL STUDY OF A PASSIVE NOX ADSORBER (PNA) FOR THE REDUCTION

OF COLD START DIESEL EMISSIONS".

Any assistance in obtaining permission to use the figure would be greatly appreciated.

Thank you for your time and consideration,

Conor Berndt

Mechanical Engineering - Graduate Student

Michigan Technological University

Email: ctberndt@mtu.edu

Phone: (906) 221-6485

MEEM B008

Shaver, Gregory M <gshaver@purdue.edu> Tue, Oct 29, 2019 at 3:33 PM

To: Conor Berndt <ctberndt@mtu.edu>

Dear Conor,

I approve. I assume you would add a citation to Mark's thesis in the caption?

Greg

[Quoted text hidden]

Conor Berndt <ctberndt@mtu.edu> Tue, Oct 29, 2019 at 3:34 PM

To: "Shaver, Gregory M" <gshaver@purdue.edu>

Greg,

Thank you very much. Yes, I would cite Mark's thesis in the figure caption and where mentioned in the text.

Kind regards,

Conor Berndt

Mechanical Engineering - Graduate Student

Michigan Technological University

Email: ctberndt@mtu.edu

Phone: (906) 221-6485

MEEM B008

[Quoted text hidden]

Shaver, Gregory M <gshaver@purdue.edu> Tue, Oct 29, 2019 at 3:36 PM

To: Conor Berndt <ctberndt@mtu.edu>

Sounds good, Conor. Best wishes finishing up.

Cheers,

[Quoted text hidden]

Conor Berndt <ctberndt@mtu.edu> Tue, Oct 29, 2019 at 3:36 PM

To: "Shaver, Gregory M" <gshaver@purdue.edu>

Thank you!

Conor Berndt

Mechanical Engineering - Graduate Student

Michigan Technological University

Email: ctberndt@mtu.edu

Phone: (906) 221-6485

MEEM B008

[Quoted text hidden]

K.3. **Copyright Permission for Thesis Figure 2.2 NOx Adsorption/Storage, Figure 2.3 NOx Desorption/Release, and Figure 2.4 Effects of H$_2$O on NOx adsorption**

Conor Berndt <ctberndt@mtu.edu> Fri, Oct 25, 2019 at 9:48 AM

To: mharold@uh.edu, samalamis@uh.edu

Hi,

I am writing to request permission to reference figures from the attached presentation from the 2018 CLEERS

conference. They would appear in the Literature Review Chapter of my master's thesis titled "AN EXPERIMENTAL

STUDY OF A PASSIVE NOX ADSORBER (PNA) FOR THE REDUCTION OF COLD START DIESEL EMISSIONS".

The figures I would like to reference are the NOx adsorption, NOx desorption, and water inhibition of NOx storage

figures.

Please let me know if you have any questions,

Thank you for your time,

Conor Berndt

Mechanical Engineering - Graduate Student

Michigan Technological University

Email: ctberndt@mtu.edu

Phone: (906) 221-6485

MEEM B008

2018CLEERS_SamMalamis_Web.pptx

3109K

Harold, Michael P <MPHarold@central.uh.edu> Fri, Oct 25, 2019 at 11:25 AM

To: Conor Berndt <ctberndt@mtu.edu>

Cc: "Malamis, Sotirios A" <samalamis@uh.edu>

Dear Conor,

That will be fine. Or you could reference the paper that is related to that presentation which will be accepted soon. It

is

S. Malamis, M.P. Harold, W.S. Epling, "Coupled NO and C3H6 Trapping, Release and Conversion on Pd-BEA:

Evaluation of The Lean Hydrocarbon NO¬x Trap," in press, Ind. Eng. Chem. Res. (2019).

The paper should appear by mid November on the IECR website.

Best wishes,

https://mail.google.com/mail/u/0?ik=8713e930df&view=pt&search=all&permthid=thread-a%3Ar-7940216985565214836&simpl=msg-a%3Ar22165828… 2/2

Mike Harold

[Quoted text hidden]

Conor Berndt <ctberndt@mtu.edu> Mon, Oct 28, 2019 at 2:06 PM

To: "Harold, Michael P" <MPHarold@central.uh.edu>

Cc: "Malamis, Sotirios A" <samalamis@uh.edu>

Dear Mike,

Thank you very much! I will use the paper citation you have provided to cite the figures.

I appreciate the timely response.

Conor Berndt

Mechanical Engineering - Graduate Student

Michigan Technological University

Email: ctberndt@mtu.edu

118

Phone: (906) 221-6485

MEEM B008

[Quoted text hidden]

K.4. Copyright Permission for Thesis Figure 2.1 ULN ATS used on a Volvo MY 13.0L Diesel Engine at SwRI

Copyright Clearance Center | Marketplace™

SAE International - License Terms and Conditions

This is a License Agreement between Conor Berndt, MS Candidate, Michigan Technological University ("You") and SAE International ("Publisher") provided by Copyright Clearance Center ("CCC"). The license consists of your order details, the terms and conditions provided by SAE International, and the CCC terms and conditions.

All payments must be made in full to CCC.

Order Date	22-Oct-2019	Type of Use	Republish in a thesis/dissertation
Order license ID	1000169-1	Publisher	SAE International
System ID	2017-01-0958	Portion	Image/photo/illustration

LICENSED CONTENT

Publication Title	Achieving Ultra Low NOX Emissions Levels with a 2017 Heavy-Duty On-Highway TC Diesel Engine and an Advanced Technology Emissions System - NOX Management Strategies	Country	United States of America
		Rightsholder	SAE International
		Publication Type	Report
Author/Editor	Sharp, Christopher		
Date	01/01/2017		

REQUEST DETAILS

Portion Type	Image/photo/illustration	Distribution	Worldwide
Number of images / photos / illustrations	1	Translation	Original language of publication
Format (select all that apply)	Electronic	Copies for the disabled?	No
Who will republish the content?	Academic institution	Minor editing privileges?	No
Duration of Use	Life of current edition	Incidental promotional use?	No
Lifetime Unit Quantity	More than 2,000,000	Currency	USD
Rights Requested	Main product		

NEW WORK DETAILS

Title	AN EXPERIMENTAL STUDY OF A PASSIVE NOX ADSORBER (PNA) FOR THE REDUCTION OF COLD START DIESEL EMISSIONS	Institution name	Michigan Technological University
		Expected presentation date	2019-11-19
Instructor name	Dr. Jeffrey D. Naber		

ADDITIONAL DETAILS

Order reference number	N/A	The requesting person / organization to appear on the license	Conor Berndt, MS Candidate, Michigan Technological University

Title, description or numeric reference of the portion(s)	Figure 4 Final Low NOx Aftertreatment System	Title of the article/chapter the portion is from	N/A
Editor of portion(s)	SAE International Journal of Engines	Author of portion(s)	Sharp, Christopher
Volume of serial or monograph	10	Issue, if republishing an article from a serial	4
Page or page range of portion	1738	Publication date of portion	2017-01-01

CCC Republication Terms and Conditions

1. Description of Service; Defined Terms. This Republication License enables the User to obtain licenses for republication of one or more copyrighted works as described in detail on the relevant Order Confirmation (the "Work(s)"). Copyright Clearance Center, Inc. ("CCC") grants licenses through the Service on behalf of the rightsholder identified on the Order Confirmation (the "Rightsholder"). "Republication", as used herein, generally means the inclusion of a Work, in whole or in part, in a new work or works, also as described on the Order Confirmation. "User", as used herein, means the person or entity making such republication.

2. The terms set forth in the relevant Order Confirmation, and any terms set by the Rightsholder with respect to a particular Work, govern the terms of use of Works in connection with the Service. By using the Service, the person transacting for a republication license on behalf of the User represents and warrants that he/she/it (a) has been duly authorized by the User to accept, and hereby does accept, all such terms and conditions on behalf of User, and (b) shall inform User of all such terms and conditions. In the event such person is a "freelancer" or other third party independent of User and CCC, such party shall be deemed jointly a "User" for purposes of these terms and conditions. In any event, User shall be deemed to have accepted and agreed to all such terms and conditions if User republishes the Work in any fashion.

3. Scope of License; Limitations and Obligations.

   3.1. All Works and all rights therein, including copyright rights, remain the sole and exclusive property of the Rightsholder. The license created by the exchange of an Order Confirmation (and/or any invoice) and payment by User of the full amount set forth on that document includes only those rights expressly set forth in the Order Confirmation and in these terms and conditions, and conveys no other rights in the Work(s) to User. All rights not expressly granted are hereby reserved.

   3.2. General Payment Terms: You may pay by credit card or through an account with us payable at the end of the month. If you and we agree that you may establish a standing account with CCC, then the following terms apply: Remit Payment to: Copyright Clearance Center, 29118 Network Place, Chicago, IL 60673-1291. Payments Due: Invoices are payable upon their delivery to you (or upon our notice to you that they are available to you for downloading). After 30 days, outstanding amounts will be subject to a service charge of 1-1/2% per month or, if less, the maximum rate allowed by applicable law. Unless otherwise specifically set forth in the Order Confirmation or in a separate written agreement signed by CCC, invoices are due and payable on "net 30" terms. While User may exercise the rights licensed immediately upon issuance of the Order Confirmation, the license is automatically revoked and is null and void, as if it had never been issued, if complete payment for the license is not received on a timely basis either from User directly or through a payment agent, such as a credit card company.

   3.3. Unless otherwise provided in the Order Confirmation, any grant of rights to User (i) is "one-time" (including the editions and product family specified in the license), (ii) is non-exclusive and non-transferable and (iii) is subject to any and all limitations and restrictions (such as, but not limited to, limitations on duration of use or circulation) included in the Order Confirmation or invoice and/or in these terms and conditions. Upon completion of the licensed use, User shall either secure a new permission for further use of the Work(s) or immediately cease any new use of the Work(s) and shall render inaccessible (such as by deleting or by removing or severing links or other locators) any further copies of the Work (except for copies printed on paper in accordance with this license and still in User's stock at the end of such period).

   3.4. In the event that the material for which a republication license is sought includes third party materials (such as photographs, illustrations, graphs, inserts and similar materials) which are identified in such material as having been used by permission, User is responsible for identifying, and seeking separate licenses (under this Service or otherwise) for, any of such third party materials; without a separate license, such third party materials may not be used.

3.5. Use of proper copyright notice for a Work is required as a condition of any license granted under the Service. Unless otherwise provided in the Order Confirmation, a proper copyright notice will read substantially as follows: "Republished with permission of [Rightsholder's name], from [Work's title, author, volume, edition number and year of copyright]; permission conveyed through Copyright Clearance Center, Inc. " Such notice must be provided in a reasonably legible font size and must be placed either immediately adjacent to the Work as used (for example, as part of a by-line or footnote but not as a separate electronic link) or in the place where substantially all other credits or notices for the new work containing the republished Work are located. Failure to include the required notice results in loss to the Rightsholder and CCC, and the User shall be liable to pay liquidated damages for each such failure equal to twice the use fee specified in the Order Confirmation, in addition to the use fee itself and any other fees and charges specified.

3.6. User may only make alterations to the Work if and as expressly set forth in the Order Confirmation. No Work may be used in any way that is defamatory, violates the rights of third parties (including such third parties' rights of copyright, privacy, publicity, or other tangible or intangible property), or is otherwise illegal, sexually explicit or obscene. In addition, User may not conjoin a Work with any other material that may result in damage to the reputation of the Rightsholder. User agrees to inform CCC if it becomes aware of any infringement of any rights in a Work and to cooperate with any reasonable request of CCC or the Rightsholder in connection therewith.

4. Indemnity. User hereby indemnifies and agrees to defend the Rightsholder and CCC, and their respective employees and directors, against all claims, liability, damages, costs and expenses, including legal fees and expenses, arising out of any use of a Work beyond the scope of the rights granted herein, or any use of a Work which has been altered in any unauthorized way by User, including claims of defamation or infringement of rights of copyright, publicity, privacy or other tangible or intangible property.

5. Limitation of Liability. UNDER NO CIRCUMSTANCES WILL CCC OR THE RIGHTSHOLDER BE LIABLE FOR ANY DIRECT, INDIRECT, CONSEQUENTIAL OR INCIDENTAL DAMAGES (INCLUDING WITHOUT LIMITATION DAMAGES FOR LOSS OF BUSINESS PROFITS OR INFORMATION, OR FOR BUSINESS INTERRUPTION) ARISING OUT OF THE USE OR INABILITY TO USE A WORK, EVEN IF ONE OF THEM HAS BEEN ADVISED OF THE POSSIBILITY OF SUCH DAMAGES. In any event, the total liability of the Rightsholder and CCC (including their respective employees and directors) shall not exceed the total amount actually paid by User for this license. User assumes full liability for the actions and omissions of its principals, employees, agents, affiliates, successors and assigns.

6. Limited Warranties. THE WORK(S) AND RIGHT(S) ARE PROVIDED "AS IS". CCC HAS THE RIGHT TO GRANT TO USER THE RIGHTS GRANTED IN THE ORDER CONFIRMATION DOCUMENT. CCC AND THE RIGHTSHOLDER DISCLAIM ALL OTHER WARRANTIES RELATING TO THE WORK(S) AND RIGHT(S), EITHER EXPRESS OR IMPLIED, INCLUDING WITHOUT LIMITATION IMPLIED WARRANTIES OF MERCHANTABILITY OR FITNESS FOR A PARTICULAR PURPOSE. ADDITIONAL RIGHTS MAY BE REQUIRED TO USE ILLUSTRATIONS, GRAPHS, PHOTOGRAPHS, ABSTRACTS, INSERTS OR OTHER PORTIONS OF THE WORK (AS OPPOSED TO THE ENTIRE WORK) IN A MANNER CONTEMPLATED BY USER; USER UNDERSTANDS AND AGREES THAT NEITHER CCC NOR THE RIGHTSHOLDER MAY HAVE SUCH ADDITIONAL RIGHTS TO GRANT.

7. Effect of Breach. Any failure by User to pay any amount when due, or any use by User of a Work beyond the scope of the license set forth in the Order Confirmation and/or these terms and conditions, shall be a material breach of the license created by the Order Confirmation and these terms and conditions. Any breach not cured within 30 days of written notice thereof shall result in immediate termination of such license without further notice. Any unauthorized (but licensable) use of a Work that is terminated immediately upon notice thereof may be liquidated by payment of the Rightsholder's ordinary license price therefor; any unauthorized (and unlicensable) use that is not terminated immediately for any reason (including, for example, because materials containing the Work cannot reasonably be recalled) will be subject to all remedies available at law or in equity, but in no event to a payment of less than three times the Rightsholder's ordinary license price for the most closely analogous licensable use plus Rightsholder's and/or CCC's costs and expenses incurred in collecting such payment.

8. Miscellaneous.

8.1. User acknowledges that CCC may, from time to time, make changes or additions to the Service or to these terms and conditions, and CCC reserves the right to send notice to the User by electronic mail or otherwise for the purposes of notifying User of such changes or additions; provided that any such changes or additions shall not apply to permissions already secured and paid for.

8.2. Use of User-related information collected through the Service is governed by CCC's privacy policy, available online here: https://marketplace.copyright.com/rs-ui-web/mp/privacy-policy

8.3. The licensing transaction described in the Order Confirmation is personal to User. Therefore, User may not assign or transfer to any other person (whether a natural person or an organization of any kind) the license created by the Order Confirmation and these terms and conditions or any rights granted hereunder; provided, however, that User may assign such license in its entirety on written notice to CCC in the event of a transfer of all or substantially all of User's rights in the new material which includes the Work(s) licensed under this Service.

8.4. No amendment or waiver of any terms is binding unless set forth in writing and signed by the parties. The Rightsholder and CCC hereby object to any terms contained in any writing prepared by the User or its principals, employees, agents or affiliates and purporting to govern or otherwise relate to the licensing transaction described in the Order Confirmation, which terms are in any way inconsistent with any terms set forth in the Order Confirmation and/or in these terms and conditions or CCC's standard operating procedures, whether such writing is prepared prior to, simultaneously with or subsequent to the Order Confirmation, and whether such writing appears on a copy of the Order Confirmation or in a separate instrument.

8.5. The licensing transaction described in the Order Confirmation document shall be governed by and construed under the law of the State of New York, USA, without regard to the principles thereof of conflicts of law. Any case, controversy, suit, action, or proceeding arising out of, in connection with, or related to such licensing transaction shall be brought, at CCC's sole discretion, in any federal or state court located in the County of New York, State of New York, USA, or in any federal or state court whose geographical jurisdiction covers the location of the Rightsholder set forth in the Order Confirmation. The parties expressly submit to the personal jurisdiction and venue of each such federal or state court.If you have any comments or questions about the Service or Copyright Clearance Center, please contact us at 978-750-8400 or send an e-mail to info@copyright.com.

v 1.1

www.manaraa.com

K.5. Copyright Permission for Thesis Figure 2.5 dCSC™ and DOC oxidation performance, Figure 2.6 CO Oxidation Comparison of DOC, PNA, and dCSC™, and Figure 2.7 HC adsorption, desorption, and conversion catalyst comparison

Copyright Clearance Center | Marketplace™

SAE International - License Terms and Conditions

This is a License Agreement between Conor Berndt, MS Candidate, Michigan Technological University ("You") and SAE International ("Publisher") provided by Copyright Clearance Center ("CCC"). The license consists of your order details, the terms and conditions provided by SAE International, and the CCC terms and conditions.

All payments must be made in full to CCC.

Order Date	22-Oct-2019	Type of Use	Republish in a thesis/dissertation
Order license ID	1000168-1	Publisher	SAE International
ISSN	1946-3960	Portion	Image/photo/illustration

LICENSED CONTENT

Publication Title	SAE International journal of fuels and lubricants	Publication Type	e-Journal
Article Title	Cold Start Concept (CSC™): A Novel Catalyst for Cold Start Emission Control	Start Page	372
		End Page	381
Author/Editor	Society of Automotive Engineers.	Issue	2
Date	01/01/2009	Volume	6
Language	English	URL	http://saefuel.saejournals.org
Country	United States of America		
Rightsholder	SAE International		

REQUEST DETAILS

Portion Type	Image/photo/illustration	Distribution	Worldwide
Number of images / photos / illustrations	3	Translation	Original language of publication
Format (select all that apply)	Electronic	Copies for the disabled?	No
Who will republish the content?	Academic institution	Minor editing privileges?	No
Duration of Use	Life of current edition	Incidental promotional use?	No
Lifetime Unit Quantity	More than 2,000,000	Currency	USD
Rights Requested	Main product		

NEW WORK DETAILS

Title	AN EXPERIMENTAL STUDY OF A PASSIVE NOX ADSORBER (PNA) FOR THE REDUCTION OF COLD START DIESEL EMISSIONS	Institution name	Michigan Technological University
		Expected presentation date	2019-11-19
Instructor name	Dr. Jeffrey D. Naber		

CCC Republication Terms and Conditions

3.4. In the event that the material for which a republication license is sought includes third party materials (such as photographs, illustrations, graphs, inserts and similar materials) which are identified in such material as having been used by permission, User is responsible for identifying, and seeking separate licenses (under this Service or otherwise) for, any of such third party materials; without a separate license, such third party materials may not be used.

3.5. Use of proper copyright notice for a Work is required as a condition of any license granted under the Service. Unless otherwise provided in the Order Confirmation, a proper copyright notice will read substantially as follows: "Republished with permission of [Rightsholder's name], from [Work's title, author, volume, edition number and year of copyright]; permission conveyed through Copyright Clearance Center, Inc. " Such notice must be provided in a reasonably legible font size and must be placed either immediately adjacent to the Work as used (for example, as part of a by-line or footnote but not as a separate electronic link) or in the place where substantially all other credits or notices for the new work containing the republished Work are located. Failure to include the required notice results in loss to the Rightsholder and CCC, and the User shall be liable to pay liquidated damages for each such failure equal to twice the use fee specified in the Order Confirmation, in addition to the use fee itself and any other fees and charges specified.

3.6. User may only make alterations to the Work if and as expressly set forth in the Order Confirmation. No Work may be used in any way that is defamatory, violates the rights of third parties (including such third parties' rights of copyright, privacy, publicity, or other tangible or intangible property), or is otherwise illegal, sexually explicit or obscene. In addition, User may not conjoin a Work with any other material that may result in damage to the reputation of the Rightsholder. User agrees to inform CCC if it becomes aware of any infringement of any rights in a Work and to cooperate with any reasonable request of CCC or the Rightsholder in connection therewith.

4. Indemnity. User hereby indemnifies and agrees to defend the Rightsholder and CCC, and their respective employees and directors, against all claims, liability, damages, costs and expenses, including legal fees and expenses, arising out of any use of a Work beyond the scope of the rights granted herein, or any use of a Work which has been altered in any unauthorized way by User, including claims of defamation or infringement of rights of copyright, publicity, privacy or other tangible or intangible property.

5. Limitation of Liability. UNDER NO CIRCUMSTANCES WILL CCC OR THE RIGHTSHOLDER BE LIABLE FOR ANY DIRECT, INDIRECT, CONSEQUENTIAL OR INCIDENTAL DAMAGES (INCLUDING WITHOUT LIMITATION DAMAGES FOR LOSS OF BUSINESS PROFITS OR INFORMATION, OR FOR BUSINESS INTERRUPTION) ARISING OUT OF THE USE OR INABILITY TO USE A WORK, EVEN IF ONE OF THEM HAS BEEN ADVISED OF THE POSSIBILITY OF SUCH DAMAGES. In any event, the total liability of the Rightsholder and CCC (including their respective employees and directors) shall not exceed the total amount actually paid by User for this license. User assumes full liability for the actions and omissions of its principals, employees, agents, affiliates, successors and assigns.

6. Limited Warranties. THE WORK(S) AND RIGHT(S) ARE PROVIDED "AS IS". CCC HAS THE RIGHT TO GRANT TO USER THE RIGHTS GRANTED IN THE ORDER CONFIRMATION DOCUMENT. CCC AND THE RIGHTSHOLDER DISCLAIM ALL OTHER WARRANTIES RELATING TO THE WORK(S) AND RIGHT(S), EITHER EXPRESS OR IMPLIED, INCLUDING WITHOUT LIMITATION IMPLIED WARRANTIES OF MERCHANTABILITY OR FITNESS FOR A PARTICULAR PURPOSE. ADDITIONAL RIGHTS MAY BE REQUIRED TO USE ILLUSTRATIONS, GRAPHS, PHOTOGRAPHS, ABSTRACTS, INSERTS OR OTHER PORTIONS OF THE WORK (AS OPPOSED TO THE ENTIRE WORK) IN A MANNER CONTEMPLATED BY USER; USER UNDERSTANDS AND AGREES THAT NEITHER CCC NOR THE RIGHTSHOLDER MAY HAVE SUCH ADDITIONAL RIGHTS TO GRANT.

7. Effect of Breach. Any failure by User to pay any amount when due, or any use by User of a Work beyond the scope of the license set forth in the Order Confirmation and/or these terms and conditions, shall be a material breach of the license created by the Order Confirmation and these terms and conditions. Any breach not cured within 30 days of written notice thereof shall result in immediate termination of such license without further notice. Any unauthorized (but licensable) use of a Work that is terminated immediately upon notice thereof may be liquidated by payment of the Rightsholder's ordinary license price therefor; any unauthorized (and unlicensable) use that is not terminated immediately for any reason (including, for example, because materials containing the Work cannot reasonably be recalled) will be subject to all remedies available at law or in equity, but in no event to a payment of less than three times the Rightsholder's ordinary license price for the most closely analogous licensable use plus Rightsholder's and/or CCC's costs and expenses incurred in collecting such payment.

8. Miscellaneous.

8.1. User acknowledges that CCC may, from time to time, make changes or additions to the Service or to these terms and conditions, and CCC reserves the right to send notice to the User by electronic mail or otherwise for the purposes of notifying User of such changes or additions; provided that any such changes or additions shall not apply to permissions already secured and paid for.

8.2. Use of User-related information collected through the Service is governed by CCC's privacy policy, available online here: https://marketplace.copyright.com/rs-ui-web/mp/privacy-policy

8.3. The licensing transaction described in the Order Confirmation is personal to User. Therefore, User may not assign or transfer to any other person (whether a natural person or an organization of any kind) the license created by the Order Confirmation and these terms and conditions or any rights granted hereunder; provided, however, that User may assign such license in its entirety on written notice to CCC in the event of a transfer of all or substantially all of User's rights in the new material which includes the Work(s) licensed under this Service.

8.4. No amendment or waiver of any terms is binding unless set forth in writing and signed by the parties. The Rightsholder and CCC hereby object to any terms contained in any writing prepared by the User or its principals, employees, agents or affiliates and purporting to govern or otherwise relate to the licensing transaction described in the Order Confirmation, which terms are in any way inconsistent with any terms set forth in the Order Confirmation and/or in these terms and conditions or CCC's standard operating procedures, whether such writing is prepared prior to, simultaneously with or subsequent to the Order Confirmation, and whether such writing appears on a copy of the Order Confirmation or in a separate instrument.

8.5. The licensing transaction described in the Order Confirmation document shall be governed by and construed under the law of the State of New York, USA, without regard to the principles thereof of conflicts of law. Any case, controversy, suit, action, or proceeding arising out of, in connection with, or related to such licensing transaction shall be brought, at CCC's sole discretion, in any federal or state court located in the County of New York, State of New York, USA, or in any federal or state court whose geographical jurisdiction covers the location of the Rightsholder set forth in the Order Confirmation. The parties expressly submit to the personal jurisdiction and venue of each such federal or state court.If you have any comments or questions about the Service or Copyright Clearance Center, please contact us at 978-750-8400 or send an e-mail to info@copyright.com.

v 1.1

124

K.6. Copyright Permissions for Thesis Figure 2.8 200-Second dCSC™ NOx Storage Capacity

3.4. In the event that the material for which a republication license is sought includes third party materials (such as photographs, illustrations, graphs, inserts and similar materials) which are identified in such material as having been used by permission, User is responsible for identifying, and seeking separate licenses (under this Service or otherwise) for, any of such third party materials; without a separate license, such third party materials may not be used.

3.5. Use of proper copyright notice for a Work is required as a condition of any license granted under the Service. Unless otherwise provided in the Order Confirmation, a proper copyright notice will read substantially as follows: "Republished with permission of [Rightsholder's name], from [Work's title, author, volume, edition number and year of copyright]; permission conveyed through Copyright Clearance Center, Inc. " Such notice must be provided in a reasonably legible font size and must be placed either immediately adjacent to the Work as used (for example, as part of a by-line or footnote but not as a separate electronic link) or in the place where substantially all other credits or notices for the new work containing the republished Work are located. Failure to include the required notice results in loss to the Rightsholder and CCC, and the User shall be liable to pay liquidated damages for each such failure equal to twice the use fee specified in the Order Confirmation, in addition to the use fee itself and any other fees and charges specified.

3.6. User may only make alterations to the Work if and as expressly set forth in the Order Confirmation. No Work may be used in any way that is defamatory, violates the rights of third parties (including such third parties' rights of copyright, privacy, publicity, or other tangible or intangible property), or is otherwise illegal, sexually explicit or obscene. In addition, User may not conjoin a Work with any other material that may result in damage to the reputation of the Rightsholder. User agrees to inform CCC if it becomes aware of any infringement of any rights in a Work and to cooperate with any reasonable request of CCC or the Rightsholder in connection therewith.

4. Indemnity. User hereby indemnifies and agrees to defend the Rightsholder and CCC, and their respective employees and directors, against all claims, liability, damages, costs and expenses, including legal fees and expenses, arising out of any use of a Work beyond the scope of the rights granted herein, or any use of a Work which has been altered in any unauthorized way by User, including claims of defamation or infringement of rights of copyright, publicity, privacy or other tangible or intangible property.

5. Limitation of Liability. UNDER NO CIRCUMSTANCES WILL CCC OR THE RIGHTSHOLDER BE LIABLE FOR ANY DIRECT, INDIRECT, CONSEQUENTIAL OR INCIDENTAL DAMAGES (INCLUDING WITHOUT LIMITATION DAMAGES FOR LOSS OF BUSINESS PROFITS OR INFORMATION, OR FOR BUSINESS INTERRUPTION) ARISING OUT OF THE USE OR INABILITY TO USE A WORK, EVEN IF ONE OF THEM HAS BEEN ADVISED OF THE POSSIBILITY OF SUCH DAMAGES. In any event, the total liability of the Rightsholder and CCC (including their respective employees and directors) shall not exceed the total amount actually paid by User for this license. User assumes full liability for the actions and omissions of its principals, employees, agents, affiliates, successors and assigns.

6. Limited Warranties. THE WORK(S) AND RIGHT(S) ARE PROVIDED "AS IS". CCC HAS THE RIGHT TO GRANT TO USER THE RIGHTS GRANTED IN THE ORDER CONFIRMATION DOCUMENT. CCC AND THE RIGHTSHOLDER DISCLAIM ALL OTHER WARRANTIES RELATING TO THE WORK(S) AND RIGHT(S), EITHER EXPRESS OR IMPLIED, INCLUDING WITHOUT LIMITATION IMPLIED WARRANTIES OF MERCHANTABILITY OR FITNESS FOR A PARTICULAR PURPOSE. ADDITIONAL RIGHTS MAY BE REQUIRED TO USE ILLUSTRATIONS, GRAPHS, PHOTOGRAPHS, ABSTRACTS, INSERTS OR OTHER PORTIONS OF THE WORK (AS OPPOSED TO THE ENTIRE WORK) IN A MANNER CONTEMPLATED BY USER; USER UNDERSTANDS AND AGREES THAT NEITHER CCC NOR THE RIGHTSHOLDER MAY HAVE SUCH ADDITIONAL RIGHTS TO GRANT.

7. Effect of Breach. Any failure by User to pay any amount when due, or any use by User of a Work beyond the scope of the license set forth in the Order Confirmation and/or these terms and conditions, shall be a material breach of the license created by the Order Confirmation and these terms and conditions. Any breach not cured within 30 days of written notice thereof shall result in immediate termination of such license without further notice. Any unauthorized (but licensable) use of a Work that is terminated immediately upon notice thereof may be liquidated by payment of the Rightsholder's ordinary license price therefor; any unauthorized (and unlicensable) use that is not terminated immediately for any reason (including, for example, because materials containing the Work cannot reasonably be recalled) will be subject to all remedies available at law or in equity, but in no event to a payment of less than three times the Rightsholder's ordinary license price for the most closely analogous licensable use plus Rightsholder's and/or CCC's costs and expenses incurred in collecting such payment.

8. Miscellaneous.

8.1. User acknowledges that CCC may, from time to time, make changes or additions to the Service or to these terms and conditions, and CCC reserves the right to send notice to the User by electronic mail or otherwise for the purposes of notifying User of such changes or additions; provided that any such changes or additions shall not apply to permissions already secured and paid for.

8.2. Use of User-related information collected through the Service is governed by CCC's privacy policy, available online here: https://marketplace.copyright.com/rs-ui-web/mp/privacy-policy

8.3. The licensing transaction described in the Order Confirmation is personal to User. Therefore, User may not assign or transfer to any other person (whether a natural person or an organization of any kind) the license created by the Order Confirmation and these terms and conditions or any rights granted hereunder; provided, however, that User may assign such license in its entirety on written notice to CCC in the event of a transfer of all or substantially all of User's rights in the new material which includes the Work(s) licensed under this Service.

8.4. No amendment or waiver of any terms is binding unless set forth in writing and signed by the parties. The Rightsholder and CCC hereby object to any terms contained in any writing prepared by the User or its principals, employees, agents or affiliates and purporting to govern or otherwise relate to the licensing transaction described in the Order Confirmation, which terms are in any way inconsistent with any terms set forth in the Order Confirmation and/or in these terms and conditions or CCC's standard operating procedures, whether such writing is prepared prior to, simultaneously with or subsequent to the Order Confirmation, and whether such writing appears on a copy of the Order Confirmation or in a separate instrument.

8.5. The licensing transaction described in the Order Confirmation document shall be governed by and construed under the law of the State of New York, USA, without regard to the principles thereof of conflicts of law. Any case, controversy, suit, action, or proceeding arising out of, in connection with, or related to such licensing transaction shall be brought, at CCC's sole discretion, in any federal or state court located in the County of New York, State of New York, USA, or in any federal or state court whose geographical jurisdiction covers the location of the Rightsholder set forth in the Order Confirmation. The parties expressly submit to the personal jurisdiction and venue of each such federal or state court.If you have any comments or questions about the Service or Copyright Clearance Center, please contact us at 978-750-8400 or send an e-mail to info@copyright.com.

v 1.1